On the Improvement of Algebraic Model for Prediction of Turbulent Flows

Qiu Jifeng

Department of Mechanical Engineering

Keio University

In Partial Fulfillment of the Requirements
for the Degree of
Ph.D. in Engineering

March 2009

Acknowledgements

First of all, I would like to express my gratitude to my supervisor, Professor Shinnosuke Obi, for his invaluable advice, guidance and encouragement throughout my studies. Professor Obi's professional and linguistic advice as well as his personal support made study a great experience and joy for me. I am also deeply grateful for Professor Shigeaki Masuda, who has retired since March of 2007, and Assistant Professor Koji Fukagata for their help and encouragement on my study. Also, I would like to thank Professor Zhenping Feng from Xi'an Jiaotong University of China for his continuous care and help.

Very special thanks go to Professor Thomas B. Gatski for his commitment to our collaborative work. During our numerous discussions, which he always had time for, Professor Gatski guided me with his great knowledge and professionalism for the study.

I take this opportunity to thank all my colleagues over the years, particularly to Mr. Rio Yokota, Mr. Yoshitsugu Naka, Mr. Alexandre Suryadi, Ms. Jing Hui. There was so much enjoyable time when we studied together. Their kind and patient support have been very important to my study and myself.

I am very grateful to the members of the thesis committee: Professor Fujihiro Hamba, Professor Akiko Matsuo and Professor Toshihisa Ueda for their valuable comments on the thesis manuscript.

I would like to thank my parents, my sister and my brother for their love, support and encouragement during all these years. I am deeply grateful to my dear wife, Yuanyuan Guo for her support and patience.

Finally, I would like to acknowledge the financial support I have taken for my study: Japanese Government MEXT Scholarship, Yamaoka Foundation, Keio University 21st century COE Program, Keio University GCOE Program, The Research Grant of Keio Leading-edge Laboratory of Science & Technology.

Abstract

The present research aims at developing algebraic Reynolds stress model (ARSM), which is feasible and accurate to simulate engineering turbulent flows. The study has been focused on the assessment and modification of the diffusive transport assumption, which is necessary and crucial to derive ARSM. By using the budget and asymptotic analyses, it is shown that the current diffusive transport assumption tends to fail in the near-wall region. Furthermore, based on above analyses, an alternative form of diffusive transport constraint is proposed for the near-wall region.

The similar methodology has also been applied to the algebraic heat flux model (AHFM). As a result, an alternative diffusive transport constraint has been proposed. Preliminary evaluation results have shown that the improvement of consequently resulted model can also be expected by employing the proposed constraint. In addition, the frame invariant concept is invoked in this study to extend the original advection assumption for flows associated with rotation and curvature effects. Moreover, the frame invariant form of AHFM is derived by using the extended weak-equilibrium condition.

To this end, some key issues concerning the basic performance of RANS models have been recognized, such as the modeling of pressure-strain rate, modeling of pressure transport term. With further study, the improvement of such models can advance the RANS modeling fundamentally, which also naturally applies to the algebraic models. It is also noted that, although the a priori tests have proved the proposed alternative constraints can improve the resultant algebraic models potentially, the more detailed tests should be performed to validate the proposed alternative constraints.

Contents

List of Figures

List of Tables

Nomenclature

Roman Symbols

$\mathcal{D}$	The diffusive transport of turbulent kinetic energy
$\mathcal{D}_{i\theta}$	The diffusive transport term in the heat flux transport equation
$\mathcal{D}_{ij}^{\nu}$	Viscous diffusion of Reynolds stress
$\mathcal{D}_{ij}^{p}$	Pressure transport of Reynolds stress
$\mathcal{D}_{ij}^{t}$	Turbulent transport of Reynolds stress
$\overline{u_i\theta}$	The turbulent heat flux
$\partial\Theta/\partial x_j$	The gradient of temperature
$\phi_{i\theta}$	The pressure temperature-gradient correlation term
τ_{ij}	The Reynolds stress
$\tilde{P}$	The instantaneous pressure
$\tilde{U}_i$	The instantaneous velocity
$\varepsilon_{i\theta}$	The dissipation term in the heat flux transport equation
b_{ij}	The Reynolds stress anisotropy tensor ($2b_{ij} = a_{ij}$)
k	Turbulent kinetic energy
k_θ	The temperature variance

P	The ensemble mean pressure
p	The fluctuating pressure
P/ε	The production-dissipation ration
$P_{i\theta}$	The production term in the heat flux transport equation
P_{ij}	Turbulent production of Reynolds stress
Pr	The Prandtl number
Q_{ij}	The orthogonal transformation tensor
Re	Reynolds number
Ri_t	The Richardson number
Ro	The rotation number
S_{ij}	The strain-rate tensor
U^+	The velocity normalized by the bulk velocity
u_τ	The wall shear velocity
$u_{\tau p}$	The wall shear velocity for pressure side
$u_{\tau s}$	The wall shear velocity for suction side
U_i	The ensemble mean velocity
u_i	The fluctuating velocity
W_{ij}	The vorticity tensor
y	The distance normal to the wall
y^+	The local coordinate
$\mathbf{I}$	The identity tensor
$\mathbf{T}^{(n)}$	The tensor basis

Greek Symbols

α The thermal diffusivity

δ_{ij} The Kronecker unit tensor

ϵ_{ijk} The permutation tensor

ν The kinematics viscosity

ν_t Eddy viscosity

ω The dissipation per unit turbulent kinetic energy or specific dissipation rate

Ω_{ij} The rotation tensor

ϕ_{ij} Redistribution tensor of Reynolds stress

Π_{ij} Velocity pressure-gradient correlation

ρ Density

τ_θ Time scale

ε The dissipation rate of turbulent kinetic energy

ε_{ij} Turbulent dissipation rate of Reynolds stress

ξ_i The normalized turbulent heat flux

Other Symbols

$\{\}$ The trace operation

Acronyms

AHFM Algebraic Heat Flux Model

ARSM Algebraic Reynolds Stress Model

CFD Computation Fluid Dynamics

DNS Direct Numerical Simulation

EVM Eddy Viscosity Models

LES Large Eddy Simulation

NLEVM Nonlinear Eddy Viscosity Models

RANS Reynolds averaged Navier-Stokes

Chapter 1

Introduction

1.1 General Background

The computation fluid dynamics (CFD) is widely used in aerodynamics, propulsion, power generation, pollution, automotive, electrical and civil engineering, as a tool of design, optimization, prediction of off-design performances of such industrial applications. Despite various other complexities, turbulence is the major obstacle for accurate and reliable CFD simulations. Turbulence can have positive or negative effects on the flow, the mixing, the dilution and the heat and mass transfer, and it is important for engineers to be able to predict the effects in the design process. Hence, the simulation of turbulence plays an essential part in most CFD calculations.

Three major techniques are nowadays in use for research and design purposes regarding turbulent fluid flows. Direct numerical simulation (DNS), which solves the Navier-Stokes equations together with the continuity equation without introducing any model, is able to represent all the details of the complex turbulent fluctuating motion. Although, it requires every large computational resource and time. In addition, the number of grid points and the cost required increase roughly with Re^3 (Pope, 2000), which limits the applicability of this approach to low or moderate Reynolds number and simple geometry flows. In large eddy simulations (LES), the larger three-dimensional unsteady turbulent motions are represented in a direct fashion, whereas, the effects of the smaller-scale motions are modeled. Accordingly, LES can be used to calculate relatively high Reynolds number flows, but the proper resolving the near-wall regions poses the problems, where a special near-wall treatment has to be introduced

(Rodi, 2006). Therefore, DNS and LES are nowadays mainly applied to low Reynolds number flows in simple geometry for scientific rather than practical purposes (Celik, 2005; Hadžić, 1999; Hanjalić, 2005*b*; Hellsten, 2004). It is noted that the DNS and LES have been a very useful tool on the development and validation of turbulence models by providing the very detailed description of fluid flow, also turbulent heat transfer. Particularly, with the aid of DNS and LES, a term-by-term modeling of the transport equation can be undertaken, which is not feasible from the experimental database. Additionally, the DNS and LES database can be used to develop the low Reynolds number models, which require a more sophisticated expression in the near-wall region.

The single-point statistical modeling of turbulence is nowadays the most widely spread approach to predict turbulent flows for practical purposes, which is the so-called Reynolds averaged Navier-Stokes (RANS) modeling. As a consequence, the second-moment correlations of fluctuating quantities appear in the RANS equations. By the level at which these correlations are modeled, several approaches have been developed. A mathematically and physically well founded approach in the framework of RANS modeling is the second moment closure, from which the second moment correlations obtain their solution from differential transport equations. The eddy viscosity models (EVM) relate the unknown Reynolds stresses to mean flow parameters, such as velocity gradients, and an eddy viscosity ν_t. The eddy viscosity can be seen essentially as product of characteristic velocity scale and corresponding length scale. This type of turbulent models is thought to be most widely used turbulence one in practical applications, although some serious fundamental deficiencies have been well documented in the literature. The nonlinear eddy viscosity models (NLEVM) and the Algebraic models, currently still under development, are a promising way to overcome the deficiencies of conventional EVMS. Particularly, much research effort has been paid to the further development of algebraic models, and it is suggested that long-term research should be supported on algebraic models (Johansson, 2002).

As pointed out by Hanjalić (2005*b*), an industrial user nowadays has very broad options of the available RANS models, which is reversely making users more difficult to make a choice in regard to which models should be used for which application. Paradoxically, there seems to be not much incentive for fundamental research in the conventional RANS modeling facing various needs for innovation. Among those research activities, some interesting directions may be identified, such as the elliptic

blending model (Manceau, 2005), the new wall function (Craft *et al.*, 2004), the further improvement of algebraic models (Gatski & Wallin, 2004; Hamba, 2006), et. al. Additionally, some new approaches, which seem to depart from the conventional RANS strategies have attracted more research activities, such as unsteady RANS, multi-scale RANS, transient RANS, hybrid RANS/LES, and so on, which are supposed to bring better physical justification and feasibility.

However, it may be noticed that some key issues concerning the basic performance of RANS models have still remained, such as the modeling of pressure-strain rate, modeling of pressure transport term. With further study, the improvement of such model can advance the RANS modeling fundamentally.

1.2 Introduction of ARSM

Among various RANS approaches, the eddy viscosity model (EVM) has received the most consideration and has been applied to many problems, due to its simple form and affordable computation cost. However, an EVM eventually fails to represent many complex features of turbulent flows. The differential Reynolds stress models (DRSM) include significantly more flow physics, and its application to complex flows is an active area of research (Haase *et al.*, 2006). In parallel with such efforts, there is a considerable renewed interest in developing the algebraic approximations for transport equations of anisotropy tensor (Johansson, 2002), which is the so-called algebraic Reynolds stress model.

The explicit algebraic Reynolds stress model (EARSM) has been considered as an alternative to EVM. Positioned at an intermediate level between EVM and DRSM, the EARSM extends the linear Boussinesq hypothesis by introducing a more general polynomial representation that should allow for the prediction of more complex flow physics. This general algebraic relation is obtained by first simplifying the differential transport equation for the Reynolds stress anisotropy tensor. This simplification results in a corresponding implicit algebraic equation (ARSM) for the Reynolds stress anisotropy components. The EARSM is then obtained from a tensor polynomial representation of the anisotropy components whose terms are functions of the strain rate and vorticity tensors as well as additional scalar parameters. The EARSM thus inherits the

simplicity and (some level of) robustness of the eddy viscosity models but also retains the potential for representing the turbulence anisotropy.

The general weak-equilibrium condition (Rodi, 1972, 1976) is used to derive the implicit ARSM from the differential transport equation of Reynolds stress anisotropy. The equilibrium state is of such state that the production equals dissipation with negligible convective and transport effects. For flows away this state, Rodi introduced the more general weak-equilibrium assumption, which is the advection and diffusive transport in $\overline{u_i u_j}$ are proportional to that of the k. For the mean convection term, this condition assumes that mean flow advection in inertial flows for the Reynolds stress anisotropy tensor b_{ij} ($= \tau_{ij}/2k - \delta_{ij}/3$) is zero,

$$\frac{Db_{ij}}{Dt} = 0 \ , \tag{1.1}$$

where $\tau_{ij} = \overline{u_i u_j}$. For the diffusive transport term, the weak-equilibrium condition yields that the entire transport term of τ_{ij} is proportional to that of the turbulent kinetic energy k, that is

$$\mathcal{D}_{ij} - \frac{\tau_{ij}}{k}\mathcal{D} = 0, \tag{1.2}$$

where $\mathcal{D}_{ij}$ represents the entire transport term of the Reynolds stress. It can be partitioned and written as

$$\begin{aligned} \mathcal{D}_{ij} &= \mathcal{D}^t_{ij} + \mathcal{D}^p_{ij} + \mathcal{D}^\nu_{ij} \\ &= -\frac{\partial}{\partial x_k}\overline{u_i u_j u_k} - \frac{\partial}{\partial x_k}\left(\overline{\frac{p}{\rho}u_i}\delta_{jk} + \overline{\frac{p}{\rho}u_j}\delta_{ik}\right) + \nu\nabla^2\tau_{ij} \ , \end{aligned} \tag{1.3}$$

where $\mathcal{D}^t_{ij}$ is the turbulent transport, $\mathcal{D}^p_{ij}$ is the pressure transport and $\mathcal{D}^\nu_{ij}$ is the viscous diffusion, with $\mathcal{D} = \mathcal{D}_{ii}/2$ in Eq. (1.2). The current study focuses on the weak-equilibrium condition associated with Eq. (1.2).

The validity of the weak-equilibrium condition greatly depends on the nature of the flow. When the spatial change of the turbulent flow is moderate and the energy balance is in equilibrium, this assumption is well supported. However, in formulating implicit ARSM equations in flows relative to non-inertial frames or with flow curvature, this assumption does not hold. As originally suggested by Rodi & Scheuerer (1983), a generalized condition that can include the effects of system rotation or streamline curvature becomes necessary in order to accurately predict such flows (Rumsey *et al.*, 2001, 2000).

The weak-equilibrium condition associated with Eq. (1.1) has been the focus of some recent studies that have attempted to develop the appropriate form for the anisotropy equilibrium assumption in both non-inertial frames and fields where streamline curvature effects persist (Gatski & Jongen, 2000; Gatski & Wallin, 2004; Girimaji, 1997; Hamba, 2006; Wallin & Johansson, 2002). Wallin & Johansson (2002), Gatski & Wallin (2004) and Hamba (2006) have all recently shown that the condition $Db_{ij}/Dt + \Omega_{ik}b_{kj} - b_{ik}\Omega_{kj} = 0$ in the non-inertial frame is incorrect where Ω_{ij} is the rotation rate tensor associated with the angular rotation rate vector ω_m of the non-inertial frame coordinates, and the extra term $\Omega_{ik}b_{kj} - b_{ik}\Omega_{kj}$ is necessary to include the motion of flow itself. Therefore, the appropriate form for the anisotropy equilibrium assumption in the non-inertial frames are $Db_{ij}/Dt = 0$. Hamba (2006) has also pointed out that the extended assumption of anisotropy equilibrium can also be objective if the co-rotational derivative is introduced.

The second assumption (Eq. (1.2)), based on constraints applicable to the entire transport term (Gatski & Rumsey, 2001), is also necessary in deriving the implicit algebraic Reynolds stress equations. However, this assumption has received much less attention since it becomes important only in near-wall regions of inhomogeneous turbulent flows and is less amenable to analysis than the condition on the Reynolds stress anisotropy itself. Nevertheless, system rotation and streamline curvature can greatly influence the diffusion and transport process of turbulent flows. This can be observed from the DNS and LES (Andersson & Kristoffersen, 1993; Grundestam *et al.*, 2008; Kim *et al.*, 1987; Kristoffersen & Andersson, 1993; Lamballais *et al.*, 1998) of rotating turbulent channel flow. This suggests that the question of whether the current assumption for diffusive transport can hold in flows involving rotation and curvature effects should be investigated.

1.3 Introduction of AHFM

There are currently considerable research activities directed toward developing the model for the prediction of heat transfer in turbulent flows. With the similar reason of ARSM, the interest on deriving the algebraic approximation approach has been increasing for predicting turbulent heat transfer. Numerous works have been devoted to develop the sophisticate algebraic model for turbulent heat flux, such as Abe &

Suga (2001); Dol *et al.* (1997); Hattori *et al.* (2006); Lai & So (1990); Rogers *et al.* (1989); Rokni (2000); Shabany & Durbin (1997); So & Sommer (1996), among others. Recently, Wikström *et al.* (2000) showed that the systematic modeling approach of forming implicit algebraic relation for turbulent heat flux and proposed a method to obtain the fully explicit form out of an implicit relation by using Caylay-Hamilton theorem for two- and three-dimensional flows. So *et al.* (2004) presented the method to derive an explicit algebraic model for two-dimensional incompressible non-isothermal turbulent flows with the aid of tensor representation theory. The works mentioned above contribute to the development of algebraic model for turbulent heat flux, while those works are limited to flows in the inertial frames. Consequently, the appropriate form of algebraic model for turbulent heat flux in the non-inertial frames has been left unexplored.

The general algebraic relation is first obtained by a simplification of the differential transport equations of turbulent heat flux by invoking the weak-equilibrium condition. Analogous to the derivation of ARSM, this weak equilibrium condition assumes that the advection of turbulent normalized heat flux is zero. The original advection assumption is only valid for inertial frames. As for the non-inertial frames, the proper form of this assumption is left unexplored. The same issue encountered for the derivation of algebraic model for Reynolds stress anisotropies has been well resolved by invoking the frame-invariant concept to account for rotation and curvature effects correctly (Gatski, 2004; Gatski & Wallin, 2004; Girimaji, 1997; Hamba, 2006; Speziale, 1998, 1979; Weis & Hutter, 2003). As pointed out by Hamba (2006), the frame-invariant property is not only the requirement for mathematical description of turbulent flow, it also serves as highly useful constraint and tool to form constitutive equations (Hamba, 2006; Speziale, 1998). By invoking the frame-invariant concept, the resultant constitutive equations for Reynolds stress anisotropies are independent of the reference frames, whether inertial or non-inertial. It has been shown that the resultant frame-invariant algebraic model for Reynolds stress anisotropies is capable to include the system rotation and streamline curvature effects (Gatski & Wallin, 2004; Jongen *et al.*, 1998*a*,*b*). Thus, it is straightforward to extend this methodology to the modeling of turbulent heat flux in non-inertial frames. By applying this frame-invariant constraint, a reference frame free algebraic heat flux model can be derived, which accounts for the system rotation and streamline curvature effects. Nagano & Hattori (2003) gave

the assessment of explicit expression for turbulent heat flux. It is readily observed that the algebraic formulation employed for turbulent heat flux in their work is not frame invariant. As a matter of fact, the rotation effects are not fully accounted for. The above example shows that frame invariant constraint is an omissible constraint for formulating the algebraic models for turbulent heat flux.

Moreover, the weak-equilibrium condition assumes that the diffusion and transport in the budget of turbulent normalized heat flux equation are negligible. This treatment is known as the diffusive transport constraint. As another constraint to derive the AHFM, the diffusive transport constraint removes the differential terms, which are associated with the diffusion and transport processes. Obviously, its validity is crucial for resulting an accurate AHFM. Wikström *et al.* (2000) investigated the validity of diffusive transport constraint by comparing the characteristic magnitudes of individual terms in the transport equation for turbulent normalized heat flux. They concluded that the diffusive transport constraint is appropriate for the streamwise component except near the wall. For the wall-normal component, this constraint is not well supported even in the center of the channel. However, their work was limited in the inertial frames, the validity of this constraint in the non-inertial frames certainly needs to be investigated further, for AHFM be applied to flows involving rotation and curvature effects.

1.4 The objective

The present study aims at the development of algebraic models for prediction of Reynolds stresses and turbulent heat fluxes. By using DNS data, the detailed behavior of each term in the transport equations of Reynolds stresses and turbulent heat fluxes for the near-wall region is understood through the budget and asymptotic analyses. Such understanding gives the possibilities to assess and modified the diffusive transport constraints, which are important in the derivation of algebraic models both for Reynolds stresses and turbulent heat fluxes. In addition, the frame invariant concept is invoked in this study to extend the original advection assumption for flows associated with rotation and curvature effects. Moreover, the frame invariant form of AHFM is derived by using the extended weak-equilibrium condition.

1.5 Outline

A general review of turbulent flows, concerning the concept of RANS modeling is first given in chapter 2. In this chapter, it contains an outline of the turbulence models beginning with a brief introduction about the statistical modeling both for turbulent Reynolds stresses and heat fluxes. Several modeling approaches are discussed in the framework of the second-moment turbulence closure. Special attention is paid to the algebraic model, which is becoming more favorable for engineering flows.

In chapter 3, some computational examples by differential Reynolds stress model, nonlinear eddy viscosity model and linear viscosity model, as well as some critical observations, are provided for the case of fully developed rotating channel flow. By these examples, the ability of representing the rotation effects, which appears usually important in the practical applications, is revealed.

Chapter 4 presents the study on the assessment and modification of diffusive transport constraint for derivation of algebraic Reynolds stress models. This study focuses on the validity and modification of the diffusive transport assumption in fully developed rotating channel flow. This is accomplished by an *a priori* assessment using the DNS data of Kristoffersen & Andersson (1993).

In Chapter 5, it includes the work on the advancement of algebraic heat flux model. The weak equilibrium condition is assessed, and a tempt is made to extend the weak equilibrium condition to noninertial frames. An alternative form of diffusive transport constraint is proposed and evaluated using DNS data.

Finally, conclusions drawn from the range of present study as well as perspectives for future work are given in Chapter 5.

Chapter 2

The Second-Moment Turbulence Modeling

2.1 Modeling of turbulent Reynolds stresses

The instantaneous velocity and pressure fields in an impressible turbulent flow under isothermal conditions are solutions of the instantaneous continuity and Navier-Stokes equations given by

$$\frac{\partial \hat{U}_i}{\partial x_i} = 0, \tag{2.1a}$$

$$\frac{\partial \hat{U}_i}{\partial t} + \hat{U}_k \frac{\partial \hat{U}_i}{\partial x_k} = -\frac{1}{\rho}\frac{\partial \hat{P}}{\partial x_i} + \nu \frac{\partial^2 \hat{U}_i}{\partial x_k \partial x_k}, \tag{2.1b}$$

where ρ and ν are density and kinematic viscosity of the fluid, $\hat{U}_i$ are instantaneous velocity vector components and $\hat{P}$ is the instantaneous pressure. According to the Reynolds-averaged approach, the instantaneous velocity and pressure are decomposed into a time mean and a fluctuating part give by

$$\hat{U}_i = U_i + u_i, \quad \hat{P} = P + p, \tag{2.2}$$

where the capital symbols (U_i, P) represent a time mean and the lower-case symbols (u_i, p) represent the fluctuating part. This averaging leads to the Reynolds-averaged continuity equation and the Reynolds-averaged Navier-Stokes (RANS) equations for

incompressible isothermal turbulent flow of a Newtonian fluid, which can be written as (Durbin & Pettersson, 2001)

$$\frac{\partial U_i}{\partial x_i} = 0, \tag{2.3a}$$

$$\frac{\partial U_i}{\partial t} + U_j \frac{\partial U_i}{\partial x_j} = -\frac{1}{\rho}\frac{\partial P}{\partial x_i} + \nu \nabla^2 U_i - \frac{\partial \overline{u_i u_j}}{\partial x_j}. \tag{2.3b}$$

Eq. (2.3b) can be rearranged to arrive at a well-known form

$$\frac{\partial U_i}{\partial t} + U_j \frac{\partial U_i}{\partial x_j} = -\frac{1}{\rho}\frac{\partial P}{\partial x_i} + \frac{1}{\rho}\frac{\partial}{\partial x_j}\left(\mu \frac{\partial U_i}{\partial x_j} - \rho \overline{u_i u_j}\right), \tag{2.4}$$

where the terms, $-\rho\overline{u_i u_j}$, are collected with the traditional normal and shear stress terms $\mu \partial U_i / \partial x_j$. By this way, it is readily to tell that the averaged effect of turbulent advection, $-\rho\overline{u_i u_j}$ has the similar mathematical representation form as the viscous stress $\mu(\partial U_i/\partial x_j + \partial U_j/\partial x_i)$ and they are both second tensor variables. This fact indicates that these two terms may be controlled by the similar mechanism. Therefore, $-\rho\overline{u_i u_j}$ is generally treated as a "stress" also, namely *Reynolds stress*. Even though this apparent stress is $-\rho\overline{u_i u_j}$, it is convenient and conventional to refer to $\overline{u_i u_j}$ as the Reynolds stress.

The extract transport equation for Reynolds stress tensor $\overline{u_i u_j}$ is given as

$$\frac{D\overline{u_i u_j}}{Dt} = P_{ij} + \phi_{ij} + \mathcal{D}^{\nu}_{ij} + \mathcal{D}^{t}_{ij} + \mathcal{D}^{p}_{ij} - \varepsilon_{ij}, \tag{2.5}$$

where the right-side represents the rate of change of τ_{ij} produced by the turbulent production P_{ij}, the redistribution ϕ_{ij}, the viscous diffusion $\mathcal{D}^{\nu}_{ij}$, the turbulent transport $\mathcal{D}^{t}_{ij}$, the pressure transport $\mathcal{D}^{p}_{ij}$ and the turbulent dissipation rate ε_{ij}. These terms are

given by

$$P_{ij} = -\left(\overline{u_i u_k}\frac{\partial U_j}{\partial x_k} + \overline{u_j u_k}\frac{\partial U_i}{\partial x_k}\right), \tag{2.6a}$$

$$\phi_{ij} = \overline{\frac{p}{\rho}\left(\frac{\partial u_i}{\partial x_j} + \frac{\partial u_j}{\partial x_i}\right)}, \tag{2.6b}$$

$$\mathcal{D}^{\nu}_{ij} = \frac{\partial}{\partial x_k}\nu\frac{\partial \overline{u_i u_j}}{\partial x_k}, \tag{2.6c}$$

$$\mathcal{D}^{t}_{ij} = -\frac{\partial}{\partial x_k}\overline{u_i u_j u_k} - \frac{\partial}{\partial x_k}\overline{u_i u_j u_k}, \tag{2.6d}$$

$$\mathcal{D}^{p}_{ij} = -\frac{\partial}{\partial x_k}\left(\overline{\frac{p}{\rho}u_i}\delta_{jk} + \overline{\frac{p}{\rho}u_j}\delta_{ik}\right), \tag{2.6e}$$

$$\varepsilon_{ij} = 2\nu\overline{\frac{\partial u_i}{\partial x_k}\frac{\partial u_j}{\partial x_k}}. \tag{2.6f}$$

Note that in the incompressible form of the $\overline{u_i u_j}$ equations, it is customary to decompose the velocity pressure-gradient correlation Π_{ij} into a term ϕ_{ij} that represents redistribution of energy among the components and a term $\mathcal{D}^{p}_{ij}$ that represents the pressure-related transport:

$$\begin{aligned}\Pi_{ij} =& \phi_{ij} + \mathcal{D}^{p}_{ij} \\ =& -\left(\overline{\frac{1}{\rho}u_i\frac{\partial p}{\partial x_j}} + u_i\frac{\partial p}{\partial x_j}\right).\end{aligned}$$

The annotations for the terms in the budgets of Reynolds stress transport equation, Eq. (2.5) indicate physical interpretations.

- **Production** P_{ij} This term represents the rate at which the energy is transferred from mean flow to turbulent fluctuations.

- **Redistribution** ϕ_{ij} The terminology, redistribution, implies that it redistribute the energy among components of Reynolds stresses without altering the total energy. The fact that the trace of this term is zero also proves its role. The qualitative effect of redistribution is to shift the energy from the larger components of $\overline{u_i u_j}$ into smaller ones, which makes the flow tend to be isotropic.

- **Viscous diffusion** $\mathcal{D}^{\nu}_{ij}$ This term transports the energy in space by molecular process. This transport is in a conservative way, without generating or destroying the energy.

- **Turbulent transport** $\mathcal{D}_{ij}^t$ The physical effect of the transport term is to spread the Reynolds stresses in space. Since turbulent transport can be expressed with the divergence of the flux, it is also a conservative term.

- **Pressure transport** $\mathcal{D}_{ij}^p$ This term is named as transport term since it is also of conservative form. However, this is a quite ambiguous terminology since pressure effects are non-local and instantaneous, while transport occurs slowly, down local gradients.

- **Dissipation rate** ε_{ij} This term represents the decay of the turbulence, which implies that it dissipates the energy of turbulence into heat. The components of ε_{ij} allow individual components of Reynolds stresses to dissipate at a different rate.

For the practice of turbulence modeling, the equations for turbulent kinetic energy k and its dissipation rate ε are usually involved. The equations for k and ε define the dynamics of turbulent kinetic energy, and illustrate the major physical mechanisms in a turbulent flow within the framework of Reynolds-averaging approach.

The exact k equation is derived by taking the half of the trace of Eq. (2.5):

$$\frac{Dk}{Dt} = P + \mathcal{D} - \varepsilon, \tag{2.7}$$

where the turbulent kinetic energy $k = 1/2\overline{u_i u_i}$. The terms on the right-hand side P, $\mathcal{D}$ and ε, can be interpreted as production of k, diffusion/transport of k and dissipation rate of k, which are (Hanjalić, 2005*a*)

$$P = -\overline{u_i u_j}\frac{\partial U_i}{\partial x_j}, \tag{2.8a}$$

$$\mathcal{D} = \frac{\partial}{\partial x_j}\left(\nu\frac{\partial k}{\partial x_j} - \frac{1}{2}\overline{u_i u_j u_j} - \frac{1}{\rho}\overline{p u_i}\right), \tag{2.8b}$$

$$\varepsilon = \nu\overline{\left(\frac{\partial u_i}{\partial x_j}\right)^2}. \tag{2.8c}$$

The exact ε equation is given by (Mansour *et al.*, 1988)

$$\frac{D\varepsilon}{Dt} = P_\varepsilon^1 + P_\varepsilon^2 + P_\varepsilon^3 + P_\varepsilon^4 + \mathcal{D}_\varepsilon^\nu + \mathcal{D}_\varepsilon^t + \mathcal{D}_\varepsilon^p - Y, \tag{2.9}$$

where the dissipation rate of kinetic energy $\varepsilon = 1/2\varepsilon_{ii}$. The different terms on the right-hand side of Eq. (2.9) can be identified as

$$P_\varepsilon^1 = -2\nu\overline{\frac{\partial u_i}{\partial x_l}\frac{\partial u_k}{\partial x_l}\frac{\partial U_i}{\partial x_k}} \quad \text{Mixed Production,} \tag{2.10a}$$

$$P_\varepsilon^2 = -2\nu\overline{\frac{\partial u_l}{\partial x_i}\frac{\partial u_l}{\partial x_k}\frac{\partial U_i}{\partial x_k}} \quad \text{Production by mean velocity gradient,} \tag{2.10b}$$

$$P_\varepsilon^3 = -2\nu\overline{u_k\frac{\partial u_i}{\partial x_l}\frac{\partial^2 U_i}{\partial x_k \partial x_l}} \quad \text{Gradient production,} \tag{2.10c}$$

$$P_\varepsilon^4 = -2\nu\overline{\frac{\partial u_i}{\partial x_k}\frac{\partial u_i}{\partial x_l}\frac{\partial u_k}{\partial x_l}} \quad \text{Turbulent production,} \tag{2.10d}$$

$$\mathcal{D}_\varepsilon^\nu = \frac{\partial}{\partial x_k}\nu\frac{\partial \varepsilon}{\partial x_k} \quad \text{Viscous diffusion,} \tag{2.10e}$$

$$\mathcal{D}_\varepsilon^t = -\frac{\partial}{\partial x_k}\overline{u_k\varepsilon} \quad \text{Turbulent transport,} \tag{2.10f}$$

$$\mathcal{D}_\varepsilon^p = -\frac{\partial}{\partial x_k}\left(\frac{2\nu}{\rho}\overline{\frac{\partial p}{\partial x_i}\frac{\partial u_k}{\partial x_i}}\right) \quad \text{Pressure transport,} \tag{2.10g}$$

$$Y = -2\overline{\left(\nu\frac{\partial^2 u_i}{\partial x_k \partial x_l}\right)} \quad \text{Dissipation.} \tag{2.10h}$$

It has been shown that the Reynolds-averaged Navier-Stokes equations contain undefined variables (second moments $\overline{u_i u_j}$) as a consequence of averaging previously. To close the equation set, these variables need to be supplemented. In order to overcome this problem, the transport equations of Reynolds stresses, Eq. (2.5), of kinetic energy, Eq. (2.7) and of dissipation rate, Eq. (2.9) are introduced. The transport equations for the second moments contain some terms of third moments. The transport equations for third moments can also be derived by multiplying the transport equation of second moments $\overline{u_i u_j}$ with the fluctuating velocity u_k and averaging, which includes terms of higher-order moments. This problem is known as the *Turbulence Closure Problem*.

The development of turbulent closure models with the framework of Reynolds-averaged Navier-Stokes approach has been the subject of intense study and numerous reviews (Gatski, 2004; Reynolds, 1976; Speziale, 1991). A significant number of closure models have been proposed, which range from the simple algebraic specification of turbulent velocity and length scales to the solution of full differential transport models. Basically, there are three levels of closure models currently employed in the community of computational fluid dynamics: eddy-viscosity model, algebraic model

and differential Reynolds stress model. These three levels of modeling strategy will be introduced in the following sections.

2.1.1 Differential Reynolds stress model

Differential Reynolds Stress Model (DRSM) is virtually the most natural and logical level in the framework of Reynolds-averaged Navier-Stokes approach. The DRSM aims to obtain a numerically solvable set of transport equations for each Reynolds stress component and the dissipation rate of kinetic energy. This is quite attractive in principle, since all the physical processes governing the evolution of the Reynolds stresses are included in the equations. Among those processes, the very important production term and also the advection by mean flow can be employed without any modeling. This is the main motivation of the DRSM approach (Hellsten, 2004). On the other hand, some other higher-order correlations, which are very important for evolution of the Reynolds stresses, have to be modeled. The modeling of these terms basically consists of the subject of developing DRSM. To model these terms appropriately, the proper physical understanding, the religious mathematical description and the rational assumption are necessary most of the time. It is argued that the DRSMs do not show always an indisputable superiority over other levels of models. One of the reasons is that more terms need to be modeled. While this offers a better opportunity to include the important processes, the advantage may be annulled if some of the terms are modeled wrongly (Hanjalić, 2005*a*).

The basic concepts of the DRSM were defined by Chou (1945) earlier, then Rotta made an important and lasting contribution as RS model (Rotta, 1951). In the 1970s, the DRSM gained more attention in the wake of the important work by Hanjalić & Launder (1972) and Launder *et al.* (1975). Since those years, many researchers have contributed to this field and proposed numerous models. The modeling work involves combinations of physical insight and assumptions on the specific term's behavior with some self-consistent mathematical descriptions to obtain an expression of the term, which is explicit in the certain dependent variables, that is Reynolds stresses $\overline{u_i u_j}$, mean velocity U_i, strain-rate tensor S_{ij}, vorticity tensor W_{ij}, kinetic energy k and its dissipation rate ε.

The definitions for S_{ij} and W_{ij} are as following

$$S_{ij} = \frac{1}{2}\left(\frac{\partial U_i}{\partial x_j} + \frac{\partial U_j}{\partial x_i}\right), \tag{2.11}$$

$$W_{ij} = \frac{1}{2}\left(\frac{\partial U_i}{\partial x_j} - \frac{\partial U_j}{\partial x_i}\right). \tag{2.12}$$

Note that the sum of symmetric strain-rate tensor S_{ij} and antisymmetric vorticity tensor W_{ij} is the velocity gradient tensor ($S_{ij} + W_{ij} = \partial U_i/\partial x_j$).

In the exact transport equation for Reynolds stresses, Eq. (2.5), the production term (P_{ij}) can be treated exactly, while certain models are required for the dissipation term (ε_{ij}), diffusion/transport term ($\mathcal{D}_{ij}$) and redistribution term (ϕ_{ij}). Extensive research effort has been given to the modeling of above terms. In the following chapter, an example will be given to illustrate the details of DRSM for the case of fully developed rotating channel flow.

2.1.2 Algebraic Reynolds stress model

Among various RANS approaches, the eddy viscosity model (EVM) has received the most consideration and has been applied to many problems, due to its simple form and affordable computation cost. However, an EVM eventually fails to represent many complex features of turbulent flows. The differential Reynolds stress models (DRSM) include significantly more flow physics, but the application to industrial flows is still challenging (Haase *et al.*, 2006). Faced with higher demands on prediction accuracy in more complex flow situations, the need for more accurate and efficient RANS models has become important.

The explicit algebraic Reynolds stress model (EARSM) has been considered as an alternative to EVM. Positioned at an intermediate level between EVM and DRSM, the EARSM extends the linear Boussinesq hypothesis by introducing a more general polynomial representation that should allow for the prediction of more complex flow physics. This general algebraic relation is obtained by first simplifying the differential transport equation for the Reynolds stress anisotropy tensor. This simplification results in a corresponding implicit algebraic equation (ARSM) for the Reynolds stress anisotropy components. The EARSM is then obtained from a tensor polynomial representation of the anisotropy components whose terms are functions of the strain rate and

vorticity tensors as well as additional scalar parameters. The EARSM thus inherits the simplicity and (some level of) robustness of the eddy viscosity models but also retains the potential for representing the turbulence anisotropy.

Algebraic Reynolds stress models are written directly in terms of the turbulent stresses and therefore do not rely on the Boussinesq approximation. This enables these models to predict some degree of anisotropy compared to the eddy viscosity model. Whereas, when applying the implicit algebraic model to the two- or three-dimensional flow, one usually finds some numerical issues raised. This is because that the equation system of algebraic relations needs to be solved directly for the Reynolds stresses, especially there are no diffusive terms contained in the algebraic Reynolds stress model. To alleviate the above numerical difficulties, much effort has been devoted to the development of explicit algebraic Reynolds stress models. However, a lot of mathematical steps are necessary to make the algebraic relations explicit. The benefit to performing all of these additional works during the formulation of the model is that resultant explicit algebraic stress models provide a significant cost savings compared to the differential equations of the full Reynolds stress model.

The very first ARSM in turbulent flow was developed by Rodi (1976) from DRSM equations. The following developments of ARSM were concentrated on the explicit form of the algebraic relations. As will shown in later section, the nonlinearity of implicit algebraic relations forms the major obstacle to derive explicit ARSM and the studies so far differ mainly by the treatment of production-dissipation ration P/ε appearing in the implicit form of ARSM. Accordingly, the model proposal can be catalogized into three major approaches.

Implicit P/ε

Pope (1975) proposed the idea of using ten tensor groups to form a consistent explicit relation was proposed, as well as the relation for two-dimensional flow with leaving the production-dissipation ration (P/ε) in the implicit form. This approach was later extended and solved for three-dimensional flows by Taulbee (1992), Taulbee *et al.* (1994).

Universal constant for P/ε

A different approach was taken by Gatski & Speziale (1993), where the equilibrium value for P/ε in homogeneous shear flow was assumed to be a universal constant. Thus this model is considered only exactly self-consistent in equilibrium homo-

geneous shear flow and might be inconsistent to extend this model beyond the equilibrium flows. Actually, the assumption of a constant P/ε resulted in a model that produces the wrong asymptotic behavior in rapid distorted flows and also may become singular under some circumstances. Therefore, some additional corrections have been proposed, such as Gatski & Speziale (1993), Speziale & Xu (1996), Rumsey *et al.* (1999), Jongen & Gatski (1998*a*), Antonello & Masi (2007), to improve the consistency condition. Extensions of EARSMs to account for anisotropic dissipation rate have been proposed by Xu & Speziale (1996), and extended to inhomogeneous flows by Jongen *et al.* (1998*a*).

Solving P/ε

The P/ε can be obtained by solving a third-order polynomial equation for two-dimensional flows, as proposed by Girimaji (1996), Johansson & Wallin (1996), Wallin & Johansson (2000) extended it to the compressible flow. The rotation and curvature effects are included by Wallin & Johansson (2002). Grundestam *et al.* (2005*b*), Grundestam *et al.* (2005*a*) derived the EARSM based on a nonlinear pressure strain-rate model. In this approach, the solution for two-dimensional flows are extended to three-dimension as first approximation.

2.1.2.1 Weak-equilibrium condition

As a matter of fact, the derivation of three mentioned above ARSMs has to invoke the weak-equilibrium assumption inevitably. The general weak-equilibrium condition (Rodi, 1972, 1976) is used to derive the implicit ARSM from the differential transport equation of Reynolds stress anisotropy. For the mean convection term, this condition assumes that mean flow advection in inertial flows for the Reynolds stress anisotropy tensor b_{ij} ($= \tau_{ij}/2k - \delta_{ij}/3$) is zero,

$$\frac{Db_{ij}}{Dt} = 0 \,, \tag{2.13}$$

where $\tau_{ij} = \overline{u_i u_j}$. Note that the Reynolds stress anisotropy tensor b_{ij} here is different from previously used a_{ij}, and the relation between this two parameters is $2b_{ij} = a_{ij}$. Both of them are used widely for the turbulence modeling in the framework of Reynolds-averaged approach. For the diffusive transport term, the weak-equilibrium

condition yields that the entire transport term of τ_{ij} is proportional to that of the turbulent kinetic energy k, that is

$$\mathcal{D}_{ij} - \frac{\tau_{ij}}{k}\mathcal{D} = 0, \tag{2.14}$$

where $\mathcal{D}_{ij}$ represents the entire transport term of the Reynolds stress. It can be partitioned and written as

$$\begin{aligned} \mathcal{D}_{ij} &= \mathcal{D}^t_{ij} + \mathcal{D}^p_{ij} + \mathcal{D}^\nu_{ij} \\ &= -\frac{\partial}{\partial x_k}\overline{u_i u_j u_k} - \frac{\partial}{\partial x_k}\left(\overline{\frac{p}{\rho}u_i}\delta_{jk} + \overline{\frac{p}{\rho}u_j}\delta_{ik}\right) + \nu\nabla^2\tau_{ij}\ , \end{aligned} \tag{2.15}$$

where $\mathcal{D}^t_{ij}$ is the turbulent transport, $\mathcal{D}^p_{ij}$ is the pressure transport and $\mathcal{D}^\nu_{ij}$ is the viscous diffusion, with $\mathcal{D} = \mathcal{D}_{ii}/2$ in Eq. (2.14).

The validity of the weak-equilibrium condition greatly depends on the nature of the flow. When the spatial change of the turbulent flow is moderate and the energy balance is in equilibrium, this assumption is well supported. However, in formulating implicit ARSM equations in flows relative to non-inertial frames or with flow curvature, this assumption does not hold. As suggested by Rodi & Scheuerer (1983), a generalized condition that can include the effects of system rotation or streamline curvature becomes necessary in order to accurately predict such flows (Rumsey *et al.*, 2001, 2000). In the later section, more detailed discussion will be addressed on this issue.

2.1.2.2 Rodi ARSM

Virtually, Rodi's ARSM (Rodi, 1976) is the starting basis of many other ARSMs developed later, therefore, it will briefly reviewed here. Rodi postulated that

$$\frac{D\tau_{ij}}{Dt} - \frac{\tau_{ij}}{k}\frac{Dk}{Dt} = 0, \tag{2.16a}$$

$$\mathcal{D}_{ij} - \frac{\tau_{ij}}{k}\mathcal{D} = 0, \tag{2.16b}$$

where the $\tau_{ij} = \overline{u_i u_j}$ is the Reynolds stress tensor. Note that the Eq. (2.16a) is equivalent with Eq. (2.13). By invoking the above weak equilibrium condition, one has

$$\frac{D\tau_{ij}}{Dt} = P_{ij} + \phi_{ij} - \varepsilon_{ij} = \frac{\tau_{ij}}{k}\left(P - \varepsilon\right). \tag{2.17}$$

Rodi (1976) proposed a set of simultaneous algebraic equations for modeling τ_{ij} using the model of Launder *et al.* (1975)for ϕ_{ij} and the isotropic model for ε_{ij}, that is

$$\frac{\tau_{ij}}{k}(P-\varepsilon) = P_{ij} - C_1\frac{\varepsilon}{k}\left(\tau_{ij} - \frac{2}{3}\delta_{ij}k\right) - C_2\left(P_{ij} - \frac{2}{3}\delta_{ij}P\right) - \frac{2}{3}\varepsilon\delta_{ij}. \tag{2.18}$$

By rearranging the above equation, one has

$$\tau_{ij} = k\left[\frac{2}{3}\delta_{ij} + \frac{1-C_2}{C_1 - 1 + P/\varepsilon}\frac{\left(P_{ij} - \frac{2}{3}\delta_{ij}P\right)}{\varepsilon}\right]. \tag{2.19}$$

For the Reynolds stress anisotropy tensor b_{ij}, Eq. (2.19) can be transformed as

$$b_{ij} = \frac{\frac{1}{2}(1-C_2)}{C_1 - 1 + P/\varepsilon}\frac{\left(P_{ij} - \frac{2}{3}\delta_{ij}P\right)}{\varepsilon}. \tag{2.20}$$

Eq. (2.20) implies that the Reynolds stress anisotropy tensor b_{ij} is directly proportional to the production anisotropy.

As can be seen, the τ_{ij} appears on both side of Eq. (2.20), which makes this ARSM implicit, therefore, this model is prone to instability in practical computations. For steady state problems, very small under-relaxation factor has to be used and for unsteady state problems, very small time step has to be used in order to obtain convergence (Taulbee (1992)). In addition, the second term of Eq. (2.19) may become singular , when its denominator $C_1 - 1 + P/\varepsilon$ approaches zero. To prevent this numerical instability, Rosenau (1989) proposed regularized version of Rodi's ARSM to overcome the possible singular behavior of Eq. (2.19). It can be concluded that the above-mentioned drawbacks coming along the implicity nature, will compromise the advantage of ARSM possessing. Naturally, pursuing the explicit formulation for τ_{ij} or b_{ij} becomes the major direction for developing ARSM, and two typical works will be reviewed in the following sections.

2.1.2.3 Gatski and Speziale ARSM

The differential transport equation for the Reynolds stress anisotropy tensor b_{ij} is given by (Gatski & Rumsey, 2001)

$$\begin{aligned}\frac{Db_{ij}}{Dt} &= \frac{1}{2k}\left(\frac{D\tau_{ij}}{Dt} - \frac{\tau_{ij}}{k}\frac{Dk}{Dt}\right)\\ &= -b_{ij}\left(\frac{P}{k}-\varepsilon\right) - \frac{2}{3}S_{ij} - \left(b_{ik}S_{kj} + S_{ik}b_{kj} - \frac{2}{3}b_{mn}S_{mn}\delta_{ij}\right)\\ &\quad + (b_{ik}W_{kj} - W_{ik}b_{kj}) + \frac{\phi_{ij}}{2k} + \frac{1}{2k}\left(\mathcal{D}_{ij} - \frac{\tau_{ij}}{k}\mathcal{D}\right)\,, \end{aligned} \tag{2.21}$$

where ϕ_{ij} is the pressure-strain rate correlation modeled by Speziale *et al.* (1991)

$$\begin{aligned}\phi_{ij} =& -\left(C_1^0 + C_1^1\frac{P}{\varepsilon}\right)\varepsilon b_{ij} + C_2 k S_{ij}\\ &+ C_3 k\left(b_{ik}S_{jk} + b_{jk}S_{ik} - \frac{2}{3}b_{mn}S_{mn}\right) - C_4 k\left(b_{ik}W_{kj} - W_{ik}b_{kj}\right)\,. \end{aligned} \tag{2.22}$$

By introducing the weak-equilibrium condition (Eqs. (2.13) and (2.14)) and substituting the pressure-strain correlation given by Eq. (2.22) into Eq. (2.21), one obtains the implicit form of the ARSM

$$\begin{aligned}0 =& -\frac{b_{ij}}{a_4} - a_3\left(b_{ik}S_{kj} + S_{ik}b_{kj} - \frac{2}{3}b_{mn}S_{mn}\delta_{ij}\right)\\ &- a_1 S_{ij} + a_2\left(b_{ik}W_{kj} - W_{ik}b_{kj}\right). \end{aligned} \tag{2.23}$$

The coefficients in this implicit form are given by

$$\begin{aligned} c_w &= \frac{C_4 - 4}{C_4 - 2}, \quad a_1 = \frac{2}{3} - \frac{C_2}{2},\\ a_2 &= 1 - \frac{C_4}{2}, \quad a_3 = 1 - \frac{C_3}{2},\\ a_4 &= \tau\left[\left(\frac{C_1^1}{2}+1\right)\frac{P}{\varepsilon} + \frac{C_1^0}{2} - 1\right]^{-1} = \tau\left[\gamma_1 + \gamma_0\frac{P}{\epsilon}\right]^{-1}, \end{aligned} \tag{2.24}$$

with $C_1^0 = 3.4$, $C_1^1 = 1.8$, $C_3 = 1.25$, $C_4 = 0.40$ and $\tau = k/\varepsilon$. These coefficients are obtained directly from the SSG pressure strain-rate correlation model.

Eq. (2.23) can be rewritten in matrix notation as

$$-\frac{1}{a_4}\mathbf{b} - a_3\left(\mathbf{bS} + \mathbf{Sb} - \frac{2}{3}\{\mathbf{bS}\}\mathbf{I}\right) + a_2\left(\mathbf{bW} - \mathbf{Wb}\right) = \mathbf{R}, \tag{2.25}$$

where $\{\}$ is the trace operation, e.g. $\{\mathbf{bS}\} = b_{ij}S_{ji}$. $\mathbf{I}$ is the identity tensor. For current linear pressure strain-rate model the isotropic dissipation rate, it follows that $\mathbf{R} = a_1\mathbf{S}$. However, the $\mathbf{R}$ can contain any known symmetric, traceless tensor (Jongen & Gatski, 1998*b*).

Eq. (2.23) forms the so-called implicit ARSM and can be solved by an interaction procedures numerically. However, such procedures can be numerically stiff for most of the cases, especially for the complex flow. Therefore, it is desirable to arrive at an explicit form of Eq. (2.23), still the algebraic character remains. The first attempt was done by Pope (1975), who proposed that a general expression for the tensor b_{ij} may be formed with S_{ij} and W_{ij} by using a three-term basis for two-dimensional flows. This form can be written as

$$\mathbf{b} = \sum_{n=1}^{3} \alpha_n \mathbf{T}^{(n)}, \tag{2.26}$$

where $\mathbf{T}^{(1)} = \mathbf{S}$, $\mathbf{T}^{(2)} = \mathbf{SW} - \mathbf{WS}$ and $\mathbf{T}^{(3)} = \mathbf{S}^2 - 1/3\,\{\mathbf{S}^2\}\,\mathbf{I}$ form the three-term integrity basis. The α_n are scalar expansion coefficients which need to be determined.

Eq. (2.25) can be solved by projecting this algebraic relation onto the tensor basis $\mathbf{T}^{(m)}$ itself. For this solution, the scalar product of Eq. (2.25) is formed with each of the tensors $\mathbf{T}^{(m)}$, $(m = 1, 2, ...N)$ (Gatski & Rumsey, 2001; Gatski & Speziale, 1993; Jongen, 1998). This procedure leads to the following system of equations:

$$\sum_{n=1}^{N} \alpha_n \Bigg[-\frac{1}{a_4}\left(\mathbf{T}^{(n)}, \mathbf{T}^{(m)}\right) - 2a_3\left(\mathbf{T}^{(n)}\mathbf{S}, \mathbf{T}^{(m)}\right) + 2a_2\left(\mathbf{T}^{(n)}\mathbf{W}, \mathbf{T}^{(m)}\right) \Bigg] = \left(\mathbf{R}, \mathbf{T}^{(m)}\right), \tag{2.27}$$

where the scalar product is defined as $\left(\mathbf{T}^{(n)}, \mathbf{T}^{(m)}\right) = \left\{\mathbf{T}^{(n)}\mathbf{T}^{(m)}\right\}$. In a more compact form

$$\sum_{n=1}^{N} \alpha_n \mathbf{A} = \left(\mathbf{R}, \mathbf{T}^{(m)}\right), \tag{2.28}$$

with $\mathbf{A}$ being the $N \times N$ matrix, whose definition for two-dimensional flow is

$$A_{nm} = \begin{bmatrix} -\frac{1}{a_4}\eta^2 & -2a_2\eta^4\mathcal{R}^2 & -\frac{1}{3}a_3\eta^4 \\ 2a_2\eta^4\mathcal{R}^2 & -\frac{2}{a_4}\eta^4\mathcal{R}^2 & 0 \\ -\frac{1}{3}a_3\eta^4 & 0 & -\frac{1}{6a_4}\eta^4 \end{bmatrix}. \tag{2.29}$$

The inversion of $\mathbf{A}$ leads to the following expressions for the representation coefficients

$$\alpha_1 = -\frac{a_4}{\alpha_0 \eta^2}\left(\{\mathbf{RS}\} + 2a_2 a_4 \{\mathbf{RWS}\} - 2a_3 a_4 \left\{\mathbf{RS}^2\right\}\right), \tag{2.30a}$$

$$\alpha_2 = a_4\left[a_2\alpha_1 + \frac{\{\mathbf{RWS}\}}{\eta^4 \mathcal{R}^2}\right], \tag{2.30b}$$

$$\alpha_3 = -a_4\left[a_3\alpha_1 + \frac{6\left\{\mathbf{RS}^2\right\}}{\eta^4}\right], \tag{2.30c}$$

where $\alpha_0 = 1 - 2a_3^2 a_4^2 \eta^2 + 2a_2^2 a_4^2 \eta^2 \mathcal{R}^2$, $\mathcal{R}^2 = -\{\mathbf{W}^2\}/\{\mathbf{S}^2\}$ and $\eta^2 = \{\mathbf{S}^2\}$. As stated previously, since $\mathbf{R}$ can be any symmetric traceless tensor, the Eq. (2.30) is the general solution valid for two-dimensional flow. In the ARSM of Gatski & Speziale (1993), the $\mathbf{R} = a_1\mathbf{S}$ as a consequence of using linear pressure strain-rate model and isotropic dissipation model. This fact yields a quite simplication of the right-hand side of Eq. (2.28) with only one non-zero entry for $\left(\mathbf{R}, \mathbf{T}^{(m)}\right)$

$$\left(\mathbf{R}, \mathbf{T}^{(m)}\right) = \begin{bmatrix} \{\mathbf{RS}\} \\ -2\{\mathbf{RWS}\} \\ \{\mathbf{RS}^2\} \end{bmatrix} = \begin{bmatrix} a_1\eta^2 \\ 0 \\ 0 \end{bmatrix}. \tag{2.31}$$

Then the α_n can be further simplized as

$$\alpha_1 = -\frac{a_1 a_4}{\alpha_0}, \tag{2.32a}$$

$$\alpha_2 = a_4 a_2 \alpha_1, \tag{2.32b}$$

$$\alpha_3 = -2a_3 a_4 \alpha_1. \tag{2.32c}$$

Substituting of Eq. (2.32) into Eq. (2.26), one obtains the explicit algebraic form for the Reynolds stress anisotropy tensor $\mathbf{b}$

$$\mathbf{b} = \alpha_1\left[\mathbf{S} + a_2 a_4 (\mathbf{SW} - \mathbf{WS}) - 2a_3 a_4\left(\mathbf{S}^2 - \frac{1}{3}\left\{\mathbf{S}^2\right\}\mathbf{I}\right)\right], \tag{2.33}$$

or for the Reynolds stress tensor τ

$$\tau = \frac{2}{3}k\mathbf{I} + 2k\alpha_1\left[\mathbf{S} + a_2 a_4 (\mathbf{SW} - \mathbf{WS}) - 2a_3 a_4\left(\mathbf{S}^2 - \frac{1}{3}\left\{\mathbf{S}^2\right\}\mathbf{I}\right)\right]. \tag{2.34}$$

It should be noted that, in Eq. (2.34), the a_4 is a function of P/ε, as shown in Eq. (2.24). Gatski & Speziale (1993) treated the P/ε to be constant, then the expression

above can be simplified. A different approach, which accounted the variation of P/ε is proposed later by Ying & Canuto (1996) and Girimaji (1996).

According to the definition, the production-dissipation ration can be easily expressed as

$$\frac{P}{\varepsilon} = -2\frac{k}{\varepsilon}\left\{\mathbf{bS}\right\}. \tag{2.35}$$

The insertation of above relation to Eq. (2.24) leads to the following expression for a_4

$$a_4 = \left[\gamma_1 - 2\frac{k}{\varepsilon}\gamma_0\alpha_1\eta^2\right]\frac{k}{\varepsilon}. \tag{2.36}$$

From Eqs. (2.32) and (2.36), one can derive the following cubic expression for α_1

$$\gamma_0^2\alpha_1^3 - \frac{\gamma_0\gamma_1}{\eta^2(k/\varepsilon)}\alpha_1^2 + \frac{1}{4\eta^4(k/\varepsilon)^2}\left[\gamma_1^2 - 2\left(\frac{k}{\varepsilon}\right)^2\gamma_0 a_1\eta^2 - 2\eta^2\left(\frac{k}{\varepsilon}\right)^2\left(\frac{a_3^2}{3} - \mathcal{R}^2 a_2^2\right)\right]\alpha_1 + \frac{\gamma_1 a_1\eta^2}{4\eta^6(k/\varepsilon)} = 0. \tag{2.37}$$

To obtain the proper solution of this equation, Jongen & Gatski (1998*b*) lean on an asymptotic analysis whereby the correct solution is the root with lowest real part of the above polynomial.

Once again, be noted, that above explicit form of ARSM is for the two-dimensional flows. Whereas, Jongen & Gatski (1998*b*) argued that Eq. (2.34) can be used as an approximation in the case of general three-dimensional flows. Actually, the exact solution for three-dimensional flows consists of ten independent tensor basis, which will be numerically difficult for practical applications, more details can be referred to Jongen (1998).

2.1.2.4 Wallin and Johansson ARSM

Different with approach taken by Gatski & Speziale (1993), Wallin & Johansson (2000) (hereafter as WJ) proposed a new explicit algebraic Reynolds stress model. The major difference between the models of Gatski & Speziale (1993) and Wallin & Johansson (2000) may be considered as the difference of adopted pressure strain-rate model. On the other hand, the issue regarding the production-dissipation ratio p/ε remains here, and solved by a cubic equation as well. The procedure of deriving WJ model will be reviewed briefly.

The weak-equilibrium condition is still invoked for deriving the WJ model, and the following implicit algebraic equation can be arrived

$$(P-\varepsilon)\,a_{ij} = P_{ij} - \frac{2}{3}P\delta_{ij} - \varepsilon_{ij} + \frac{2}{3}\varepsilon\delta_{ij} + \phi^s_{ij} + \phi^r_{ij}, \tag{2.38}$$

where pressure strain-rate term ϕ_{ij} is split into two terms, namely show part ϕ^s_{ij} and rapid part ϕ^r_{ij}. The rest terms have the same expression as shown in Eq. (2.5). Apparently, in the WJ model, the isotropic dissipation rate model is also adopted. Note that the original nomenclature is kept here for Reynolds stress anisotropy tensor $a_{ij}(=2b_{ij})$.

To close the Eq. (2.38), the ϕ^s_{ij} and ϕ^r_{ij} have to be modeled. In WJ model, the models of Rotta (1951) and Launder *et al.* (1975) for slow part and rapid part are adopted, respectively, which are

$$\phi^s_{ij} = -C_1\varepsilon a_{ij}, \tag{2.39}$$

$$\begin{aligned}\phi^r_{ij} = &-\frac{C_2+8}{11}\left(P_{ij}-\frac{2}{3}P\delta_{ij}\right) - \frac{30C_2-2}{55}k\left(\frac{\partial U_i}{\partial x_j}+\frac{\partial U_j}{\partial x_i}\right)\\ &-\frac{8C_2-2}{11}\left(-\overline{u_iu_k}\frac{\partial U_k}{\partial x_j} - \overline{u_ju_k}\frac{\partial U_k}{\partial x_i}\right).\end{aligned} \tag{2.40}$$

The constant C_2 in the ϕ^r_{ij} was originally suggested to be 0.4 by Launder *et al.* (1975), but more recent studies have suggested a higher value close to $5/9$, such as Lumley (1978), Shabbir & Shih (1992), Taulbee (1992). By substituting Eqs. (2.39) and (2.40) into Eq. (2.38) and setting the $C_2 = 5/9$, one can obtain an implicit algebraic relation for Reynolds stress tensor a_{ij}

$$\left(C_1 - 1 + \frac{P}{\varepsilon}\right)a_{ij} = -\frac{15}{8}S^\tau_{ij} + \frac{4}{9}\left(a_{ik}W^\tau_{kj} - W^\tau_{ik}a_{kj}\right), \tag{2.41}$$

where $S^\tau_{ij} = S_{ij}k/\varepsilon$ and $W^\tau_{ij} = W_{ij}k/\varepsilon$. Eq. (2.41) can be rewritten in a matrix notation

$$N\mathbf{a} = -\frac{6}{5}\mathbf{S}^\tau + \left(\mathbf{a}\mathbf{W}^\tau - \mathbf{W}^\tau\mathbf{a}\right), \tag{2.42}$$

where N is related the production dissipation ration by

$$N = \frac{9}{4}\left\{C_1 + 1 + \frac{P}{\varepsilon}\right\}. \tag{2.43}$$

Once again, the explicit representation of Eq. (2.42) is required to avoid the numerical difficulties. Following the procedure proposed by Pope (1975), Wallin & Johansson (2000) proposed a general relation for the Reynolds stress anisotropy tensor $\mathbf{a}$ using ten tensor basis in terms of $\mathbf{S}^\tau$ and $\mathbf{W}^\tau$ for three-dimensional flows

$$\begin{aligned}\mathbf{a} = &\beta_1\mathbf{S}^\tau + \beta_2\left(\mathbf{S}^{\tau 2} - \frac{1}{3}II_S\mathbf{I}\right) + \beta_3\left(\mathbf{W}^{\tau 2} - \frac{1}{3}II_W\mathbf{I}\right)\\ &+ \beta_4\left(\mathbf{S}^\tau\mathbf{W}^\tau - \mathbf{W}^\tau\mathbf{S}^\tau\right) + \beta_5\left(\mathbf{S}^{\tau 2}\mathbf{W}^\tau - \mathbf{W}^\tau\mathbf{S}^{\tau 2}\right)\\ &+ \beta_6\left(\mathbf{S}^\tau\mathbf{W}^{\tau 2} + \mathbf{W}^{\tau 2}\mathbf{S}^\tau - \frac{2}{3}IV\mathbf{I}\right) + \beta_7\left(\mathbf{S}^{\tau 2}\mathbf{W}^\tau + \mathbf{W}^\tau\mathbf{S}^{\tau 2} - \frac{2}{3}V\mathbf{I}\right)\\ &+ \beta_8\left(\mathbf{S}^\tau\mathbf{W}^\tau\mathbf{S}^{\tau 2} - \mathbf{S}^{\tau 2}\mathbf{W}^\tau\mathbf{S}^\tau\right) + \beta_9\left(\mathbf{W}^\tau\mathbf{S}^\tau\mathbf{W}^{\tau 2} - \mathbf{W}^{\tau 2}\mathbf{S}^\tau\mathbf{W}^\tau\right)\\ &+ \beta_{10}\left(\mathbf{W}^\tau\mathbf{S}^{\tau 2}\mathbf{W}^{\tau 2} - \mathbf{W}^{\tau 2}\mathbf{S}^{\tau 2}\mathbf{W}^\tau\right), \end{aligned} \tag{2.44}$$

where the β_n $(1 \leq n \leq 10)$ coeffcients may be functions of the five independent invariants in terms of $\mathbf{S}^\tau$ and $\mathbf{W}^\tau$. These invariant are given by

$$II_S = \left\{\mathbf{S}^{\tau 2}\right\}, \tag{2.45a}$$

$$II_W = \left\{\mathbf{W}^{\tau 2}\right\}, \tag{2.45b}$$

$$III_S = \left\{\mathbf{S}^{\tau 3}\right\}, \tag{2.45c}$$

$$IV = \left\{\mathbf{S}^\tau\mathbf{W}^{\tau 2}\right\}, \tag{2.45d}$$

$$V = \left\{\mathbf{S}^{\tau 2}\mathbf{W}^{\tau 2}\right\}. \tag{2.45e}$$

By inserting Eq. (2.44) into Eq. (2.42) and using the Cayley-Hamilton theorem to reduce the higher-order tensor groups, one can obtain the β_n-coefficients. For two-dimensional flows, there are three independent groups: $\mathbf{S}^\tau$, $(\mathbf{S}^{\tau 2} - II_\mathbf{S}\mathbf{I})$ and $(\mathbf{S}^\tau\mathbf{W}^\tau - \mathbf{W}^\tau\mathbf{S}^\tau)$, and only β_1 and β_4 are non-zero coefficients. Then, the representation for $\mathbf{a}$ can be formed as

$$\mathbf{a} = \beta_1\mathbf{S}^\tau + \beta_4\left(\mathbf{S}^\tau\mathbf{W}^\tau - \mathbf{W}^\tau\mathbf{S}^\tau\right), \tag{2.46}$$

where

$$\beta_1 = -\frac{6}{5}\frac{N}{N^2 - 2II_W}, \tag{2.47a}$$

$$\beta_2 = -\frac{6}{5}\frac{1}{N^2 - 2II_W}. \tag{2.47b}$$

$$\tag{2.47c}$$

From Eqs. (2.43), (2.47) and (2.42), one can obtain a cubic equation for the unknown N

$$N^3 - C_1' N^2 - \left(\frac{27}{10} II_S + 2 II_W\right) N + 2 C_1' II_W = 0, \tag{2.48}$$

where $C_1' = 9\left(C_1 - 1\right)/4$.

The above N-equation can be solved in a closed form with the solution for the positive root being

$$N = \begin{cases} \dfrac{C_1'}{3} + \left(P_1 + \sqrt{P_2}\right)^{1/3} + \text{sign}\left(P_1 + \sqrt{P_2}\right)\left|P_1 + \sqrt{P_2}\right|^{1/3} & P_2 \geq 0, \\ \dfrac{C_1'}{3} + \left(P_1^2 + P_2\right)^{1/6} \cos\left(\dfrac{1}{3}\arccos\left[\dfrac{P_1}{\sqrt{P_1^2 - P_2}}\right]\right) & P_2 < 0, \end{cases} \tag{2.49}$$

where the P_1 and P_2 are defined as

$$P_1 = \left(\frac{C'^2}{27} + \frac{9}{20} II_S - \frac{2}{3} II_W\right) C_1', \tag{2.50a}$$

$$P_2 = P_1^2 - \left(\frac{C'^2}{9} + \frac{9}{10} II_S + \frac{2}{3} II_W\right)^3. \tag{2.50b}$$

For three-dimensional flows, the N-equation is of six order, where the analytical solution can not be obtained. Therefore, Wallin & Johansson (2000) suggested to use Eq. (2.48) as an approximation. Accordingly, the β_n coefficients are

$$\beta_1 = -\frac{6}{5} \frac{N\left(2N^2 - 7II_W\right)}{\left(N^2 - 2II_W\right)\left(2N^2 - II_W\right)}, \tag{2.51a}$$

$$\beta_2 = -\frac{72}{5} \frac{N^{-1} IV}{\left(N^2 - 2II_W\right)\left(2N^2 - II_W\right)}, \tag{2.51b}$$

$$\beta_4 = -\frac{12}{5} \frac{\left(N^2 - 2II_W\right)}{\left(N^2 - 2II_W\right)\left(2N^2 - II_W\right)}, \tag{2.51c}$$

$$\beta_6 = -\frac{36}{5} \frac{N}{\left(N^2 - 2II_W\right)\left(2N^2 - II_W\right)}, \tag{2.51d}$$

$$\beta_9 = \frac{36}{5} \frac{1}{\left(N^2 - 2II_W\right)\left(2N^2 - II_W\right)}, \tag{2.51e}$$

where all other coefficients are zero.

Naji *et al.* (2004) evaluated the GS and WJ models for the turbulent flow through a square duct which involves a secondary flow and significant anisotropy between the turbulent Reynolds stress tensor components. An a priori evaluation of these models

is made using direct numerical simulation (DNS) results of Navier-Stokes equations. Comparisons of results from EASM and from DNS shows that these models are able to predict reasonably well such flows. It is concluded that the GS model, which is of a three tensor basis should be more convenient for engineering applications, and can be used as an optimal approximation for three-dimensional flows.

2.1.2.5 Inclusion of rotation effects

Turbulent flows are known to be sensitive to the system rotation effects. It is also clear that the differential Reynolds stress models are capable to capture these non-inertial effects. Therefore, it is understandable that the ARSMs, which derived from the differential Reynolds stress model, can inherit the ability to represent the system rotation effects. However, this sensitivity is partially lost through the weak-equilibrium assumption invoked in order to derive the ARSM. It has been shown that, in principle, this deficiency can be removed by extending the weak-equilibrium condition to non-inertial frames, such as Speziale (1979), Speziale (1998), Weis & Hutter (2003), Gatski & Wallin (2004), Hamba (2006). The common agreement is that, the extra term $b_{ik}\Omega_{kj} - \Omega_{ik}b_{kj}$ should be included into Eq. (2.23) to fully account for the non-inertial effects, where Ω_{ij} is the system rotation rate tensor.

As a result, for the GS model, the rotation effects can be included by the following implicit algebraic model.

$$\begin{aligned} 0 = &- \frac{b_{ij}}{a_4} - a_3 \left(b_{ik}S_{kj} + S_{ik}b_{kj} - \frac{2}{3}b_{mn}S_{mn}\delta_{ij} \right) \\ &- a_1 S_{ij} + a_2 \left(b_{ik}{W^*}_{kj} - W^*_{ik}b_{kj} \right), \end{aligned} \tag{2.52}$$

where

$$W^*_{ij} = W_{ij} + \frac{1}{a_2}\Omega_{ij}. \tag{2.53}$$

The above result shows that, to include the rotation effects through an extended weak-equilibrium condition, the resultant implicit algebraic equation is only altered through a change in vorticity tensor. Since Eq. (2.52) is an implicit equation for b_{ij} in the inertial frame, it needs to be transformed into the non-inertial frame to preserve the frame-invariant property, which is given by

$$0 = -\frac{\bar{b}_{ij}}{a_4} - a_3\left(\bar{b}_{ik}\bar{S}_{kj} + \bar{S}_{ik}\bar{b}_{kj} - \frac{2}{3}\bar{b}_{mn}\bar{S}_{mn}\delta_{ij}\right) - a_1\bar{S}_{ij} + a_2\left(\bar{b}_{ik}\bar{W}^*_{kj} - \bar{W}^*_{ik}\bar{b}_{kj}\right), \tag{2.54}$$

where

$$\bar{W}_{ij} = W^*_{ij} - \epsilon_{ijk}\Omega_k = W_{ij} + \frac{1}{a_2}\Omega_{ij} - \epsilon_{ijk}\Omega_k, \tag{2.55}$$

and the tensor Ω_{ij} is simply related to the rotation rate Ω_k by

$$\Omega_{ij} = -\epsilon_{ijk}\Omega_k. \tag{2.56}$$

So that

$$\bar{W}_{ij} = W_{ij} - \left(1 + \frac{1}{a_2}\right)\epsilon_{ijk}\Omega_k, \tag{2.57}$$

where ϵ_{ijk} is the permutation tensor.

For the WJ model, the similar methodology is adopted to include the rotation effects, details can be found in Wallin (2000), Wallin & Johansson (2002), Grundestam (2006), et al.

2.1.3 Eddy viscosity model

The concept behind the eddy viscosity models is that the unknown Reynolds stresses, a consequence from the Reynolds averaging procedure, are modeled using mean flow parameters, such as velocity gradients, and an eddy viscosity ν_t, which was proposed by Boussinesq more than a century ago

$$\overline{u_i u_j} = -\nu_t\left(x, y, z\right)\left(\frac{\partial U_i}{\partial x_j} + \frac{\partial U_j}{\partial x_i}\right) + \frac{2}{3}k\delta_{ij}. \tag{2.58}$$

The expression for the Reynolds stresses can be algebraic, linear or non-linear, by which the eddy viscosity models can be further sub-divided into four classes, which are algebraic (zero-equation) models, one-equation models, two-equation models and non-linear models. By definition, an n-equation model indicates that a model that requires solutions of n additional differential transport equations in addition to those expressing conservation of mass, momentum and energy. In the context of eddy viscosity model, these additional differential transport equations are supposed to provide the velocity

scale and the length scale (Bredberg, 2001) for the formulation of eddy viscosity ν_t, which is

$$\nu_t = u \cdot l, \tag{2.59}$$

where u is the velociy scale and l is the length scale.

The two-equation level of closure attempts to develop the transport equations both for the velocity scale and length scale of flow. In the context of two-equation closure, many different models have been proposed. The main difference among these models is the choice of the length scale quantity. The mostly used two-equation model is that of k-ε model, which uses the dissipation rate, ε, appearing in the k-equation to construct the eddy viscosity. Another widely used two-equation model is the k-ω model, where the ω is the dissipation per unit turbulent kinetic energy or specific dissipation rate (Wilcox, 1993).

The $k-\varepsilon$ type of two-equations models uses the turbulent energy k to constitute the velocity scale, $k^{1/2}$, and the turbulent energy dissipation rate ε to constitute the turbulent length scale, formally $k^{3/2}/\varepsilon$. Thus, the eddy viscosity ν_t is given by the relation

$$\nu_t = C_\mu \frac{k^2}{\varepsilon} = C_\mu k \tau, \tag{2.60}$$

where $\tau = k/\varepsilon$.

Note that there are several notable deficiencies with above k-ε type of models, namely linear eddy viscosity model. One is the isotropy of the eddy viscosity as consequences of Boussinesq approximation, which assumes a direct proportionality between the turbulent Reynolds stresses and the mean strain rate tensor. This very feature leads the failure for prediction of turbulent flows in some complex cases, such as the secondary motions in ducts. Another deficiencies with linear eddy viscosity model is that of insensitivity to the non-inertial effects, such as imposed rotations, since the sole dependence on the strain rate (Eq. (2.58)), which is material frame indifferent. To remedy these deficiencies, possible choices are the modification on a case-by-case or *ad hoc* basis, such as Launder *et al.* (1977), Howard *et al.* (1980), et al.; or to extend the one-term tensor representation to a nonlinear multiple terms representation, which forms the category of nonlinear eddy viscosity model, such as Speziale (1987), Taulbee (1992), Mompean *et al.* (1996), Craft *et al.* (1997) et al. It may be conclude that, in the framework of eddy viscosity model, the nonlinear eddy viscosity model approach

offers a relatively more rigorous manner for prediction of complex flows compared to that of linear eddy viscosity models. The general form for deriving the nonlinear eddy viscosity model may be expressed as

$$\tau_{ij} = \frac{2}{3}k\delta_{ij} + \sum_{n=1}^{N} \alpha_n^{'} T_{ij}^{(n)}, \tag{2.61}$$

where $T_{ij}^{(n)}$ are the tensor bases and $\alpha_n^{'}$ are the expansion coefficients which need to be determined.

Since one of the advantages with the nonlinear viscosity models is the ability of represent the anisotropy of Reynolds stress tensors, it is straightforward to reform the equations in terms of the Reynolds stress anisotropies b_{ij}, which leads to

$$b_{ij} = \sum_{n=1}^{N} \alpha_n T_{ij}^{(n)}, \tag{2.62}$$

which may be found identical to Eq. (2.26), which is used to derive algebraic Reynolds stress models. As a matter of fact, the ARSMs and NLEVMs share the same basic formulation, and in both cases, an explicit tensor representation for b_{ij} is obtained in terms of S_{ij} and W_{ij}. The identifying feature to distinguish these two types of model are the technique to obtain the expansion coefficients α_n. As shown in previous section, in the ARSM case, the projection method and Cayley-Hamilton theorem are used to obtain such coefficients in a mathematically consistent fashion from the differential Reynolds stress model; while in the case of NLEVM, the expansion coefficients are determined based on calibrations with experimental or numerical data and physical constraints. To illustrate such ideas, two examples will be given below.

Shih *et al.* (1995) proposed a quadratic model

$$\mathbf{b} = \alpha_{\mathbf{1}}\mathbf{S} + \alpha_{\mathbf{2}}\left(\mathbf{SW} - \mathbf{WS}\right). \tag{2.63}$$

The α_i coefficients are determined by applied the rapid distortion theory constraint to rapidly rotating isotropic turbulence, and the realizability constraints

$$\tau_{\beta\beta} \geq 0, \quad \text{no sum} \tag{2.64a}$$

$$\tau_{\beta\gamma}^2 \leq \tau_{\beta\beta}\tau_{\gamma\gamma}. \quad \text{Schwarz inequality} \tag{2.64b}$$

The coefficients are further optimized by comparison with experiment and numerical simulation of homogeneous shear flow and the inertial sublayer.

Craft *et al.* (1996) argued that higher-order terms are necessary in order to predict flows with complex strain fields. To this end, Craft *et al.* (1996) proposed a cubic model

$$\begin{aligned}\mathbf{b} =&\alpha_1\mathbf{S} + \alpha_2\left(\mathbf{S^2} - \frac{\mathbf{1}}{\mathbf{3}}\{\mathbf{S^2}\}\mathbf{I}\right)\\ &+ \alpha_3\left(\mathbf{SW} - \mathbf{WS}\right) + \alpha_4\left(\mathbf{W^2} - \frac{\mathbf{1}}{\mathbf{3}}\{\mathbf{W^2}\}\mathbf{I}\right)\\ &+ \alpha_5\left(\mathbf{W^2S} + \mathbf{SW^2} - \frac{\mathbf{2}}{\mathbf{3}}\{\mathbf{SW^2}\}\mathbf{I}\right) + \alpha_6\left(\mathbf{WS^2} - \mathbf{S^2W}\right).\end{aligned} \tag{2.65}$$

Calibration of above model coefficients is based on an optimization over a wide rage of flows, which include plane channel flow, circular pipe flow, axially rotating pipe flow, fully developed curved channel flow and impinging jet flows.

2.2 Modeling of turbulent heat flux

The modeling of turbulent heat fluxes is important in many engineering applications, and usually found to be carried out by invoking the Reynolds averaged analogy. This leads to the same decomposition as for the velocities, the temperature can be expressed as

$$\hat{\Theta} = \Theta + \theta, \tag{2.66}$$

where the capital symbols (Θ) represent an ensemble mean and the lower-case symbols (θ) represent the fluctuating part. This averaging leads to the Reynolds-averaged equations of turbulent mean flow without buoyancy effect as follows

$$\frac{\partial U_i}{\partial x_i} = 0, \tag{2.67a}$$

$$\frac{DU_i}{Dt} = -\frac{1}{\rho}\frac{\partial P}{\partial x_i} + \frac{\partial}{\partial x_j}\left(\nu\frac{\partial U_i}{\partial x_j} - \overline{u_i u_j}\right), \tag{2.67b}$$

$$\frac{D\Theta}{Dt} = \frac{\partial}{\partial x_j}\left(\alpha\frac{\partial \Theta}{\partial x_j} - \overline{u_j\theta}\right), \tag{2.67c}$$

where U_i is the mean velocity of the flow, P is the mean pressure. ρ and ν are the constant density and kinematic viscosity respectively. $\overline{u_i u_j}$ is the Reynolds stress, α

is the thermal diffusivity, Θ is the mean temperature and $\overline{u_i\theta}$ is the turbulent heat flux with θ being the temperature fluctuation.

The resulting unknown $\overline{u_i\theta}$ in Eq. (2.67c) causes the same problems for the temperature equation as the Reynolds stresses do for the momentum equation. Closing Eq. (2.67c) needs the supply of $\overline{u_i\theta}$, which consists the context of turbulent heat flux modeling. It should be noted that any modeling of turbulent heat flux without mentioning the velocity models is considered incomplete (So & Speziale, 1999). The temperature equations are usually modeled as scalar equations with a known velocity field. On the contrary, the closure of the velocity equations can be carried out with no regarding to the temperature field in the case of neglecting buoyancy effects. Additionally, it has been pointed out that model for the temperature field should not be a higher level than that for velocity field (Cebeci & Bradshaw, 1984).

Similar to the Reynolds stresses, the prediction of the turbulent heat fluxes can be carried out using a hierarchy of models, which consist of gradient transport models and second-order closure models (So & Speziale, 1999). The gradient transport models include the eddy viscosity model and algebraic model. To construct such models, the assumptions of dynamic similarity between temperature and velocity fields and gradient transport of heat momentum are usually invoked. Similar methodology is also often used to develop the second-order closure for turbulent heat fluxes. Well documented reviews about turbulent heat flux models can be found in So & Speziale (1999).

Also in analogy with the transport equation for Reynolds stress, the exact transport equation of turbulent heat flux in inertial frames without buoyancy effect can be given by

$$\frac{D\overline{u_i\theta}}{Dt} = P_{i\theta} + \phi_{i\theta} + \mathcal{D}_{i\theta} - \varepsilon_{i\theta}, \tag{2.68}$$

where $P_{i\theta}$ is the production term which contains the production due to the gradient of mean temperature and velocity, $\phi_{i\theta}$ is pressure temperature-gradient correlation term (also known as P&T-Corr.), $\mathcal{D}_{i\theta}$ is the combination of viscous diffusion, turbulent transport and pressure transport and $\varepsilon_{i\theta}$ is the dissipation term Dol *et al.* (1997). These

terms are given by

$$P_{i\theta} = -\overline{u_i u_j}\frac{\partial \Theta}{\partial x_j} - \overline{u_j \theta}\frac{\partial U_i}{\partial x_j}, \tag{2.69a}$$

$$\phi_{i\theta} = \overline{\frac{p}{\rho}\frac{\partial \theta}{\partial x_i}}, \tag{2.69b}$$

$$\mathcal{D}_{i\theta} = \frac{\partial}{\partial x_j}\left(\alpha\overline{\frac{\partial \theta}{\partial x_j}u_i} + \nu\theta\overline{\frac{\partial u_i}{\partial x_j}}\right) - \frac{\partial \overline{\theta u_i u_j}}{\partial x_j} - \frac{1}{\rho}\overline{\frac{\partial \theta p}{\partial x_i}}, \tag{2.69c}$$

$$\varepsilon_{i\theta} = (\alpha + \nu)\overline{\frac{\partial \theta}{\partial x_j}\frac{\partial u_i}{\partial x_j}}. \tag{2.69d}$$

It is noted that the terms containing correlations of second or higher orders in Eq.(2.68) need to be modeled. $P_{i\theta}$ can be treated in an exact manner by second or lower order variables. Generally, a transport model for turbulent heat flux can be expressed in terms of the gradient of mean velocity $\partial U_i/\partial x_j$, gradient of temperature $\partial \Theta/\partial x_j$, the Reynolds stresses $\overline{u_i u_j}$, the heat fluxes $\overline{u_i \theta}$ and some time scales.

Attention here will go to the derivation of algebraic heat flux model from the differential transport model for turbulent heat flux established by Wikström *et al.* (2000) and So *et al.* (2004). During this process, the weak-equilibrium condition is invoked to obtain the algebraic relations for turbulent heat flux in analogy with the derivation of algebraic Reynolds stress models.

To obtain the algebraic relation for normalized turbulent heat flux, the turbulent kinetic energy $k(=\overline{u_i u_i}/2)$ and the temperature variance $k_\theta(=\overline{\theta^2}/2)$ are also necessary. Their transport equations can be expressed as

$$\frac{Dk}{Dt} = \mathcal{D}_k + P_k - \varepsilon_k, \tag{2.70a}$$

$$\frac{Dk_\theta}{Dt} = \mathcal{D}_\theta + P_\theta - \varepsilon_\theta. \tag{2.70b}$$

In analogy with the derivation of transport equation for Reynolds stress anisotropy $b_{ij}(=\overline{u_i u_j}/2k - \delta_{ij}/3)$ (Gatski & Wallin, 2004), one can obtain the transport equation for normalized turbulent heat flux $\xi_i(=\overline{u_i\theta}/(k^{1/2}k_\theta^{1/2}))$ (Hattori *et al.*, 2006; So *et al.*, 2004; Wikström *et al.*, 2000)

$$\frac{D\xi_i}{Dt} = \frac{1}{k^{1/2}k_\theta^{1/2}}(P_{i\theta} + \phi_{i\theta} - \varepsilon_{i\theta}) - \frac{\xi_i}{2}\left[\tau_k\left(\frac{P_k}{\varepsilon_k} - 1\right) + \tau_\theta\left(\frac{P_\theta}{\varepsilon_\theta} - 1\right)\right] + \mathcal{D}_i^a, \tag{2.71}$$

where $\tau_k = \varepsilon_k/k$ and $\tau_\theta = \varepsilon_\theta/k_\theta$ are time scales. Note that the concept of normalized heat flux itself directly conflicts with the linearity principle proposed by Pope (1983), which has been often preferred to be abandoned in many scalar transport models, such as Hattori *et al.* (2006); So *et al.* (2004); Wikström *et al.* (2000). The term $\mathcal{D}_i^a$ is the diffusion and transport of ξ_i, which reads

$$\mathcal{D}_i^a = \frac{D_{i\theta}}{k^{1/2}k_\theta^{1/2}} - \frac{1}{2}\xi_i\left(\frac{\mathcal{D}_\theta}{k_\theta} + \frac{\mathcal{D}_k}{k}\right). \tag{2.72}$$

Eq.(2.71) provides the full description for the transport equation of ξ_i, which is the basis to derive the algebraic model. By invoking the weak-equilibrium condition (So *et al.*, 2004; Wikström *et al.*, 2000), i. e.,

$$\frac{D\xi_i}{Dt} = 0, \tag{2.73a}$$

$$\mathcal{D}_i^a = 0, \tag{2.73b}$$

one can reduce Eq.(2.71) to an approximated form for normalized turbulent heat flux ξ_i:

$$0 = \frac{1}{k^{1/2}k_\theta^{1/2}}\left(P_{i\theta} + \phi_{i\theta} - \varepsilon_{i\theta}\right) - \frac{\xi_i}{2}\left[\tau_k\left(\frac{P_k}{\varepsilon_k} - 1\right) + \tau_\theta\left(\frac{P_\theta}{\varepsilon_\theta} - 1\right)\right]. \tag{2.74}$$

To achieve the AHFM, the specific models for the pressure temperature-gradient correlation $\phi_{i\theta}$ and the dissipation term $\varepsilon_{i\theta}$ are neccesary. A rather general model for the combined effect of $\phi_{i\theta}$ and $\varepsilon_{i\theta}$ that has been studied by Wikström *et al.* (2000) is considered here, which can be written as

$$\begin{aligned}\phi_{i\theta} - \varepsilon_{i\theta} = & -\left(C_{1\theta} + C_{5\theta}\frac{k}{\varepsilon k_\theta}\overline{u_{j\theta}}\frac{\partial\Theta}{\partial x_j}\right)\frac{\varepsilon}{k}\overline{u_{i\theta}} + C_{2\theta}\overline{u_{j\theta}}\frac{\partial U_i}{\partial x_j} \\ & + C_{3\theta}\overline{u_{j\theta}}\frac{\partial U_j}{\partial x_i} + C_{4\theta}\overline{u_i u_j}\frac{\partial\Theta}{\partial x_j},\end{aligned} \tag{2.75}$$

where $C_{1\theta} \sim C_{5\theta}$ are model coefficients.

Substituting Eq.(2.75) into Eq.(2.74), and after further generalization, one obtains

$$\begin{aligned}0 \;=\; & -C_b\left(2b_{ij} + \frac{2\delta_{ij}}{3}\right)\Theta_j - C_S S_{ij}\xi_j - C_W W_{ij}\xi_j \\ & -\frac{\xi_i}{2}\left\{\tau_k\left(\frac{P_k}{\varepsilon_k} - 1 + 2C_{1\theta}\right) + \tau_\theta\left[\frac{P_\theta}{\varepsilon_\theta}\left(1 - 2C_{5\theta}\right) - 1\right]\right\},\end{aligned} \tag{2.76}$$

where $C_b = 1 - C_{4\theta}$, $C_S = 1 - C_{2\theta} - C_{3\theta}$, $C_W = 1 - C_{2\theta} + C_{3\theta}$ and $\Theta_i = (k/k_\theta)^{1/2}(\partial\Theta/\partial x_i)$. The strain-rate tensor S_{ij} and vorticity tensor W_{ij} are given as

$$S_{ij} = \frac{1}{2}\left(\frac{\partial U_i}{\partial x_j} + \frac{\partial U_j}{\partial x_i}\right), \tag{2.77a}$$

$$W_{ij} = \frac{1}{2}\left(\frac{\partial U_i}{\partial x_j} - \frac{\partial U_j}{\partial x_i}\right). \tag{2.77b}$$

Furthermore, Eq.(2.76) can be expressed by a function of specific terms such that

$$0 = f_i\left(b_{km}, S_{km}, W_{km}, \xi_m, \Theta_m\right). \tag{2.78}$$

Chapter 3

Calculation of fully developed rotating channel flow

3.1 Calculation of fully developed rotating channel flow using LS model

In this section, a calculation of fully developed rotating channel flow will be undertaken to show the performance of DRSM. Fully developed channel flow has been studied extensively to increase the understanding of the mechanics of wall-bounded turbulent flows experimentally (Johnston *et al.*, 1972; Matsubara & Alfredsson, 1996, 1998) and numerically (Alvelius, 1999; Cambon *et al.*, 1992; Grundestam *et al.*, 2008; Kristoffersen & Andersson, 1993; Lamballais *et al.*, 1996, 1998; Liu & Lu, 2007; Piomelli & Liu, 1995; Tafti & Vanka, 1991) et al. Its geometric simplicity is attractive for both experimental and theoretical investigations of complex turbulence interactions near a wall. Also the turbulent flows with system rotation are considerable interest in a variety of industrial, geophysical and astrophysical applications.

It is well established that system rotation affects both the mean motion and the turbulent structure. The interaction of the Coriolis force with the mean shear produces stabilization or destabilization of the flow near the two walls. Here, the concept of stability is related to an enhancement (destabilization) or with a damping (stabilization) of the turbulence levels compared to the non-rotating case. Along the unstable side (pressure side) of the channel, the mean shear vorticity is parallel to the rotation vector,

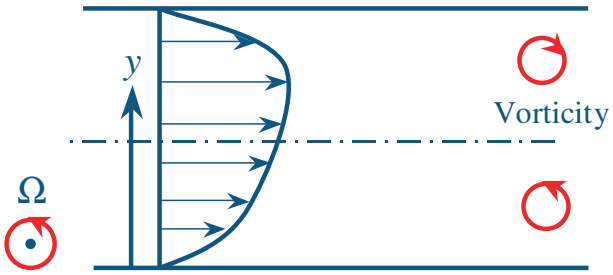

Figure 3.1: Schematics of the fully developed rotating channel flow

while along the stable side (suction side), these two vectors are anti-parallel. This situation can lead to the complete suppression of turbulence and the relaminarization of the flow on the stable side of the channel if the rotation rate is sufficiently high (Dutzler *et al.*, 2000; Pallares & Davidson, 2000).

With the development of high performance computers, it becomes possible to reveal more details of turbulent flow with DNS and LES simulation, which are also often used to test and validate the various closure models. Kristoffersen & Andersson (1993) carried out DNS of rotating channel flow at $Re = 5800$ and $Ro \leq 0.5$ .Lamballais *et al.* (1996) and Lamballais *et al.* (1998) computed rotating channel flow at $Re = 5000$ and $Ro \leq 1.5$ by DNS and $Re = 14000$ and $Ro \leq 1.5$ by LES. Also for the channel flow without system rotation, Kim *et al.* (1987) computed the channel flow at Re=5600 by DNS, a large number of turbulence statistics are computed and compared with the experimental data. In this study, the above DNS and LES calculations will play as a benchmark, to show the performance of turbulence model for the prediction of fully developed rotating channel flow.

The schematics of fully developed turbulent flow between to infinite parallel walls rotating around spanwise axis shown in Fig. 3.1 . The resulting flow, which is assumed to be incompressible, is characterized by the following mean streamwise momentum equation:

$$0 = -\frac{1}{\rho}\frac{\partial P_{eff}}{\partial x} - \frac{d}{dy}\overline{uv} + \nu\frac{d^2U}{dy^2}. \tag{3.1}$$

In the above equation, the gradient of effective pressure $P_{eff} = P - \rho\Omega^2 r^2$ is uniform in entire flow field. Also Eq. (3.1) shows that the total shear stress varies linearly across the channel as in non-rotating flow.

As to the turbulence model, the model developed by Launder & Shima (1989) is adopted because it predicts a variety of flows fairly well and also its relatively simple formulation. For clarity, some model details will be reviewed briefly here.

As shown in the exact transport equation of Reynolds stress tensor, Eq. (2.5), the turbulent production P_{ij} and viscous diffusion $\mathcal{D}^{\nu}_{ij}$ are treated in exact forms. Additionally, the Coriolis production term C_{ij} to include the rotation effects can be also treated directly. While the others terms need to be modeled.

The turbulent transport of Reynolds stress $\mathcal{D}^{t}_{ij}$ is represented by the general gradient diffusion hypothesis, as shown previously.

$$\mathcal{D}^{t}_{ij} = \frac{\partial}{\partial x_k}\left(C_s \frac{k}{\varepsilon}\overline{u_k u_l}\frac{\partial \overline{u_i u_j}}{\partial x_l}\right), \tag{3.2}$$

where the $C_s = 0.22$ here. Although this simple choice has been made for computational convenience rather than accuracy, the relative unimportance of diffusive transport in the stress budget for the boundary layers means that possible errors are unlikely to have a significant effect (Launder & Shima (1989)). In addition, the pressure transport effect has been modeled together with turbulent transport in Eq. (3.2) by adjusting the coefficient C_s.

The pressure strain-rate correlation (redistribution) term is modeled as

$$\phi_{ij} = \phi_{ij,1} + \phi_{ij,2} + \phi_{ij,3} + \phi^{w}_{ij,1} + \phi^{w}_{ij,2} + \phi^{w}_{ij,3}, \tag{3.3}$$

where

$$\phi_{ij,1} = -C_1\varepsilon a_{ij} = -C_1\varepsilon\left(\frac{\overline{u_i u_j}}{k} - \frac{2}{3}\delta_{ij}\right), \tag{3.4a}$$

$$\phi_{ij,2} = -C_2\left(P_{ij} - \frac{2}{3}\delta_{ij}P\right), \tag{3.4b}$$

$$\phi_{ij,3} = -\frac{1}{2}C_2\left(C_{ij} - \frac{2}{3}\delta_{ij}C\right), \tag{3.4c}$$

$$\phi^{w}_{ij,1} = C^{w}_{1}\frac{\varepsilon}{k}\left(\overline{u_k u_l}n_l n_k\delta_{ij} - \frac{3}{2}\overline{u_i u_k}n_j n_k - \frac{3}{2}\overline{u_j u_k}n_i n_k\right) f_w, \tag{3.4d}$$

$$\phi^{w}_{ij,2} = C^{w}_{2}\left(\phi_{kl,2}n_k n_l\delta_{ij} - \frac{3}{2}\phi_{ik,2}n_j n_k - \frac{3}{2}\phi_{jk,2}n_i n_k\right) f_w, \tag{3.4e}$$

$$\phi^{w}_{ij,3} = C^{w}_{2}\left(\phi_{kl,3}n_k n_l\delta_{ij} - \frac{3}{2}\phi_{ik,3}n_j n_k - \frac{3}{2}\phi_{jk,3}n_i n_k\right) f_w. \tag{3.4f}$$

In the above redistribution model, the f_w is the near-wall damping function, taken as

$$f_w = \frac{k^{3/2}}{2.5\varepsilon}\left(\frac{1}{y} + \frac{1}{2d-y}\right), \tag{3.5}$$

with y being the distance normal to the wall and d being the half width of the channel. Note that in the Launder & Shima (1989) redistribution model, three non-dimensional parameters A, A_2 and A_3 are employed to offer a convenient way to meet the two-component limit, which requires that the velocity fluctuation of normal to the wall falls to zero more rapidly than the other two components by continuity, as wall is approached.

The coefficients in the redistribution model here are as following

$$C_1 = 1 + 2.58AA_2^{1/4}\left\{1 - \exp\left[-\left(-0.0067Re_t\right)^2\right]\right\}, \tag{3.6a}$$

$$C_2 = 0.75A^{1/2}, \tag{3.6b}$$

$$C_1^w = -\frac{2}{3}C_1 + 1.67, \tag{3.6c}$$

$$C_2^w = \max\left[\left(\frac{2}{3}C_2 - \frac{1}{6}/C_2\right), 0\right]. \tag{3.6d}$$

For the dissipation rate of Reynolds stress tensor, ε_{ij}, the assumption of local isotropy is adopted:

$$\varepsilon_{ij} = \frac{2}{3}\delta_{ij}\varepsilon. \tag{3.7}$$

For the dissipation rate model, Launder & Shima (1989) also used these parameters, so did by the Hanjalić & Jakirlić (1993) model later. Finally, the dissipation rate of turbulence energy, ε, is obtained by solving

$$\frac{D\varepsilon}{Dt} = \frac{d}{dy}\left[\left(C_\varepsilon\frac{k^2}{\varepsilon} + \nu\right)\frac{d\varepsilon}{dy}\right] + \left(C_{\varepsilon 1} + \psi_1 + \psi_2\right)\frac{\varepsilon}{k}P - C_{\varepsilon 2}\frac{\varepsilon^2}{k}, \tag{3.8}$$

where

$$\psi_1 = 2.5A\left(\frac{P}{\varepsilon} - 1\right), \tag{3.9a}$$

$$\psi_2 = 0.3\left(1 - 0.3A_2\right)\exp\left[-\left(0.002Re_t\right)^2\right], \tag{3.9b}$$

where ψ_1 has the effect to reduce turbulence length scale, and ψ_2 controls relaminarization of turbulent flow under favorable pressure gradient. The coefficients C_ε, $C_{\varepsilon 1}$ and

Table 3.1: The terms in the transport equations of Reynolds stress tensor

Terms	$\overline{u^2}$	$\overline{uv}$	$\overline{v^2}$	$\overline{w^2}$
P_{ij}	$-2\overline{uv}\frac{dU}{dy}$	$-\overline{v^2}\frac{dU}{dy}$	0	0
ε_{ij}	$\frac{2}{3}\varepsilon$	0	$\frac{2}{3}\varepsilon$	$\frac{2}{3}\varepsilon$
C_{ij}	$4\Omega_3\overline{uv}$	$-2\Omega_3\left(\overline{u^2}-\overline{v^2}\right)$	$4\Omega_3\overline{uv}$	0
$\phi_{ij,1}$	$-C_1\frac{\varepsilon}{k}\left(\overline{u^2}-\frac{2}{3}k\right)$	$-C_1\frac{\varepsilon}{k}\left(\overline{uv}\right)$	$-C_1\frac{\varepsilon}{k}\left(\overline{v^2}-\frac{2}{3}k\right)$	$-C_1\frac{\varepsilon}{k}\left(\overline{w^2}-\frac{2}{3}k\right)$
$\phi_{ij,2}$	$-C_2\left(P_{11}-\frac{2}{3}P\right)$	$-P_{12}$	$C_2\frac{2}{3}P$	$C_2\frac{2}{3}P$
$\phi_{ij,3}$	$-2C_2\Omega_3\overline{uv}$	$-C_2\Omega_3\left(\overline{v^2}-\overline{u^2}\right)$	$2C_2\Omega_3\overline{uv}$	0
$\phi^w_{ij,1}$	$C_1^w\frac{\varepsilon}{k}\left(\overline{v^2}\right)f_w$	$C_1^w\frac{\varepsilon}{k}\left(-\frac{3}{2}\overline{uv}\right)f_w$	$C_1^w\frac{\varepsilon}{k}\left(-2\overline{v^2}\right)f_w$	$C_1^w\frac{\varepsilon}{k}\left(\overline{v^2}\right)f_w$
$\phi^w_{ij,2}$	$\frac{2}{3}C_2C_2^wPf_w$	$\frac{2}{3}C_2C_2^wP_{12}f_w$	$-\frac{4}{3}C_2C_2^wPf_w$	$\frac{2}{3}C_2C_2^wPf_w$
$\phi^w_{ij,3}$	$2C_2C^w\Omega_3\overline{uv}f_w$	$\frac{3}{2}C_2C^w\Omega_3\left(\overline{v^2}-\overline{u^2}\right)f_w$	$-4C_2C^w\Omega_3\overline{uv}f_w$	$2C_2C^w\Omega_3\overline{uv}f_w$

$C_{\varepsilon 2}$ in the above dissipation model are taken as their standard high Reynolds number values (Launder *et al.*, 1972), respectively.

Table 3.1 listed the all the terms in the transport equation of Reynolds stress tensor, excepted for the diffusive transport term, for the specific case of fully developed rotating channel, where Ω_3 is the system rotation rate.

The above equations are solved by the finite difference method with 201 non-uniform distributed nodes in the y direction to meet the grid density requirements suggested by So *et al.* (1991), and the first computational node was situated at $y^+ \leq 0.5$. The distance between each node is increased with an expansion ration of 1.05. On the solid wall, Reynolds stresses and mean velocity are set to 0, and for the dissipation rate

is:

$$\varepsilon = 2\nu \left(\frac{d\sqrt{k}}{dy} \right)^2 , \tag{3.10}$$

which represents the exact limit. The kinetic energy k is not solved directly here, and obtained by $k = \left(\overline{u^2} + \overline{v^2} + \overline{w^2} \right) /2$. The solution was assumed to have reached a steady state when the sum of absolute normalized residuals across the channel normalized with the time step, fell below 10^{-5}.

Stationary Case

First of all, the computation of fully developed channel flow without rotation is undertaken to show the basic performance of adopted DRSM here, and compared with the DNS data of Kim *et al.* (1987). The computations are carried out for Reynolds number $Re = 5600$, based on the bulk mean velocity U_m and the channel width $2d$:

$$Re = \frac{2U_m d}{\nu}. \tag{3.11}$$

To verify the grid independence, the computation with different nodes number distributed in the y direction was carried out, as shown in Fig. 3.2. Fig. 3.2a shows the non-dimensional velocity U profile normalized by the bulk velocity U_m with nodes number 51, 101, 151, 201. For the nodes number 101, 151 and 201, it shows that the velocity profile is independent from the nodes number without any discernible effect. For nodes number 51, qualitatively inconsistent profile is shown compared with those of other nodes number. For the streamwise Reynolds stress $\overline{u^2}$, similar behavior is also observed, further proved that by using the node number more that 101, the computation results can be independent from the choice of nodes number. Howsoever, in the present computation, the node number 201 is adopted for relative high resolution and easy comparison with DNS data.

The profiles of the mean velocity non-dimensionalized by the wall shear velocity are shown in Fig. 3.3, and also law of wall and log law are presented in the figure. Within the sublayer, $y^+ \leq 5$, the computational result follows the linear law as the DNS. In the logarithmic region, however, there exits a noticeable discrepancy between these two results.

The profiles of three normal Reynolds stresses normalized by the wall shear velocity u_τ and compared with DNS data are shown in Fig. 3.4, The definition for the wall

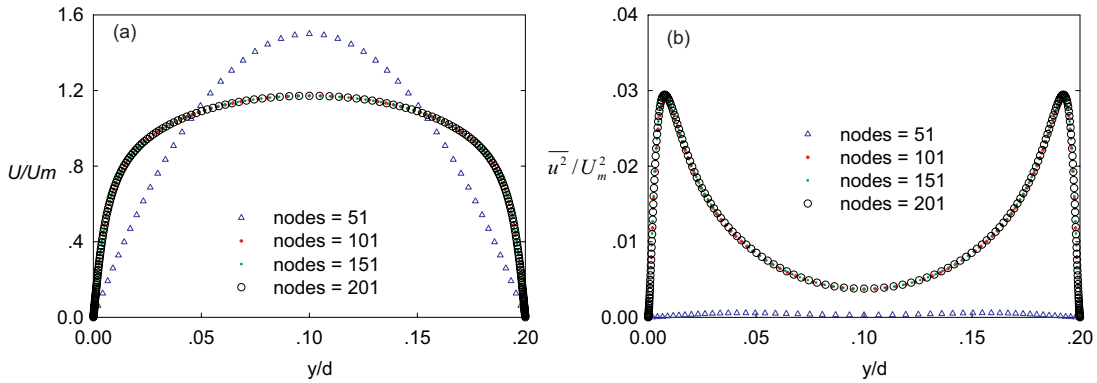

Figure 3.2: Verification of the grid independence

shear velocity in this stationary case is as following

$$u_\tau = \sqrt{\nu \frac{dU}{dy}|_{wall}}. \tag{3.12}$$

And the local coordinate y^+ is

$$y^+ = u_\tau y/\nu. \tag{3.13}$$

Although the general shape of the profiles is in good agreement, there exits some discrepancy between these model simulation and DNS data.

Excellent agreement is obtained for the Reynolds shear stress component $\overline{uv}$ as shown in Fig. 3.5 across the channel. It is worthy to note that the correct representing the Reynolds shear stress is crucial for evaluating the performance of turbulent models, since the Reynolds shear stress appears in the momentum equation.

Considering the no-slip boundary condition and continuity equation, the velocity and pressure fluctuations in the wall vicinity can be expanded as (Mansour *et al.*, 1988; Patel *et al.*, 1985; So *et al.*, 1997)

$$u^+ = b_1 y^+ + \cdots, \tag{3.14a}$$

$$v^+ = c_2 y^{+2} + \cdots, \tag{3.14b}$$

$$w^+ = b_3 y^+ + \cdots, \tag{3.14c}$$

$$\overline{uv}^+ = b_1 c_2 y^{+3} + \cdots, \tag{3.14d}$$

where wall units are used (normalized by kinematics viscosity ν and the friction velocity u_τ).

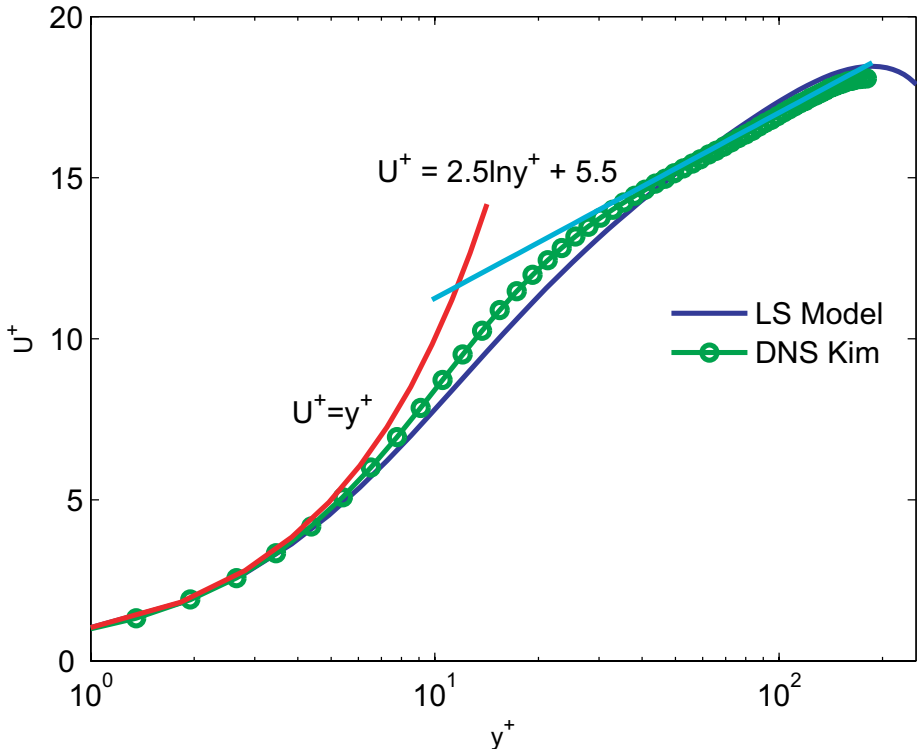

Figure 3.3: Mean velocity U^+ profile

The limiting near-wall behavior of the rms of the Reynolds stresses is shown in Fig. 3.6, where

$$u = u_{rms}/\left(4y^{+}\right), \tag{3.15a}$$

$$v = v_{rms}/\left(10^{4}y^{+2}\right), \tag{3.15b}$$

$$w = w_{rms}/\left(y^{+}\right), \tag{3.15c}$$

$$uv = uv/\left(10^{4}y^{+3}\right). \tag{3.15d}$$

It is quite obvious that the LS model can not represent the limiting wall behavior, especially for the v and $\overline{uv}$.

Rotating Case

The computations for rotating channel flow are conducted for Reynolds number $Re = 5000$ and 5800 compared with the results of DNS. For this application, different values of the rotation number are considered, which corresponds to $0 \leq Ro \leq 0.5$ at

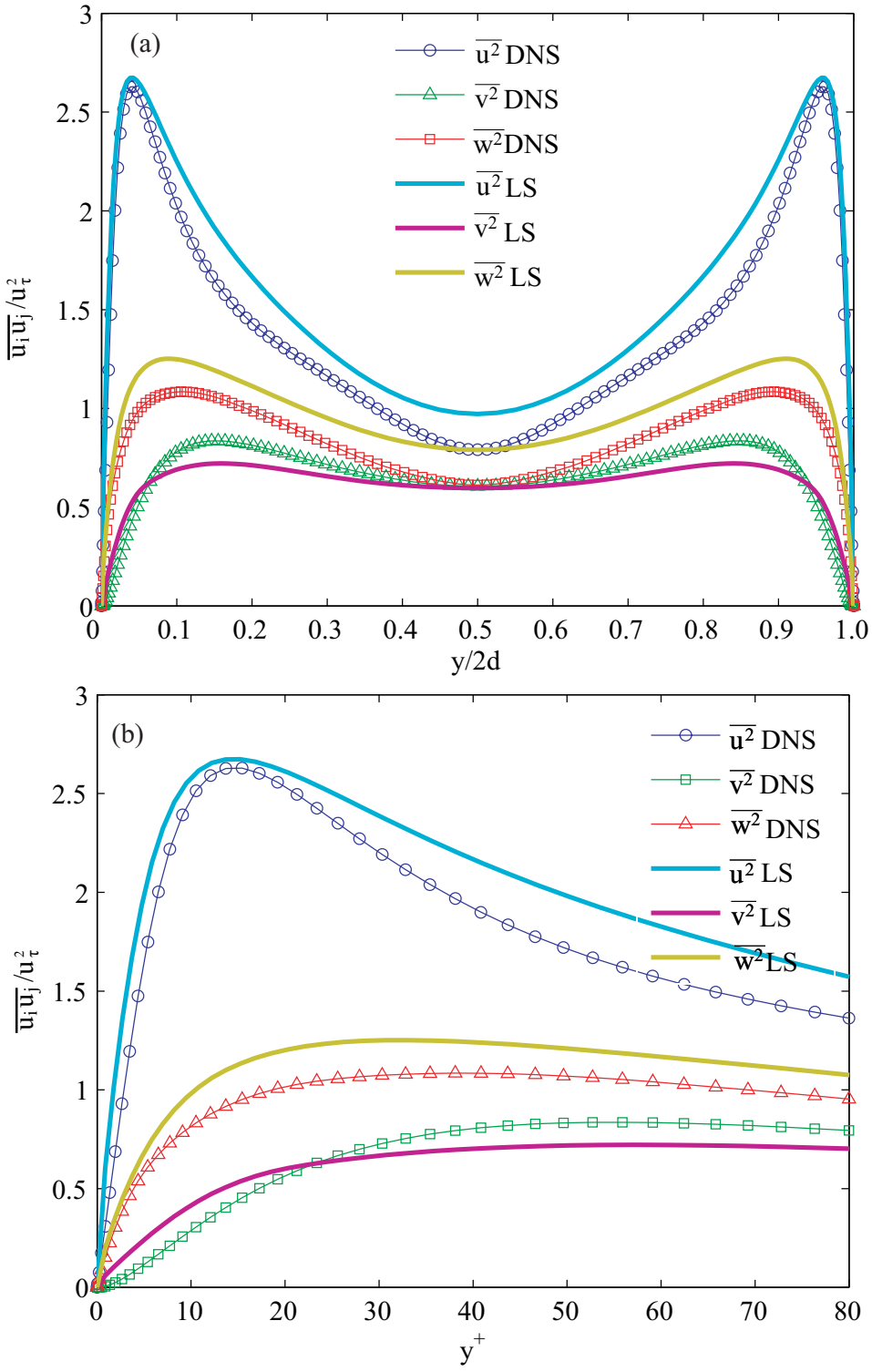

Figure 3.4: Three normal Reynolds stresses computed by LS model compared with DNS data (a) in global coordinates (b) in local coordinates

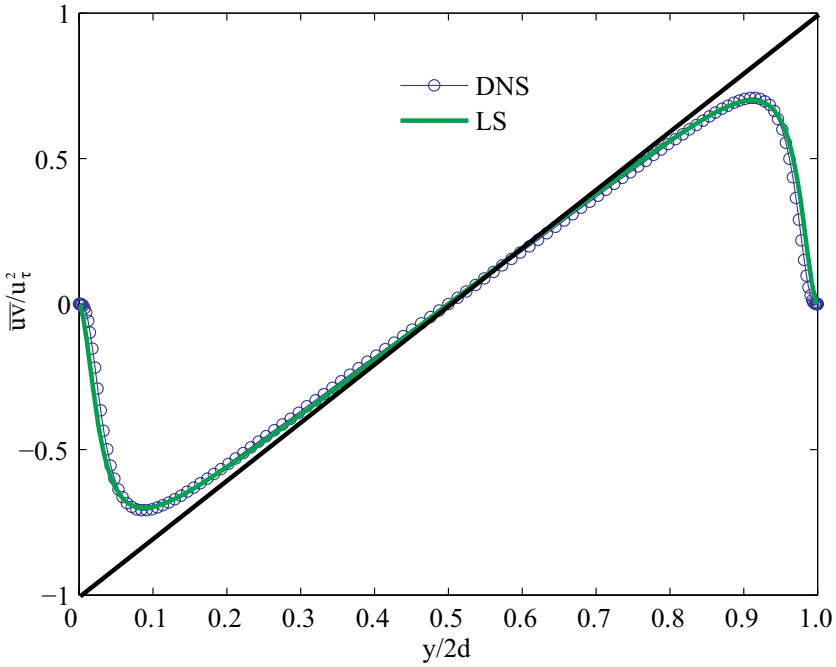

Figure 3.5: Reynolds shear stress normalized by the wall shear velocity

$Re = 5800$, and $Ro = 1.5$ at $Re = 5000$. The definition for Ro is

$$Ro = 2\Omega_3 d/U_m. \tag{3.16}$$

Fig. 3.7 compares the mean velocity represented by this work and those from DNS. The vertical axis is normalized by the bulk mean velocity U_m, and the horizontal axis by the channel width $2d$. The left ($y/2d = 0$) and right ($y/2d = 1$) hand sides of the figure correspond to the pressure and suction sides, respectively. The result by DNS indicates that the velocity profile becomes gradually asymmetric about the center as the rotation number increases. The LS model represents this tendency fairly well up to $Ro = 0.5$. As for the higher rotation, however, the LS model gives parabolic velocity profile contrary to the asymmetric one given by DNS. A true fact is that, for relatively high rotation number, e.g. $Ro = 1.5$, the turbulent flow shows the trend of relaminarization (Dutzler *et al.*, 2000; Lamballais *et al.*, 1998; Liu & Lu, 2007; Pallares & Davidson, 2000). It appears that LS model has over predicted this trend by giving a laminar-like velocity profile.

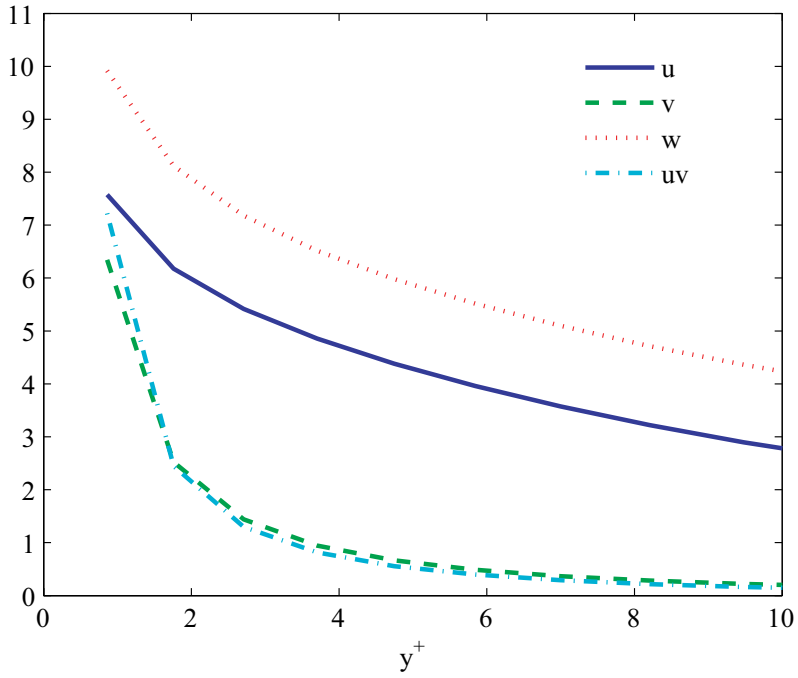

Figure 3.6: Near-wall behavior of Reynolds stresses

The three normal Reynolds stress components, $\overline{u^2}$, $\overline{v^2}$, $\overline{w^2}$ and the shear stress $\overline{uv}$ are presented in Figs. 3.8 - 3.11 with the same condition as for the mean velocity profile in Fig. 3.7. The overall tendency shown by the results of DNS is that the Reynolds stresses are damped along the suction side and enhanced along the pressure side. The computation of LS model represents the similar tendency, and shows fairly well agreement with DNS generally for Ro up to 0.5. Whereas, as was the case shown in mean velocity profile, the agreement with DNS becomes worse when the Ro increases. All the Reynolds stress components nearly vanish for $Ro = 1.5$, which corresponds to the laminar-like mean velocity profile, and once again, implies that the rotation effects are over estimated in the LS model.

Different from the definition of wall shear velocity u_τ by Eq. (3.12) in the stationary case, there are two local shear velocity for pressure side and suction side, respec-

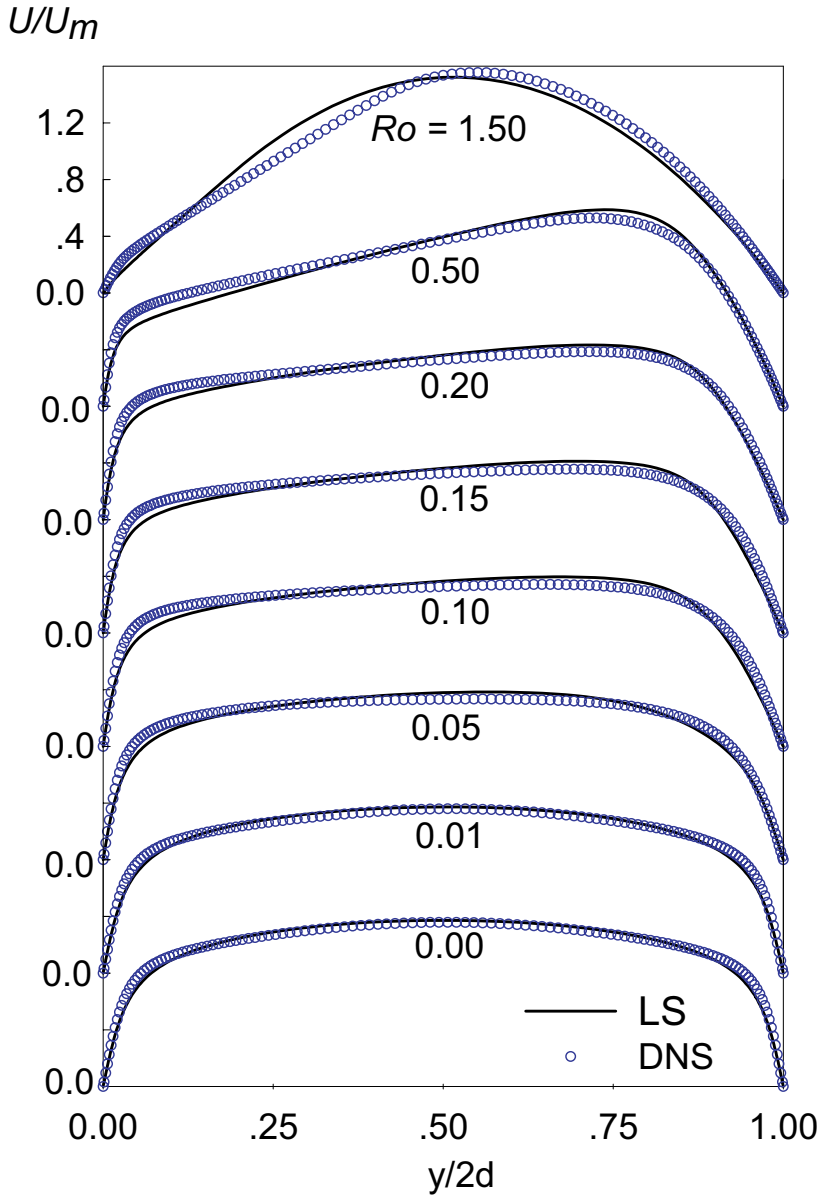

Figure 3.7: Mean velocity profile for $Re = 5800$, $Ro = 0$ - 0.5 and $Re = 5000$, $Ro = 1.5$

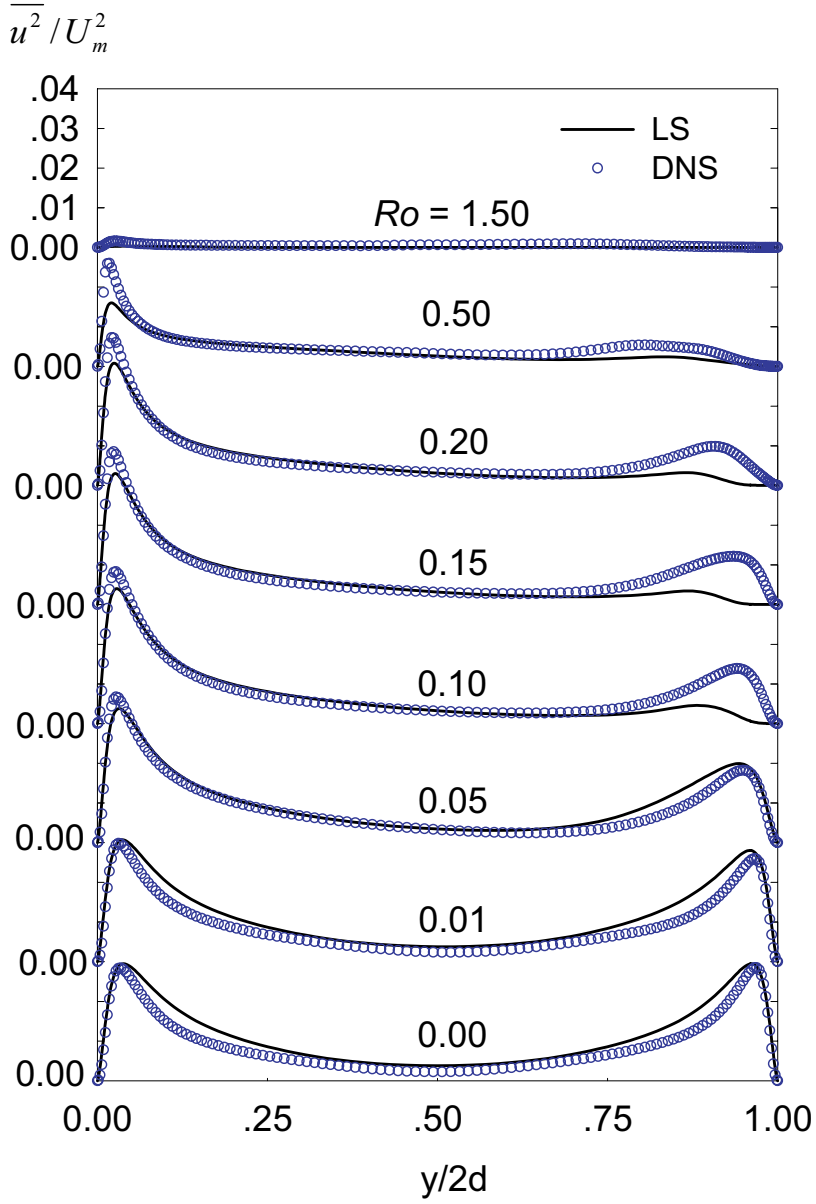

Figure 3.8: Reynolds stress $\overline{u^2}$ profile for $Re = 5800$, $Ro = 0$ - 0.5 and $Re = 5000$, $Ro = 1.5$

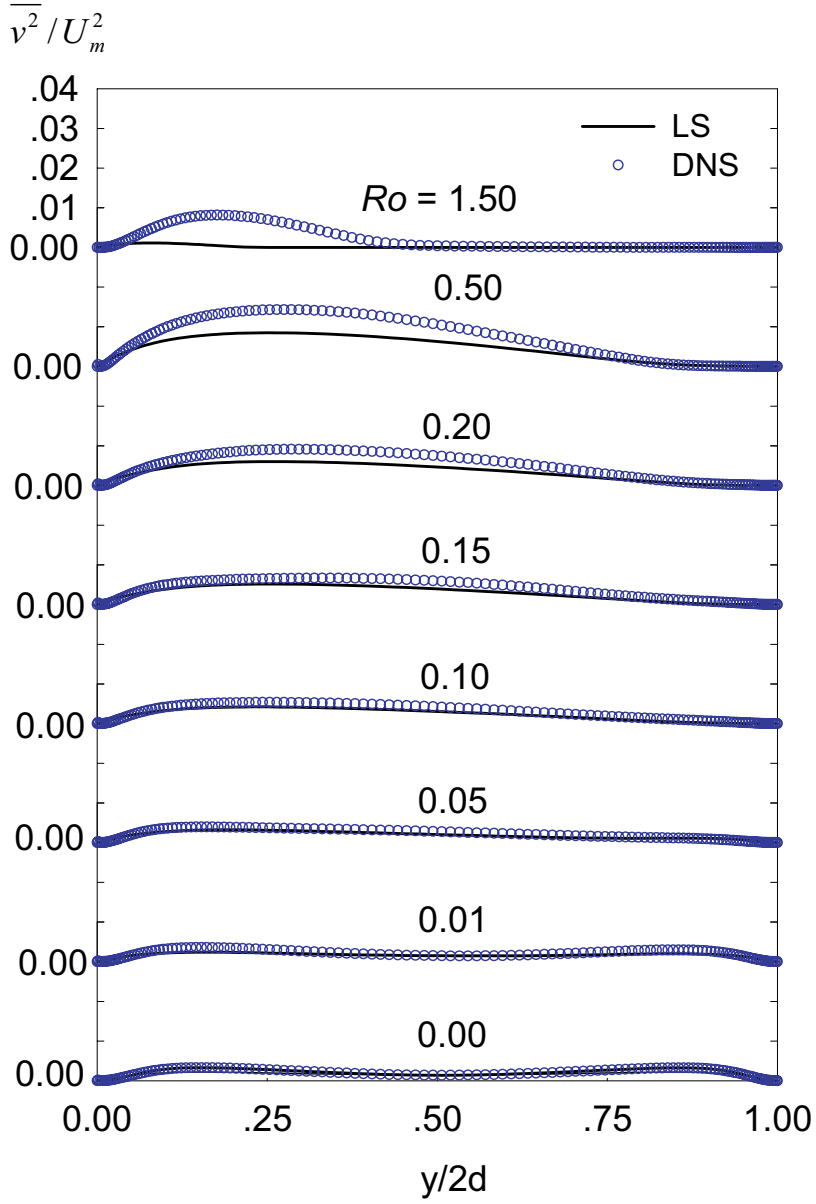

Figure 3.9: Reynolds stress $\overline{v^2}$ profile for $Re = 5800$, $Ro = 0$ - 0.5 and $Re = 5000$, $Ro = 1.5$

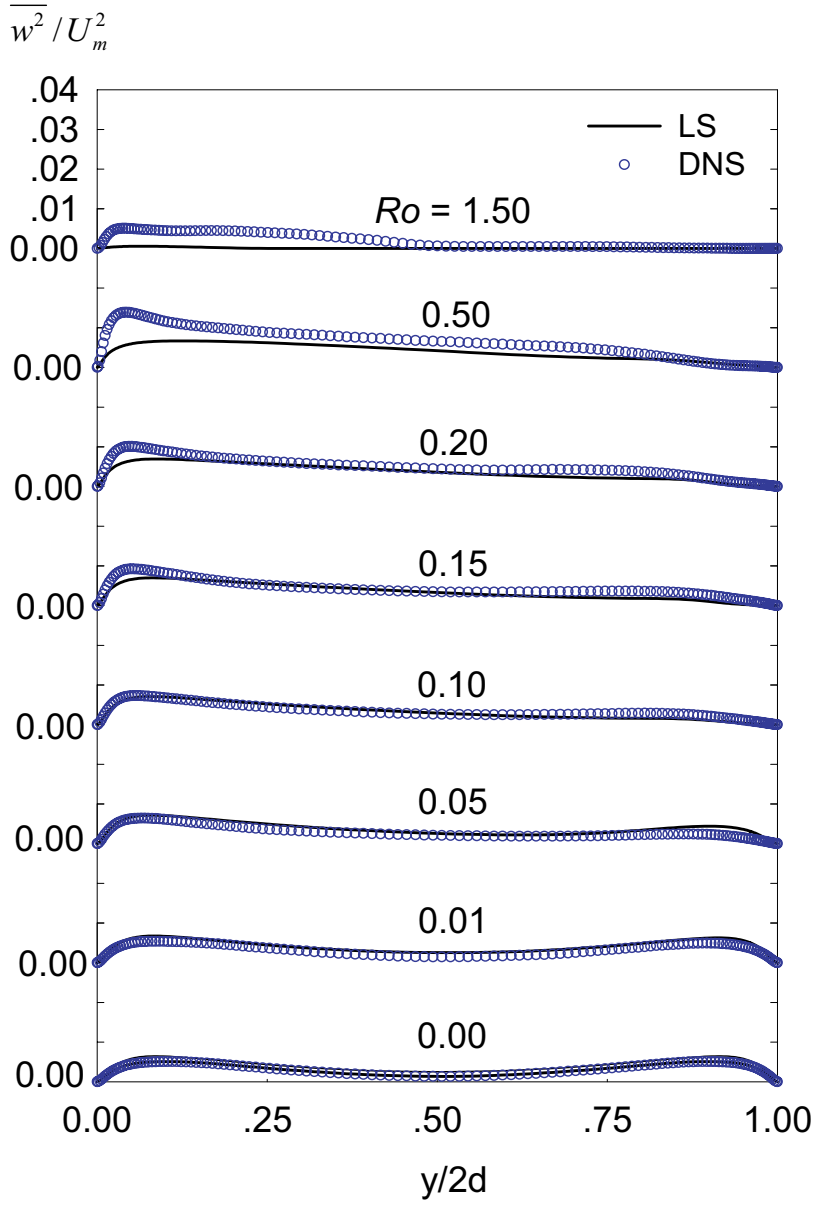

Figure 3.10: Reynolds stress $\overline{w^2}$ profile for $Re = 5800$, $Ro = 0$ - 0.5 and $Re = 5000$, $Ro = 1.5$

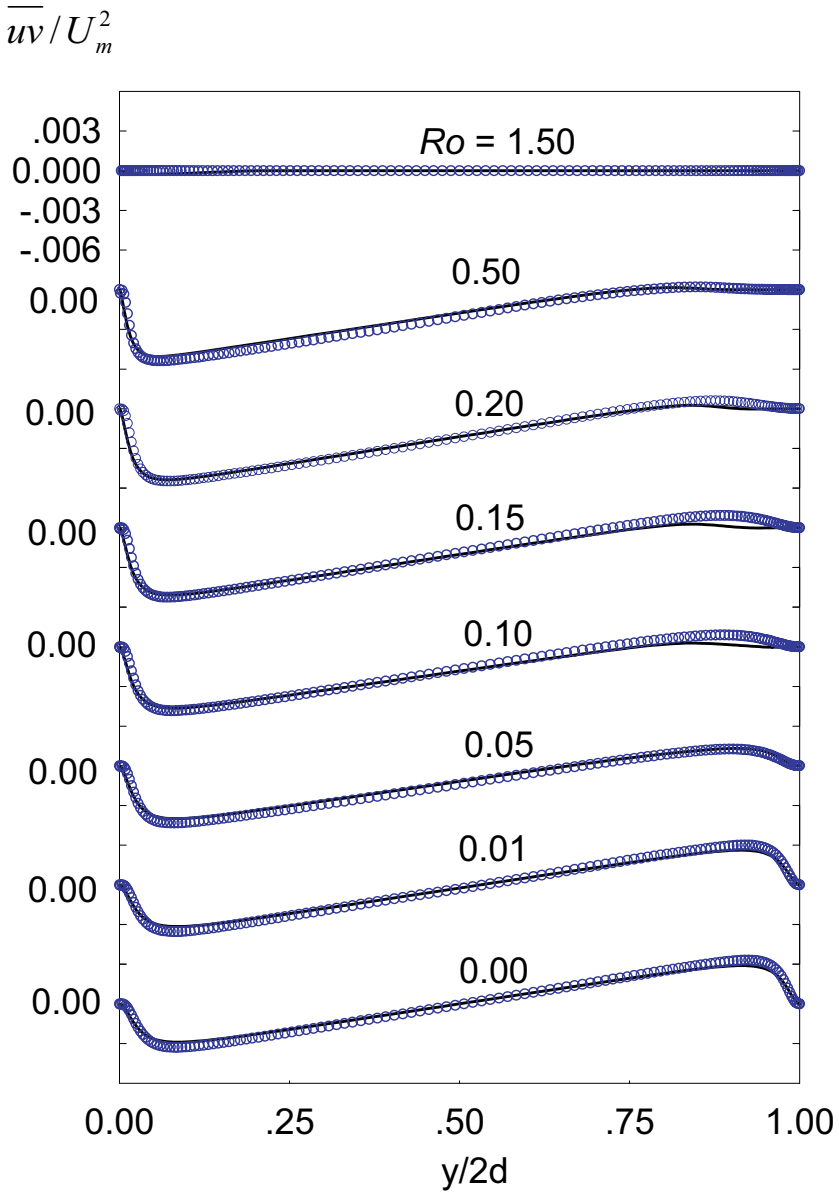

Figure 3.11: Reynolds stress $\overline{uv}$ profile for $Re = 5800$, $Ro = 0$ - 0.5 and $Re = 5000$, $Ro = 1.5$

tively:

$$u_{\tau p} = \sqrt{\nu \frac{dU}{dy}|_{p,wall}}, \tag{3.17a}$$

$$u_{\tau s} = \sqrt{\nu \frac{dU}{dy}|_{s,wall}}. \tag{3.17b}$$

Additionally, Kristoffersen & Andersson (1993) gave definition for the global shear velocity u_τ in terms of $u_{\tau p}$ and $u_{\tau s}$:

$$u_\tau^2 = \frac{1}{2}\left(u_{\tau p}^2 + u_{\tau p}^2\right). \tag{3.18}$$

It is obvious that for stationary case $(\Omega_3 = 0)$, the mean flow is symmetric with respect to the (x, z)-plane at $y = 0$ and $u_\tau = u_{\tau p} = u_{\tau s}$.

Local shear velocities, as defined in Eq. (3.17), are shown as a function of the rotation number in Fig. 3.12, also compared with those of DNS data.

The results of LS model shown in Fig. 3.12 follow the similar trend as those of Kristoffersen & Andersson (1993) and Lamballais *et al.* (1998) up to rotation number 0.5 generally, namely that the wall shear velocity is reduced on the suction side and increased on the pressure side due to stabilization and destabilization respectively. However, the results of LS model show appreciably greater rotation effect than DNS do, which implies that the LS model is somehow over-sensitive to the rotation effects. Recall that the rotation effects are included in the LS model by and only by the presence of Coriolis production and its redistribution, it is reasonable to ascribe the over-sensitivity to the model of redistribution model, since the Coriolis production is treated in an exact way.

On the other hand, for the relatively high rotation number, e.g. $Ro = 1.5$, the LS model shows its quite positive perspective, which is the ability to represent the reliminarlization phenomena. In Fig. 3.12, around the $Ro = 1.5$, the DNS of Lamballais *et al.* (1998) shows that $u_{\tau p}/u_\tau$ decreases, meanwhile the $u_{\tau s}/u_\tau$ increases. The general tendency is that the $u_{\tau p}/u_\tau$ and $u_{\tau s}/u_\tau$ tend to obtain unity eventually, which implies that the turbulent flow is relaminarlizing. The LS model represents this tendency fairly well, although it seems the flow predicted by LS model has already been

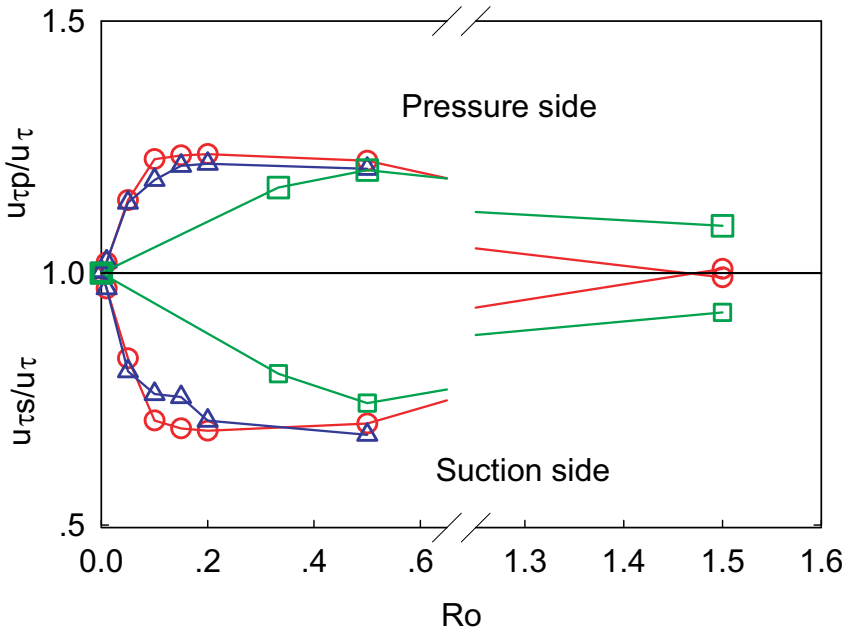

Figure 3.12: Local wall shear velocities $u_{\tau p}/u_\tau$, $u_{\tau s}/u_\tau$ as function of Ro. ◯: LS model, △: DNS by Kristoffersen & Andersson (1993), □: DNS by Lamballais *et al.* (1998).

laminarlized, since $u_{\tau p}/u_\tau$ and $u_{\tau p}/u_\tau$ are quite close to unity. This proves the previous observation that the LS seems to be over-sensitive to the rotation effects, and this is also consistent with observation of Figs. 3.8-3.11.

Fully developed turbulent flows at low Reynolds numbers in stationary and rotating channels have been simulated using a second order code with a popular differential Reynolds stress model - LS model. It shows that the LS model is able to correctly represent the global behavior of turbulence, give quite satisfactory agreement for mean velocity and Reynolds stress components both for the stationary and rotating cases. In this sense, it implies that the second-moment closure in this study does capture the main effects of rotation on the turbulence structure. In particular, the different behavior near the two walls has been traced to the fact the imposed rotating effects damp the turbulence intensity along the suction side and enhance it along the pressure side, which shows the potential that differential Reynolds stress model possesses for predicting the turbulent rotating flows.

On the other hand, however, the fact that the LS model fails to give good agreement

with DNS data for high rotation number indicates the requirement of further development for LS model. The analyses on mean velocity, Reynolds stresses, as well as the local wall shear velocities, suggest that the LS model seems to be over-sensitive to the rotation effects, which could be the future direction for the improvement of the model. Since the terms other than the pressure strain-rate are treated in an exact manner to include the rotation effects in the LS model, it is suggested that the more attention should be paid for the pressure strain-rate term, to correctly include the rotation effects.

3.2 Evaluation of eddy viscosity models considering rotation effects

As well known fact, an inherent shortcoming of eddy viscosity type of models is that they are independent of imposed system rotation. So when the EVMs are applied for curvature or rotating flow, some modifications have to be made to sensitize such models to Coriolis force. A common practice is to modify the turbulent length scale by adding rotating dependent terms to the dissipation rate equation; another way is to introduce the vorticity tensors to sensitize the rotation effects.

In this section, the predictive capability of linear and nonlinear eddy viscosity models will be evaluated systematically, for fully developed non-rotating and rotating channel flow. In this case, the imposed rotation breaks the symmetry of the flow field and may eventually lead to relaminarization on the stable side of the channel. For the EVM models, they all require the solutions of two transport equations: equation for turbulent kinetic energy and one for turbulent dissipation rate. For the incompressible, fully developed rotating channel flow, these two equations have the following simplified expressions

$$\nu_t = f_\mu C_\mu k \tau, \tag{3.19a}$$

$$0 = P - \varepsilon + D + \frac{d}{dy}\left[\left(\nu + \frac{\nu_t}{\sigma_\varepsilon}\right)\frac{dk}{dy}\right], \tag{3.19b}$$

$$0 = C^*_{\varepsilon 1} P \frac{\varepsilon}{k} - f_2 C^*_{\varepsilon 2} + E + \frac{d}{dy}\left[\left(\nu + \frac{\nu_t}{\sigma_\varepsilon}\right)\frac{d\varepsilon}{dy}\right], \tag{3.19c}$$

$$\tau = k/(\varepsilon - D). \tag{3.19d}$$

The first EVM model evaluated here is that of Howard *et al.* (1980), which is proposed to capture the rotation effects by adding rotating dependent terms to the dissipation rate equation. This model for Coriolis force effects are based on a study of curved boundary layers by Launder *et al.* (1977). In the ε equation, "on the grounds of seeking the simplest possible form", it is chosen to accommodate curvature effects by making the value of $C^*_{\varepsilon 2}$ depends on a turbulent curvature Richardson number (Ri_t).

$$Ri = \frac{-2\Omega\left(\dfrac{\partial W}{\partial x} - 2\Omega\right)}{\left(\dfrac{\partial W}{\partial x}\right)^2}. \tag{3.20}$$

Then following the practice of Launder *et al.* (1977), turbulent Richardson number is formed by replacing the mean flow time-scale represented by the denominator$(\partial W/\partial x)^2$ with a turbulence time-scale k/ε. Thus the Richardson number becomes

$$Ri_t = -2\Omega\left(\frac{k}{\varepsilon}\right)^2\left(\frac{\partial U}{\partial x} - 2\Omega\right). \tag{3.21}$$

In this Coriolis-modified eddy viscosity model, the following relations are used to close the Eq. (3.19)

$$D = -2\nu\left(\frac{\partial\sqrt{k}}{\partial y}\right)^2, \tag{3.22a}$$

$$E = 2\nu\nu_t\left(\frac{\partial S}{\partial y}\right)^2, \tag{3.22b}$$

$$f_\mu = \exp\left[-3.4\left(1 + \frac{Re_t}{50}\right)^{-2}\right], \tag{3.22c}$$

$$Re_t = \frac{k\tau}{\nu}, \tag{3.22d}$$

$$C^*_{\varepsilon 2} = \left[C_{\varepsilon 2} + 1.536S^2\tau^2\left(\frac{\Omega}{S}\right)\left(1 - \frac{\Omega}{S}\right)\right], \tag{3.22e}$$

$$f_2 = 1 - 0.3\exp\left(-Re_t^2\right), \tag{3.22f}$$

where $C_\mu = 0.09$, $C^*_{\varepsilon 1} = 1.44$, $C_{\varepsilon 2} = 1.92$, $\sigma_k = 1$, $\sigma_\varepsilon = 1.3$, and Ω is the system rotation rate. The wall boundary condition are given by $k = 0$ and $\varepsilon = 0$.

Howard *et al.* (1980) compared the solution of this model in a relatively low rotation number ($Ro = 0.21$) with the experimental data of Johnston *et al.* (1972), which

conducted experiments on water flowing in a rotating channel flow apparatus. The inclusion of a Coriols force modification to the wall function is believed to result in a markedly poor fit with the measured velocity profile. Also it is thought that the value of y^+, for the first gird spacing from the wall is too big, which was between 15 and 30.

The another eddy viscosity model reviewed here is that proposed by Shih *et al.* (1995), which introduces the vorticity tensors to the quadratic relations for Reynolds stress anisotropies

$$b_{ij} = -C_\mu^* \tau S_{ij} + c_2 \tau^2 \left(S_{ik}\overline{W}_{kj} - \overline{W}_{ik} S_{kj} \right), \tag{3.23}$$

with

$$\overline{W}_{ij} \equiv W_{ij} - \epsilon_{mij}\Omega_m, \quad \Omega_m = (0, 0, \Omega), \tag{3.24}$$

where ϵ_{ijk} is the permutation tensor.

The relations used in Shih *et al.* (1995) to close Eq. (3.19) are as

$$c_2 = -\frac{\sqrt{1 - 18C_\mu^{*2}(S\tau)^2}}{1 + 12(S\tau)^2 \left| 1 - \dfrac{\Omega}{S} \right|}, \tag{3.25a}$$

$$D = E = 0, \tag{3.25b}$$

$$f_2 = \left[1 - \exp\left(-\frac{y^+}{5.5} \right) \right]^2, \tag{3.25c}$$

$$y^+ = \frac{y u_\tau}{\nu}, \tag{3.25d}$$

$$C_\mu^* = \left[6.5 + 3\sqrt{2}\,|S\tau| \sqrt{1 - 3\frac{\Omega}{S} + \frac{9}{2}\left(\frac{\Omega}{S}\right)^2} \right]^{-1}, \tag{3.25e}$$

where u_τ is the friction velocity, $f_\mu = 1.0$, $C_\mu = 0.09$, $C_{\varepsilon 1}^* = 1.44$, $C_{\varepsilon 2}^* = 1.92$, $\sigma_k = 1$ and $\sigma_\varepsilon = 1.3$. As for the boundary condition, $k = 0$ is used at the wall, while $\varepsilon = 2\nu(\partial\sqrt{k}/\partial y)^2$ is used for the boundary condition for dissipation rate.

Once again, the Launder & Shima (1989) model is used again to compare with the EVMS, and the DNS database of Kristoffersen & Andersson (1993) is used to show the performance of above models.

As indicated from Figures 3.13-3.15, the Coriolis-modified EVM of Howard *et al.* (1980) presents quite reasonable predictions for the mean velocity and turbulent kinetic

energy at different rotation numbers. The nonlinear eddy viscosity model of Shih *et al.* (1995) fails to represent the rotation effects generally, gives unacceptable predictions for mean velocity and turbulent kinetic energy. Noted that the Coriolis-modified EVM predicts correctly the linear velocity profile on the pressure side, while the NLEVM fails to. At $Ro = 0.5$ and 1.5, it seems that NLEVM is insensitive to the rotation effects.

Once again, it is proved that the DRSM is the most rational and promising approach in the framework of RANS modeling. As shown in Figures 3.13-3.15, the DRSM gives fairly good agreement with the DNS data, and has the overall advantage compared the eddy viscosity type of model.

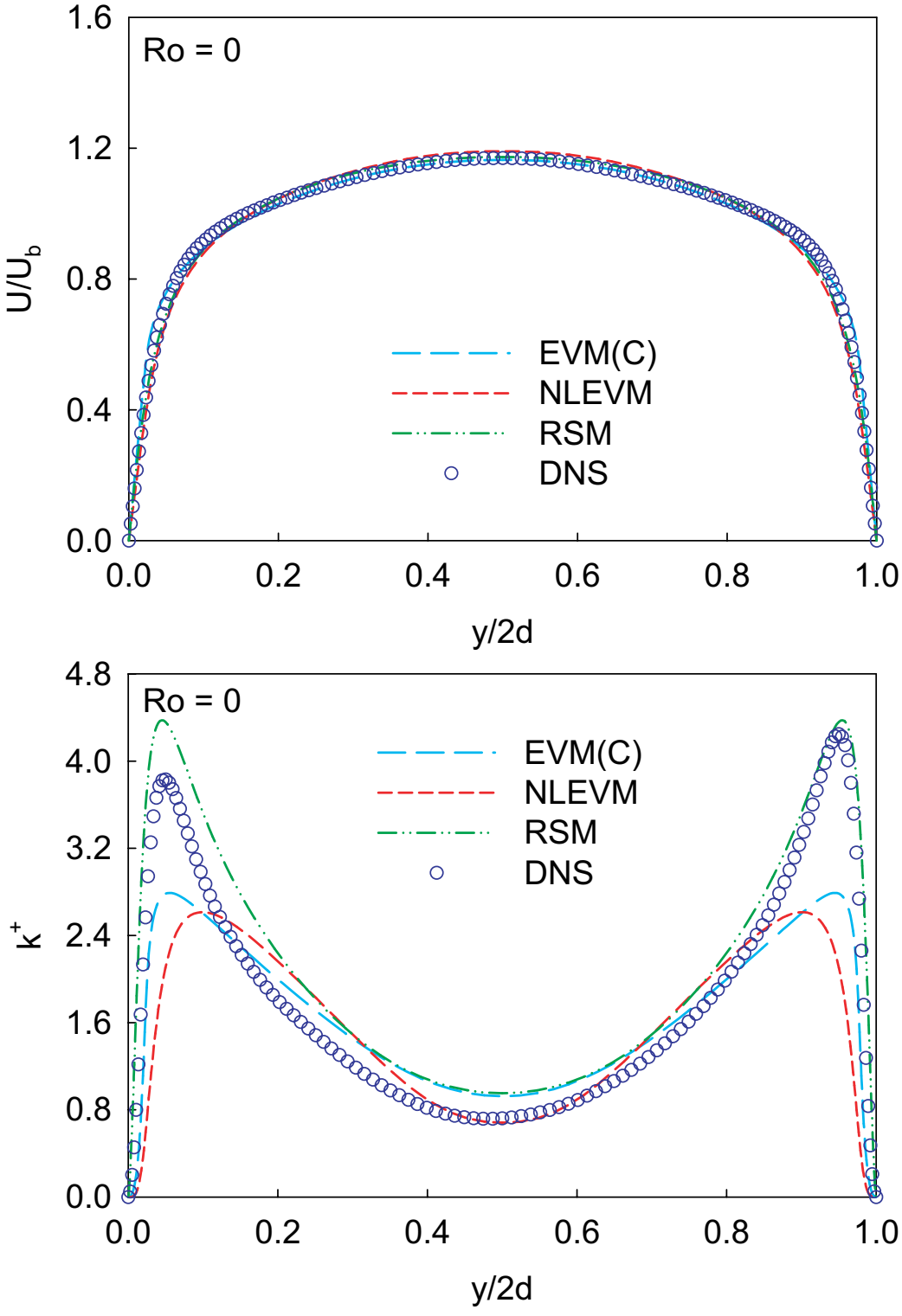

Figure 3.13: Mean velocity and turbulent kinetic energy profiles at $Ro = 0$

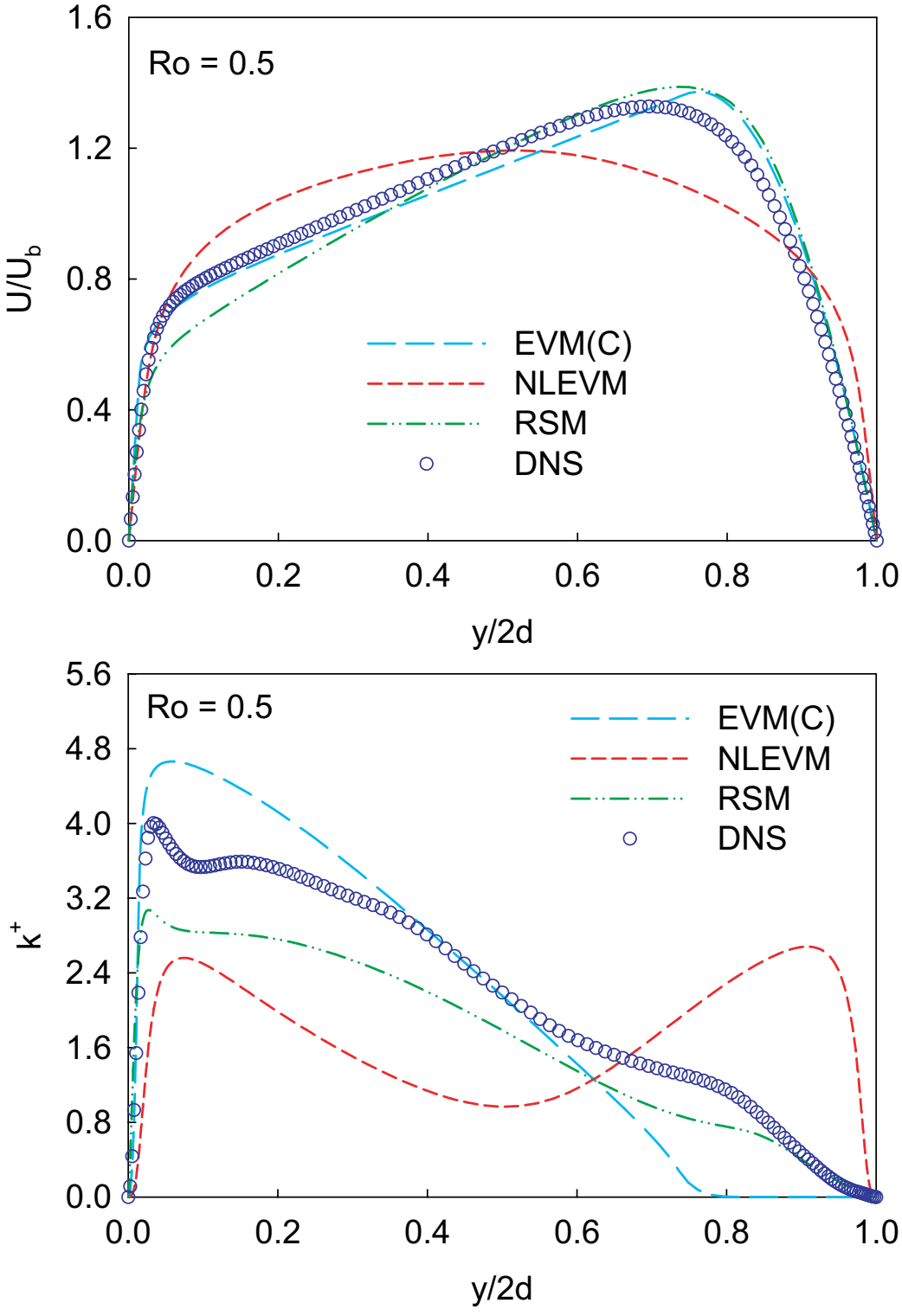

Figure 3.14: Mean velocity and turbulent kinetic energy profiles at $Ro = 0.5$

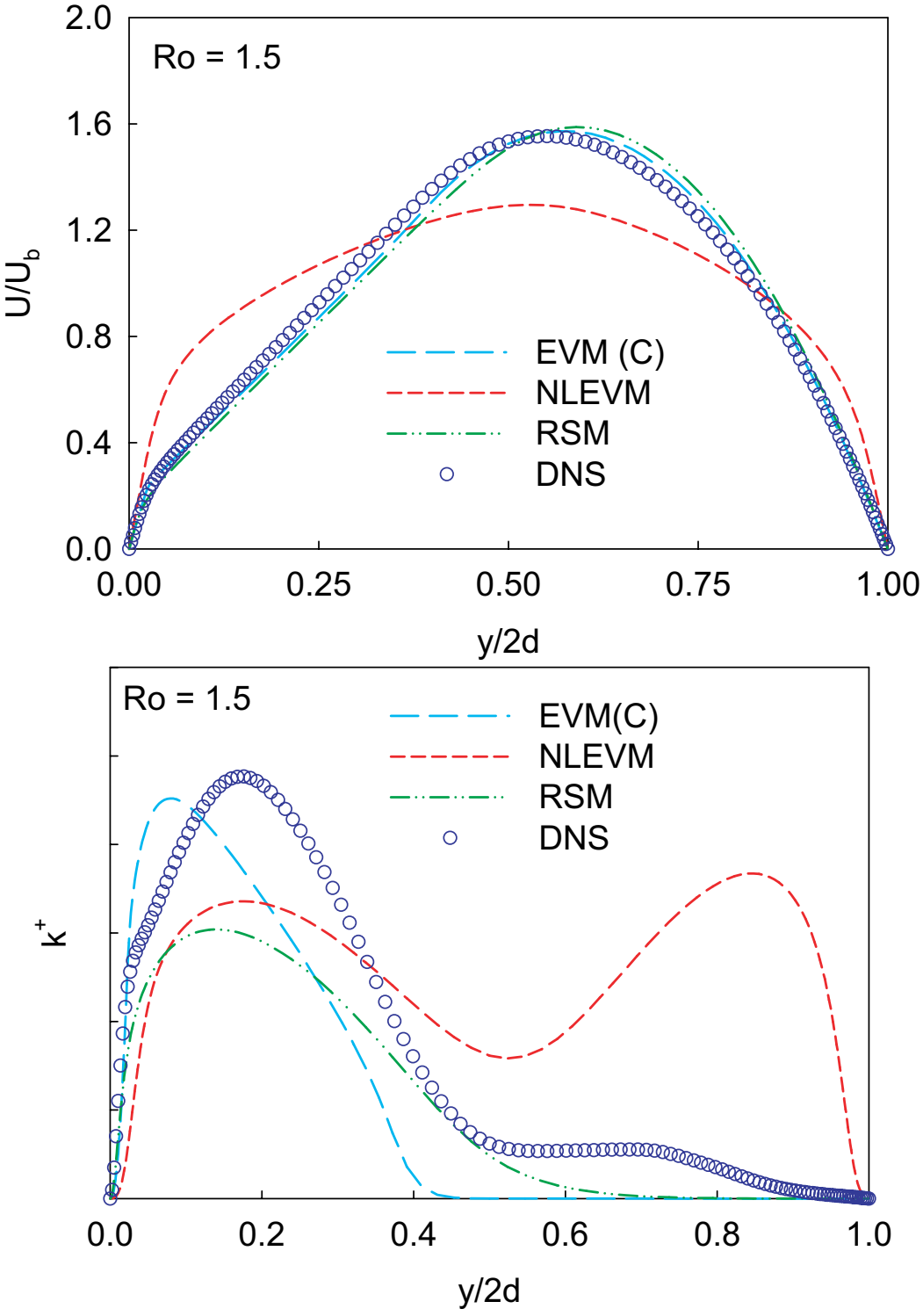

Figure 3.15: Mean velocity and turbulent kinetic energy profiles at $Ro = 1.5$

Chapter 4

Evaluation of extended weak-equilibrium conditions for Reynolds stress

4.1 Introduction

This study focuses on the validity and modification of the diffusive transport assumption in fully developed rotating channel flow. This is accomplished by an *a priori* assessment using the DNS data of Kristoffersen & Andersson (1993). This database has been selected because it has been most commonly used for model development and comparison with other DNS (Jakirlić *et al.*, 2002). Based on the asymptotic analysis of the near-wall behavior, an alternative form for the diffusive transport constraint is proposed, and evaluated using the DNS data. Results show that the newly proposed diffusive transport constraint applied to the implicit algebraic anisotropy equation more accurately accounts for the near-wall behavior than previously proposed forms. This suggests that the performance of algebraic Reynolds stress models can be improved in flows where rotation and curvature effects exist.

4.2 Evaluation of diffusive transport constraint

The fully developed rotating channel flow is adopted as a test case where the turbulence structure is strongly influenced by the Coriolis force, and differs considerably from that of the non-rotating case. There have been many experimental and computational studies of this problem (Johnston *et al.*, 1972; Kim *et al.*, 1987; Kristoffersen & Andersson, 1993; Lamballais *et al.*, 1998; Moore, 1967) that have shown that the imposed system rotation changes the dynamic structure of the turbulent flow. Consequently, the turbulence level is enhanced along the pressure side while reduced along the suction side, and the diffusive transport across the channel is increased, or changes sign. The correct representation of these rotation-induced features is an important criteria for turbulence model development.

The exact transport equation for the Reynolds stress anisotropy tensor b_{ij} in the non-inertial frame is given by

$$\begin{aligned}\frac{Db_{ij}}{Dt} &+ \Omega_{ik}b_{kj} - b_{ik}\Omega_{kj} \\ &= -b_{ij}\left(\frac{P}{k} - \frac{\varepsilon}{k}\right) - \frac{2}{3}S_{ij} - \left(b_{ik}S_{kj} + S_{ik}b_{kj} - \frac{2}{3}b_{mn}S_{mn}\delta_{ij}\right) \\ &+ \left(b_{ik}\widetilde{W}_{kj} - \widetilde{W}_{ik}b_{kj}\right) + \frac{\phi_{ij}}{2k} - \frac{1}{2k}\left(\varepsilon_{ij} - \frac{\tau_{ij}}{k}\varepsilon\right) + \frac{1}{2k}\left(\mathcal{D}_{ij} - \frac{\tau_{ij}}{k}\mathcal{D}\right), \quad (4.1)\end{aligned}$$

with S_{ij} being the mean strain rate tensor, W_{ij} being the mean vorticity tensor and $\widetilde{W}_{ij} = W_{ij} + \Omega_{ij}$, $\Omega_{ij} = \epsilon_{imj}\omega_m$ with ω_m being the system rotation rate. In Eq. (4.1), D_{ij} has the same form as shown in Eq. (1.3). The terms on the right-hand side include the pressure-strain rate correlation ϕ_{ij} and the turbulent dissipation rate ε_{ij}. These terms are given by

$$\phi_{ij} = \overline{\frac{p}{\rho}\left(\frac{\partial u_i}{\partial x_j} + \frac{\partial u_j}{\partial x_i}\right)}, \quad (4.2a)$$

$$\varepsilon_{ij} = 2\nu\overline{\frac{\partial u_i}{\partial x_k}\frac{\partial u_j}{\partial x_k}}. \quad (4.2b)$$

The other terms come from the turbulent kinetic energy equation

$$\frac{Dk}{Dt} = P - \varepsilon + \mathcal{D}, \quad (4.3)$$

where the right-hand side represents the turbulent production $P = -\tau_{ik}\partial U_i/\partial x_k$, the isotropic turbulent dissipation rate $\varepsilon = \varepsilon_{ii}/2$ and the combined effects of turbulent transport, pressure transport and viscous diffusion $\mathcal{D}$.

By invoking the assumption of anisotropy equilibrium $Db_{ij}/Dt = 0$, one can reduce and rewrite Eq. (4.1) as

$$0 = \frac{1}{2k}\left(P_{ij} + C_{ij} - \frac{\tau_{ij}}{k}P\right) + \frac{1}{2k}\phi_{ij} - \frac{1}{2k}\left(\varepsilon_{ij} - \frac{\tau_{ij}}{k}\varepsilon\right) + \frac{1}{2k}\left(\mathcal{D}_{ij} - \frac{\tau_{ij}}{k}\mathcal{D}\right), \quad (4.4)$$

$$\begin{aligned} P_{ij} &= -\tau_{ik}\frac{\partial U_j}{\partial x_k} - \tau_{jk}\frac{\partial U_i}{\partial x_k} \\ &= -\frac{4}{3}kS_{ij} - 2k\left(b_{ik}S_{kj} + S_{ik}b_{kj}\right) + 2k\left(b_{ik}W_{kj} - W_{ik}b_{kj}\right), \quad (4.5a) \\ C_{ij} &= -4k\left(\epsilon_{imk}\omega_m b_{kj} + \epsilon_{jmk}\omega_m b_{ki}\right), \quad (4.5b) \end{aligned}$$

where $P_{ij} + C_{ij} - (\tau_{ij}/k)P$ is the production term, ϕ_{ij} is the redistribution term, $\varepsilon_{ij} - (\tau_{ij}/k)\varepsilon$ is the dissipation term, and $\mathcal{D}_{ij} - (\tau_{ij}/k)\mathcal{D}$ is the diffusive transport term. Note that the rotation effects are represented by the term C_{ij}.

The validity of the original diffusive transport assumption associated with Eq. (1.2) is examined. The budget of Eq. (4.4) is evaluated using DNS data of Kristoffersen & Andersson (1993). All the dependent variables including the higher-order correlations are obtained directly from the DNS, and they have been non-dimensionalized by ν and u_τ, where ν is the kinematic viscosity and u_τ is the friction velocity. The database used here contains DNS carried out for $Re_b = 2U_b d/\nu = 4800$, with Re_b being the bulk Reynolds number based on the channel half width d and the mean flow velocity U_b. The rotation number is defined by

$$Ro = 2|\omega_m|d/U_b. \quad (4.6)$$

Figures 4.1 and 4.2 show the budget of Eq. (4.4) for the b_{11}- and b_{12}-components for the $Ro = 0.0$, 0.15 and 0.50 cases. Note that hereafter all the budget terms are multiplied by $2k$ for better illustration as the legends shown in the plots. Since the production term is shown to vanish at the wall, the redistribution term balances the diffusive transport term plus the dissipation term for all three rotation numbers. As expected, the diffusive transport term plays a crucial role in the b_{ij} transport equation

in the near-wall region. Thus, any diffusive transport constraint that neglects the diffusive transport term, such as Eq. (1.2), is unlikely to hold for the near-wall region. In the center of the channel, the absolute levels of the diffusive transport term are not negligibly small. Although this suggests that neglect of the diffusive transport term is also unlikely to hold for the center of the channel, the present study will focus on the diffusive transport constraint in the near-wall region.

Gatski & Rumsey (2001) re-examined the assumption Eq. (1.2) applied to the $\mathcal{D}_{ij}$ and proposed a modification. If Eq. (1.2) is rewritten in terms of the anisotropy tensor b_{ij},

$$\mathcal{D}_{ij} - \frac{\tau_{ij}}{k}\mathcal{D} = \mathcal{D}_{ij} - \frac{2}{3}\mathcal{D}\delta_{ij} - 2\mathcal{D}b_{ij} \ , \tag{4.7}$$

the right-hand side of Eq. (4.7) is shown to be the sum of the deviatoric part of $\mathcal{D}_{ij}$ and a term proportional to the anisotropy tensor b_{ij} with scalar coefficient $\mathcal{D}$. The term proportional to the deviatoric part of $\mathcal{D}_{ij}$ is then assumed to vanish, that is

$$\mathcal{D}_{ij} - \frac{2}{3}\mathcal{D}\delta_{ij} = 0 \ , \tag{4.8}$$

and the new constraint on diffusive transport term is then given by

$$\mathcal{D}_{ij} - \frac{\tau_{ij}}{k}\mathcal{D} = -2\mathcal{D}b_{ij} \ . \tag{4.9}$$

Applying the extended constraint to Eq. (4.4), one has the reduced transport equation for b_{ij}

$$0 = \frac{1}{2k}\left(P_{ij} + C_{ij} - \frac{\tau_{ij}}{k}P\right) + \frac{\phi_{ij}}{2k} - \frac{1}{2k}\left(\varepsilon_{ij} - \frac{\tau_{ij}}{k}\varepsilon\right) - \frac{\mathcal{D}}{k}b_{ij} \ . \tag{4.10}$$

Now consider the *a priori* evaluation of the extended constraint. The left-hand side of Eq. (4.9) is substituted with DNS data, and compared the right-side of Eq. (4.9). Additionally, considering the actual form that diffusive transport term appears in the transport equation of b_{ij}, it is more straightforward to scale both sides of Eq. (4.9) by $2k$.

For the non-rotating case, Figure 4.3 shows that this extended diffusive transport constraint gives rather larger or opposite sign values in the near-wall region for all Reynolds stress components than the DNS does. For the rotating cases, Figures 4.4-4.5 display the same trends as the non-rotating case. Thus, the extended diffusive

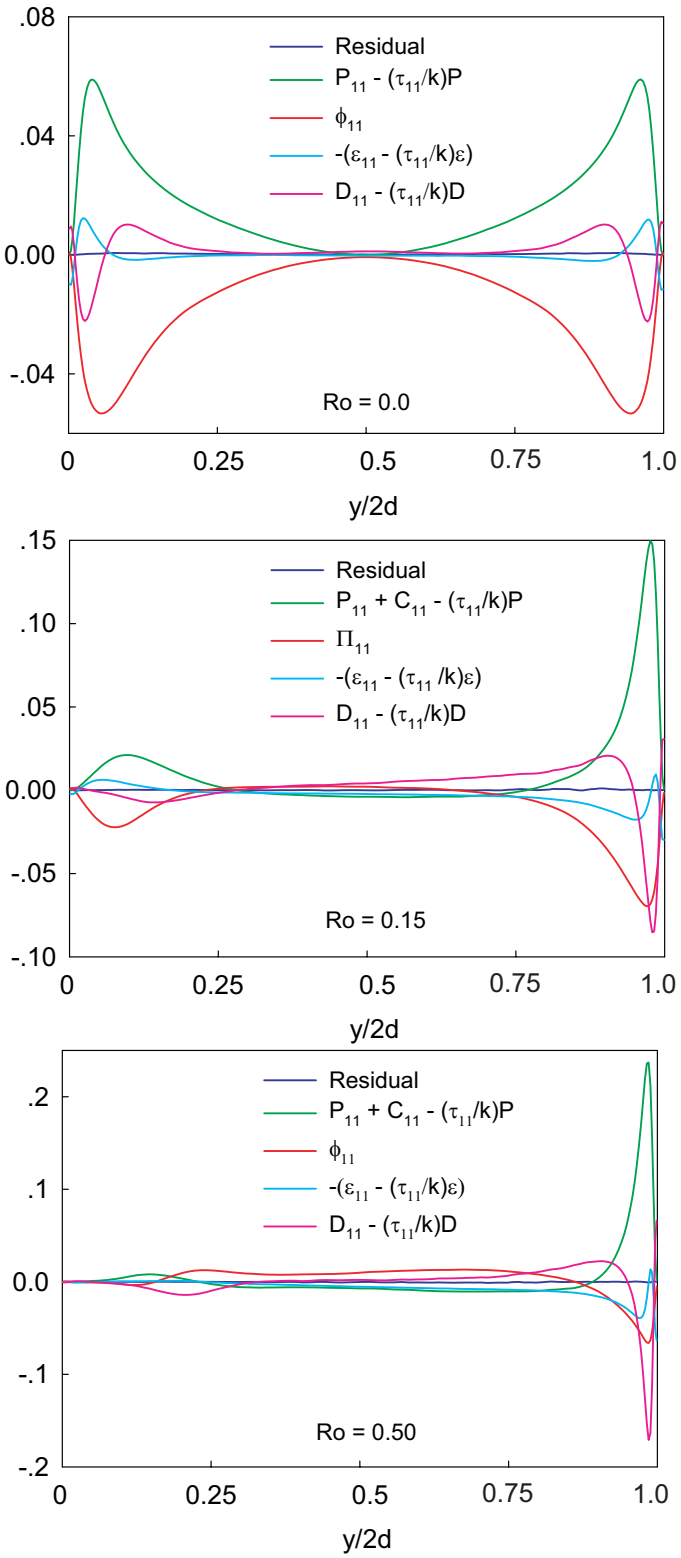

Figure 4.1: The budget of different scaled terms in Eq. (4.4) for b_{11}

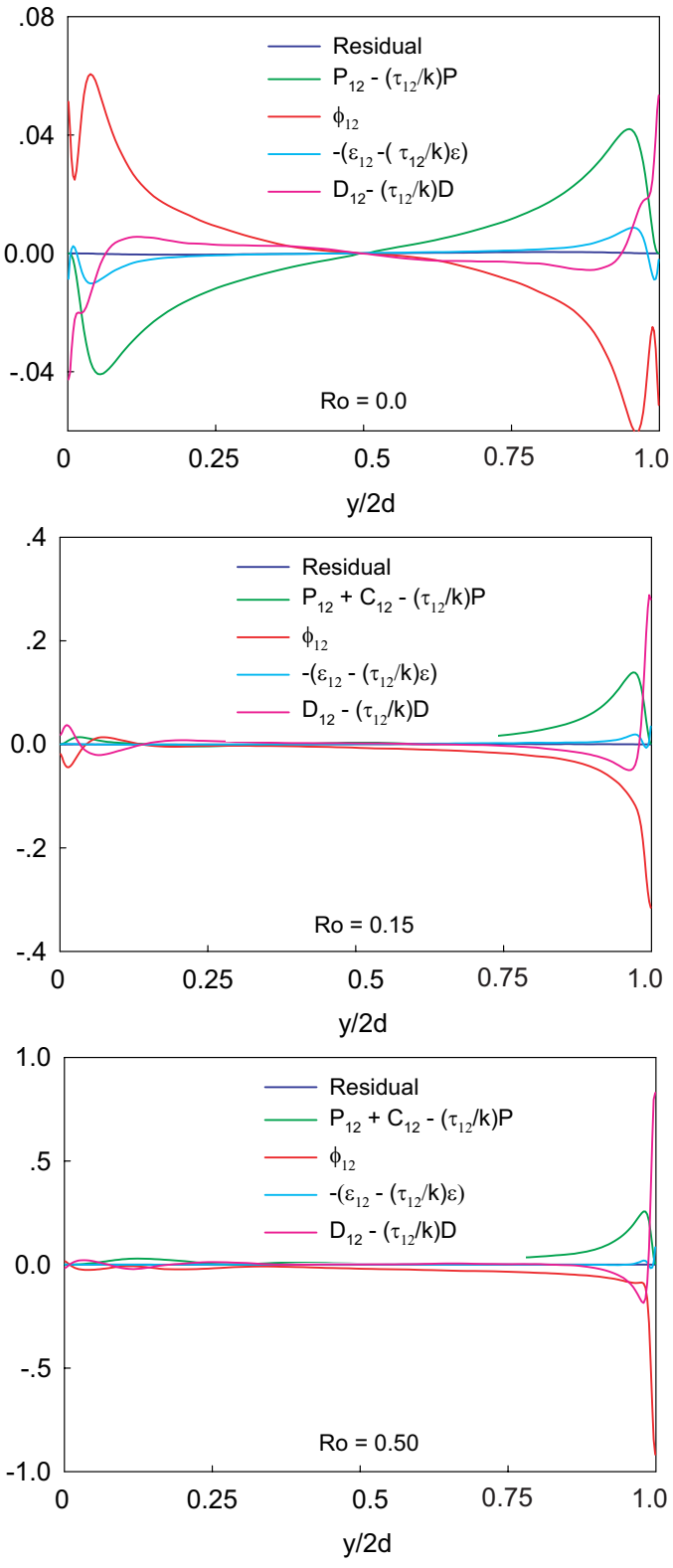

Figure 4.2: The budget of different scaled terms in Eq. (4.4) for b_{12}

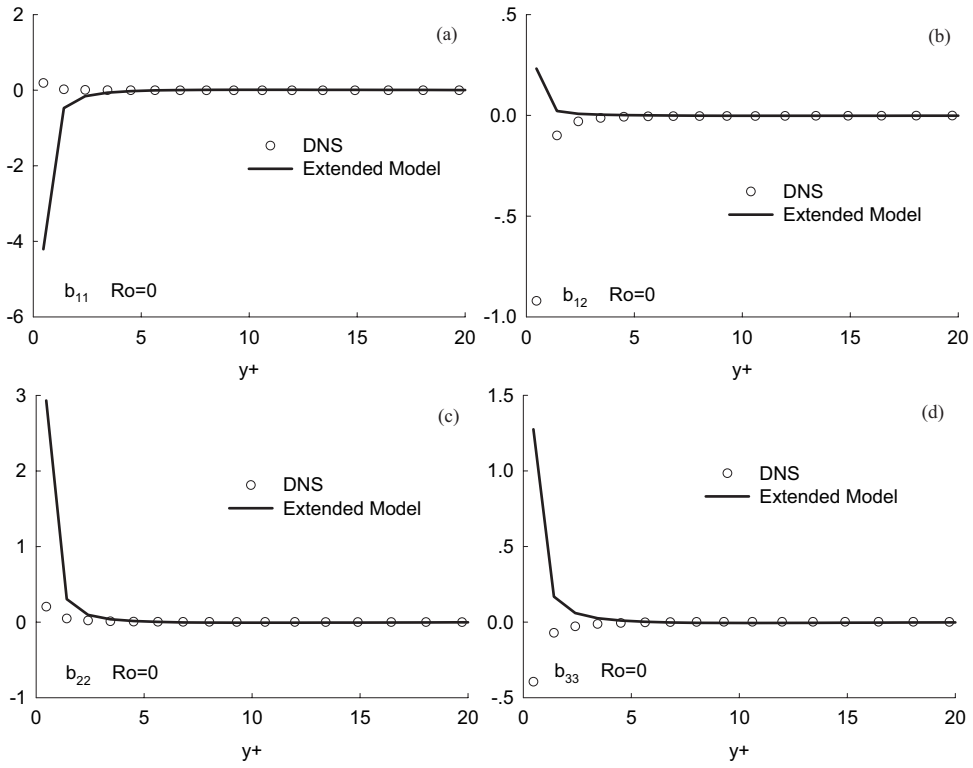

Figure 4.3: Validation of extended diffusive transport constraint for $Ro = 0$

transport constraint proposed by Gatski & Rumsey (2001) is not capable of improving the performance of ARSM in the near-wall region. While it may be a consistent first approximation to assume that a constraint on the diffusive transport term should be proportional to the Reynolds stress anisotropy b_{ij}, it is also necessary that some account be explicitly taken of the presence of the wall. Rather than pursuing such a modification, a more beneficial approach is to investigate the asymptotic behavior of the various terms in the vicinity of the wall.

4.3 Near-wall behavior of Reynolds stress equation

The discussion now will be focused on the possible modification to improve the diffusive transport constraint by the means of budget analysis. To analyze the near-wall behavior of individual terms in Eq. (4.4), the velocity and pressure fluctuations in the wall vicinity can be expanded as shown in Eq. (3.14).

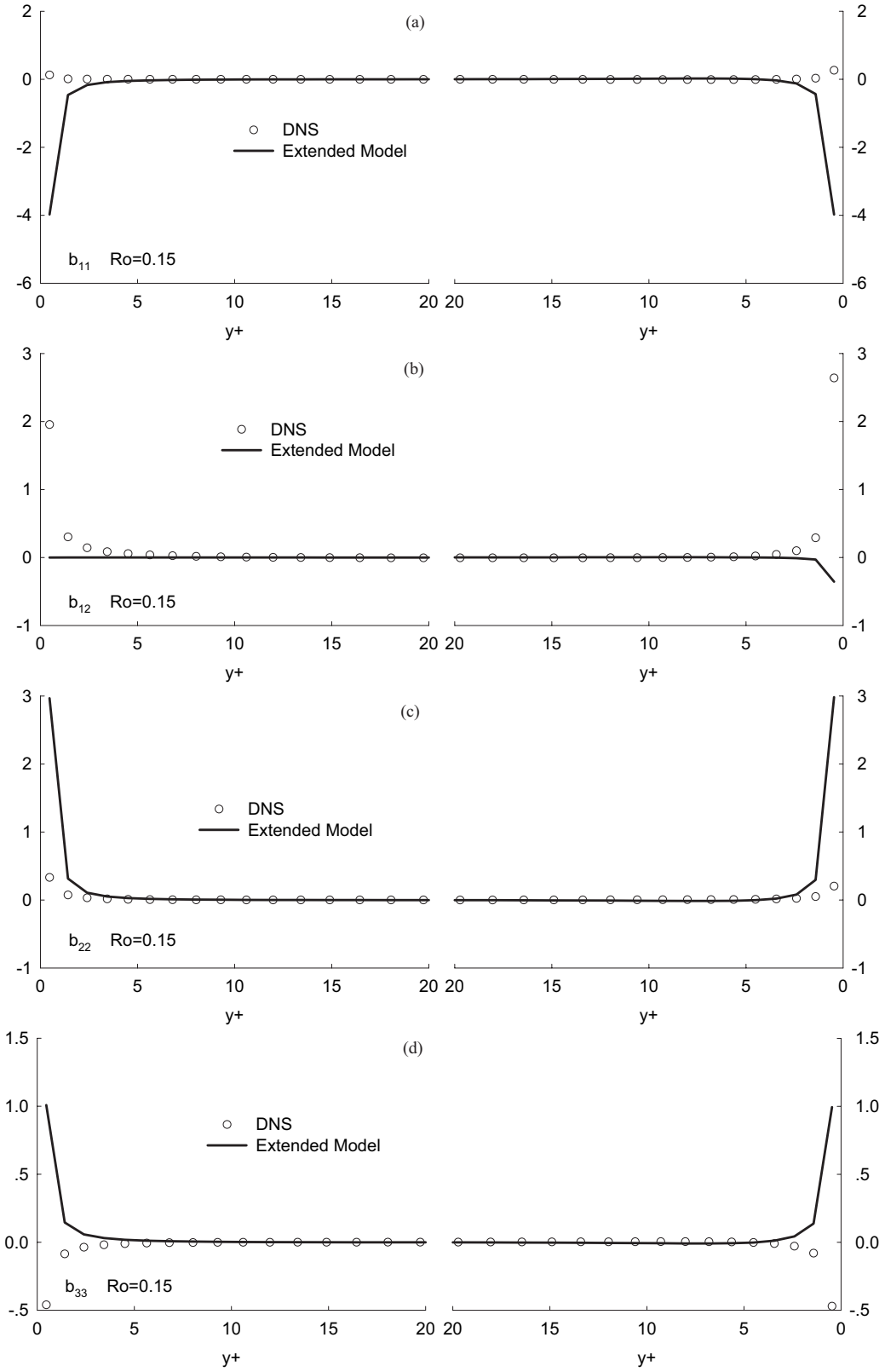

Figure 4.4: Validation of extended diffusive transport constraint for $Ro = 0.15$ (*lhs*: suction side, *rhs*: pressure side)

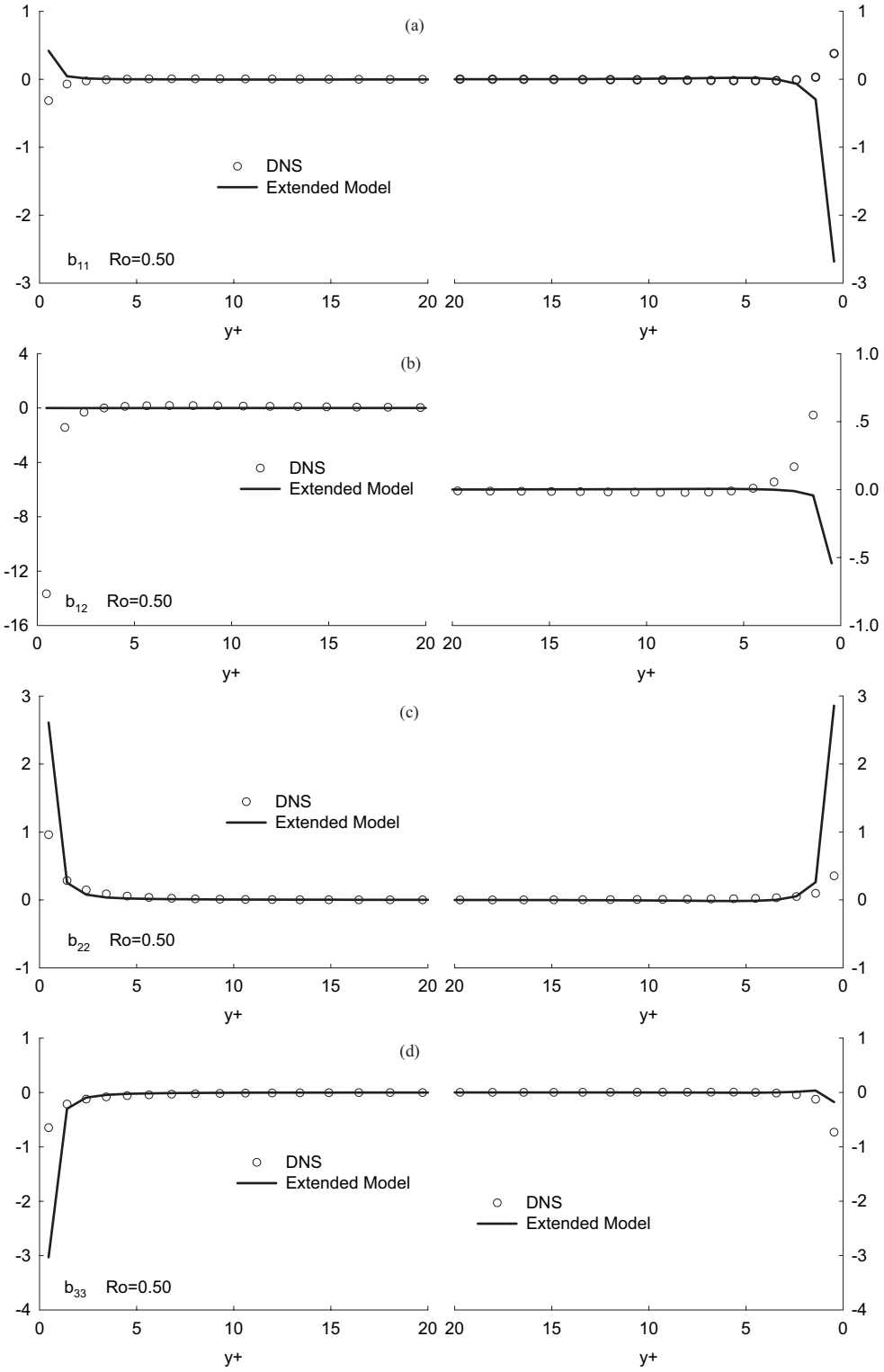

Figure 4.5: Validation of extended diffusive transport constraint for $Ro = 0.50$ (*lhs*: suction side, *rhs*: pressure side)

$$u^+ = b_1 y^+ + \cdots , \tag{4.11a}$$
$$v^+ = c_2 y^{+2} + \cdots , \tag{4.11b}$$
$$w^+ = b_3 y^+ + \cdots , \tag{4.11c}$$
$$p^+ = a_p + b_p y^+ + \cdots , \tag{4.11d}$$

where wall units are used (normalization by kinematic viscosity ν and the friction velocity u_τ).

For the b_{11} equation, the near-wall asymptotic behavior of budget can be expressed as

$$P_{11} + C_{11} - \frac{\overline{u^2}}{k} P = \left(\frac{-2\overline{b_3^2}}{\overline{b_1^2} + \overline{b_3^2}} + 4\Omega_3^+ \right) \overline{b_1 c_2} y^{+3} + \cdots , \tag{4.12a}$$
$$\phi_{11} = 2\overline{a_p b_{1,1}} y^+ + 2 \left(\overline{a_p c_{1,1}} + \overline{b_p b_{1,1}} \right) y^{+2} + \cdots , \tag{4.12b}$$
$$\varepsilon_{11} - \frac{\overline{u^2}}{k} \varepsilon = 8 \frac{\overline{b_1 c_1 b_3^2} + \overline{b_3 c_3 b_1^2}}{\overline{b_1^2} + \overline{b_3^2}} + \cdots , \tag{4.12c}$$
$$\mathcal{D}_{11} - \frac{\overline{u^2}}{k} \mathcal{D} = \frac{4\overline{b_1^2} \overline{a_p c_2} - 12\overline{b_1^2} \overline{b_3 c_3} + 12\overline{b_3^2} \overline{b_1 c_1}}{\overline{b_1^2} + \overline{b_3^2}} + \cdots . \tag{4.12d}$$

Note that the left-hand sides of the above equations are in wall unit but the symbols are retained for simplicity.

For the $Ro = 0$ case, the budget of the b_{11}-component in Figure 4.6 shows that the production term is the dominant source in the range $y^+ \geq 10$, while the redistribution term is the dominant sink. In the vicinity of the wall, the production term and redistribution term decay rapidly, while the dissipation and diffusive transport terms balance each other up to the wall. For the $Ro = 0.15$ and $Ro = 0.50$ cases, it is readily observed that the rotation effect plays a significant role in the budget, since the flow structure is significantly different compared with the non-rotating case. However, the relative balance between the different terms in the budget remains roughly similar to the non-rotating case.

Recall that in the original formulation for the ARSM, assumptions on the isotropic behavior of the tensor dissipation rate, $\varepsilon_{ij} = 2\varepsilon\delta_{ij}/3$, and the anisotropy of the diffusive transport term $\mathcal{D}_{ij} = (\tau_{ij}/k)\mathcal{D}$ are made. However, Figure 4.6 has shown that the

contributions from the dissipation rate term and the diffusive transport term balance, but are not negligible in the near-wall region. This then requires that the remaining terms in the equation balance each other in the near-wall region.

For b_{12} equation, wall asymptotic behavior of terms in Eq. (4.4) can be expressed as

$$P_{12} + C_{12} - \frac{\overline{uv}}{k}P = -2\Omega_3^+ \overline{b_1^2} y^{+2} + \cdots , \tag{4.13a}$$

$$\phi_{12} = \overline{a_p b_1} + \left(2\overline{a_p c_1} + 2\overline{c_2 b_1}\right) y^+ + \cdots , \tag{4.13b}$$

$$\varepsilon_{12} - \frac{\overline{uv}}{k}\varepsilon = 2\overline{b_1 c_2} y^+ + \cdots , \tag{4.13c}$$

$$\mathcal{D}_{12} - \frac{\overline{uv}}{k}\mathcal{D} = -\overline{a_p b_1} - 2\overline{a_p c_1} y^+ + \cdots . \tag{4.13d}$$

Figure 4.7 shows the budget of the b_{12} equation. For the non-rotating and rotating cases, the dominant source is the production term, while the dominant sink is the redistribution term through most of the channel. As the wall is approached, the dissipation term decays as $\mathcal{O}(y^+)$, and the production term decays faster as $\mathcal{O}(y^{+2})$. The redistribution term remains large, and remains in balance with diffusive transport term for $y^+ \leq 10$. The asymptotic analysis also shows that in the wall vicinity, the redistribution and diffusive transport terms decay as $\mathcal{O}(y^0)$. At the wall, the redistribution term is equal to the diffusive transport term.

In the RANS formulation, the velocity pressure-gradient term Π_{ij} is usually split into a pressure transport $\mathcal{D}_{ij}^p$ term and a redistribution term ϕ_{ij} (Mansour *et al.*, 1988). The corresponding expansions of these three terms for the b_{12}-component are

$$\Pi_{12} = -2\overline{b_1 c_2} y^+ + \cdots , \tag{4.14a}$$

$$\phi_{12} = \overline{a_p b_1} + 2\left(\overline{b_1 c_2} + \overline{a_p c_1}\right) y^+ + \cdots , \tag{4.14b}$$

$$\mathcal{D}_{12}^p = -\overline{a_p b_1} - 2\left(2\overline{b_1 c_2} + \overline{a_p c_1}\right) y^+ + \cdots . \tag{4.14c}$$

Equation (4.14) shows that the Π_{12} is of $\mathcal{O}(y^+)$ and that ϕ_{12} and $\mathcal{D}_{12}^p$ are of $\mathcal{O}(y^0)$. Thus the Π_{12} component is negligible in the near-wall region. Based on this observation, one can conclude that ϕ_{12} balances $\mathcal{D}_{12}^p$ in the near-wall region. Since the $\mathcal{D}_{12}^p$ component makes the major contribution to the diffusive transport term $\mathcal{D}_{ij} - (\tau_{ij}/k)\mathcal{D}$, it means that the diffusive transport term balances the redistribution term in the near-wall region. This is consistent with the conclusion drawn from the budget analysis

of the b_{12}-component equation. This indicates that for the b_{12}-component the original diffusive transport constraint will still fail in the near-wall region. The fact that the redistribution term balances the diffusive transport term suggests a relationship between the two in arriving at an alternative form of the diffusive transport constraint. One may use the redistribution term to represent the diffusive transport term in the near-wall region. Since the implicit ARSM is intended to replicate the predictive capabilities of the DRSM, an alternative to neglecting the diffusive transport term, is to choose a diffusive transport constraint related to the redistribution term.

Figure 4.8 shows the budget of the b_{22} equation, the redistribution term becomes negative at about $y^+ \approx 10$, while the diffusive transport term becomes large and keeps in balance with the redistribution term for $y^+ \leq 10$. Consistent with the Taylor series expansions, Figure 4.8 shows that the production term decays as $\mathcal{O}(y^{+3})$, and the dissipation term decays as $\mathcal{O}(y^{+2})$. If the velocity pressure-gradient partitioning is examined, the Π_{22} decays as $\mathcal{O}(y^{+2})$, and as with the Π_{12} component becomes negligible for $y^+ \leq 10$. Thus the diffusive transport term once again balances the redistribution term in the near-wall region. This further supports the proposal of using the redistribution term to represent the diffusive transport term in the near-wall region

Figure 4.9 shows the budget from the b_{33} equation. For $y^+ \leq 10$, the production term decays rapidly, but the diffusive transport term becomes large close to the wall and balances the redistribution and dissipation terms. This is similar to the behavior found for the b_{11}- component.

4.4 Modification of diffusive transport constraint

The above observations on the wall asymptotic behavior of the terms in the b_{ij} equations can be summarized as follows: in the b_{11}- and b_{33}-equations, the viscous dissipation stays finite on the wall, keeping balances with the viscous diffusion part in the diffusive transport process there, as well as in close proximity to the wall; in the b_{12}- and b_{22}-equations, pressure transport and redistribution stay finite in close proximity to the wall. The near-wall modeling strategy of the diffusive transport term must cope with these two different mechanisms, and this is readily accomplished by adopting the form

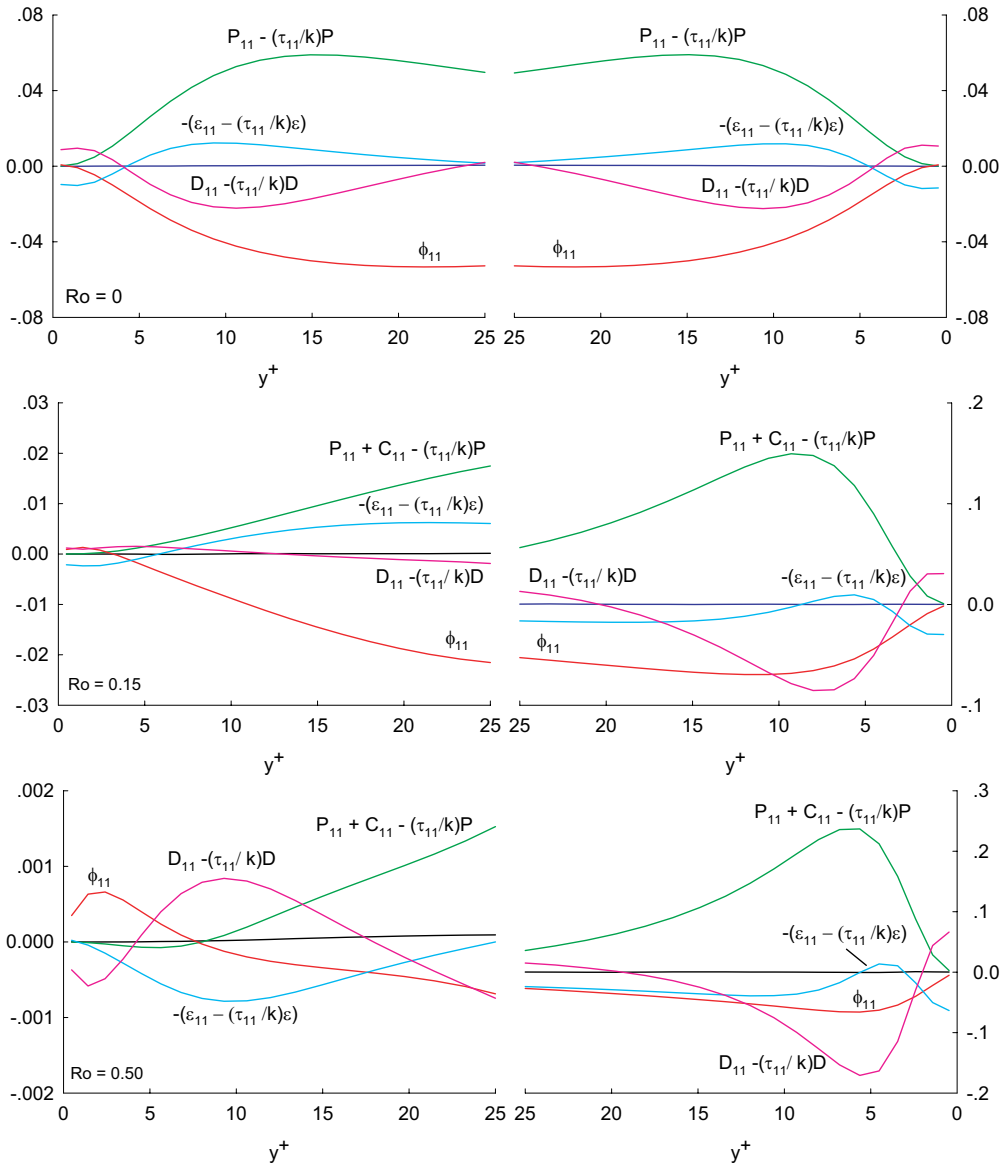

Figure 4.6: Scaled terms in the budget of b_{11} in wall coordinates (*lhs*: suction side, *rhs*: pressure side)

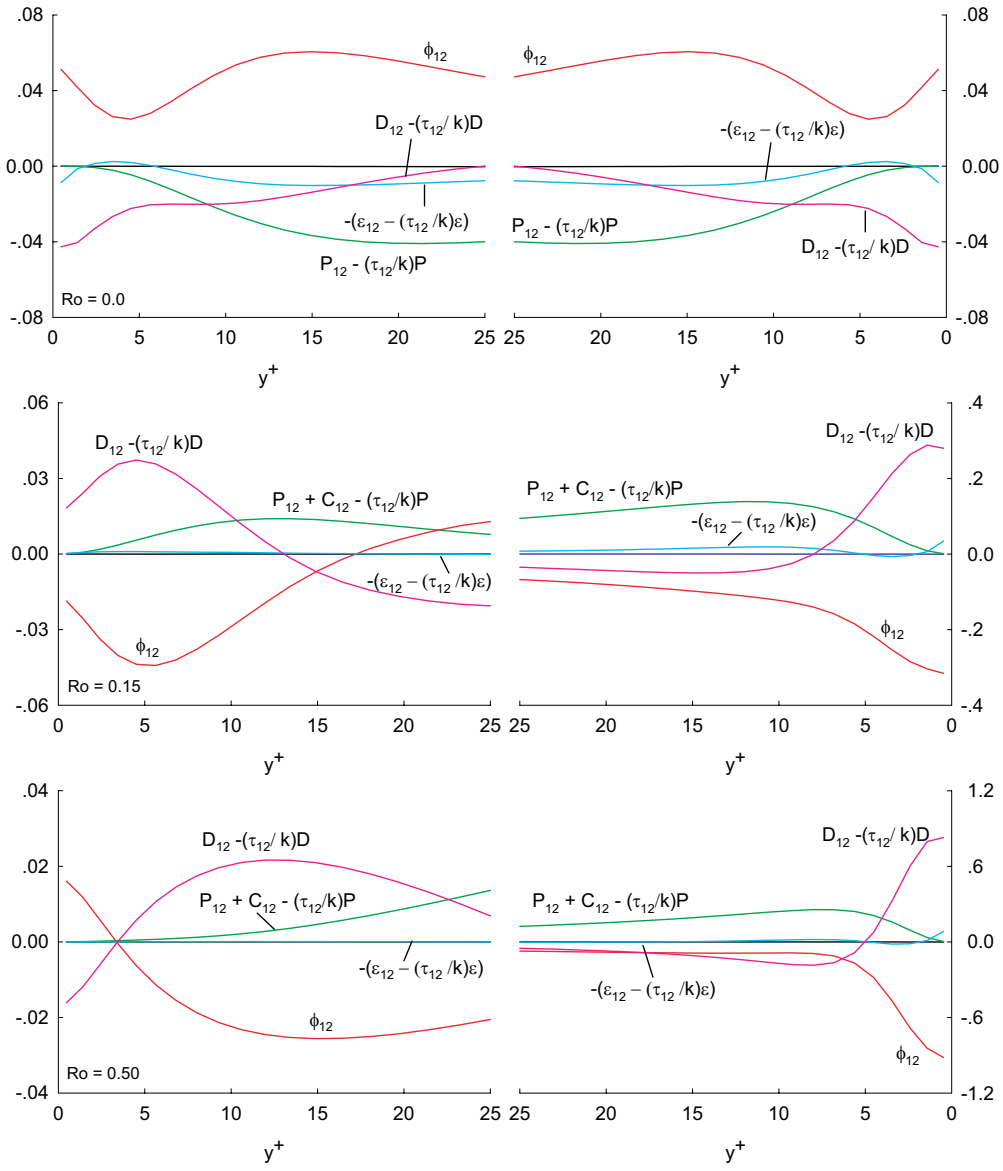

Figure 4.7: Scaled terms in the budget of b_{12} in wall coordinates (*lhs*: suction side, *rhs*: pressure side)

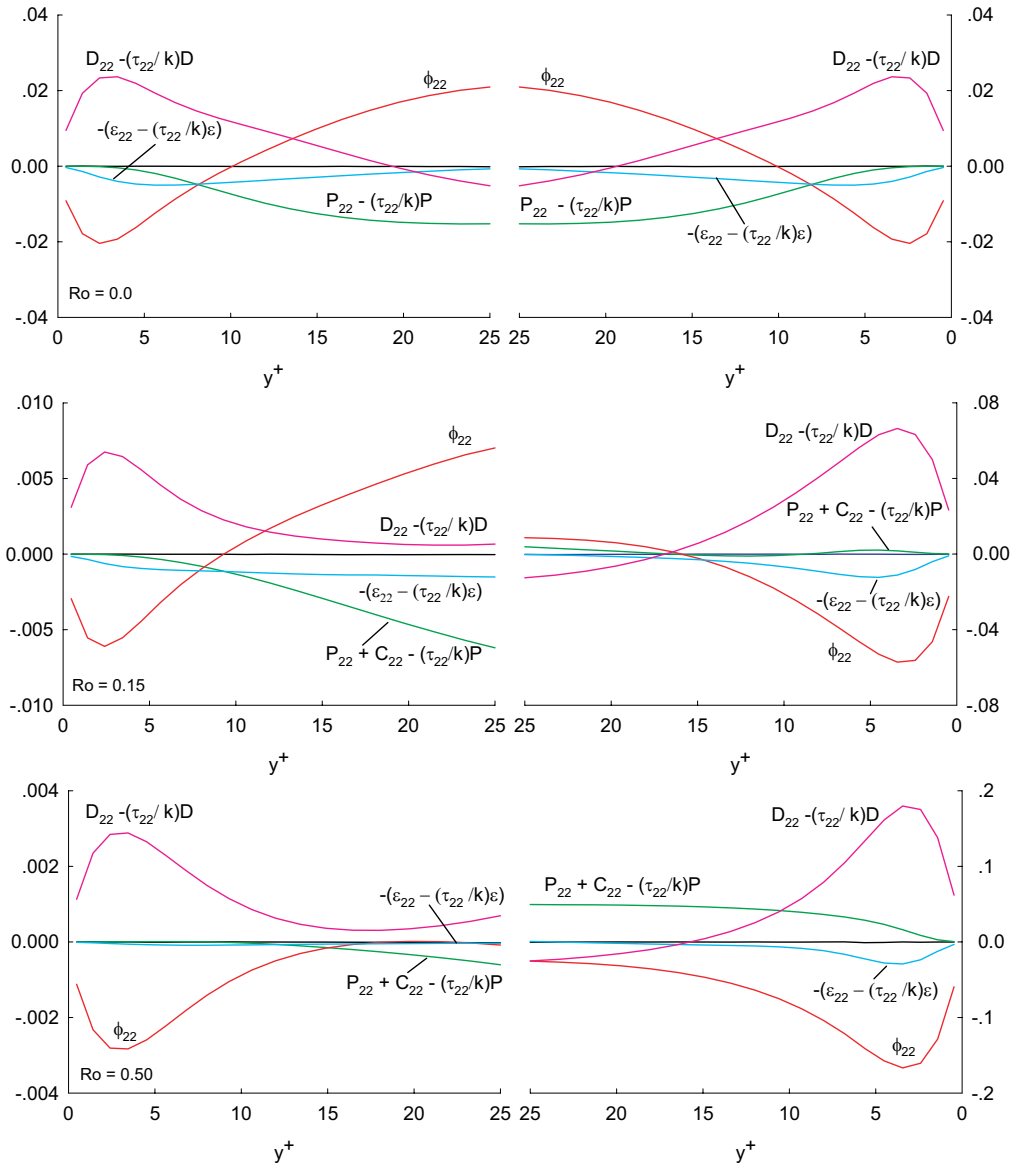

Figure 4.8: Scaled terms in the budget of b_{22} in wall coordinates (*lhs*: suction side, *rhs*: pressure side)

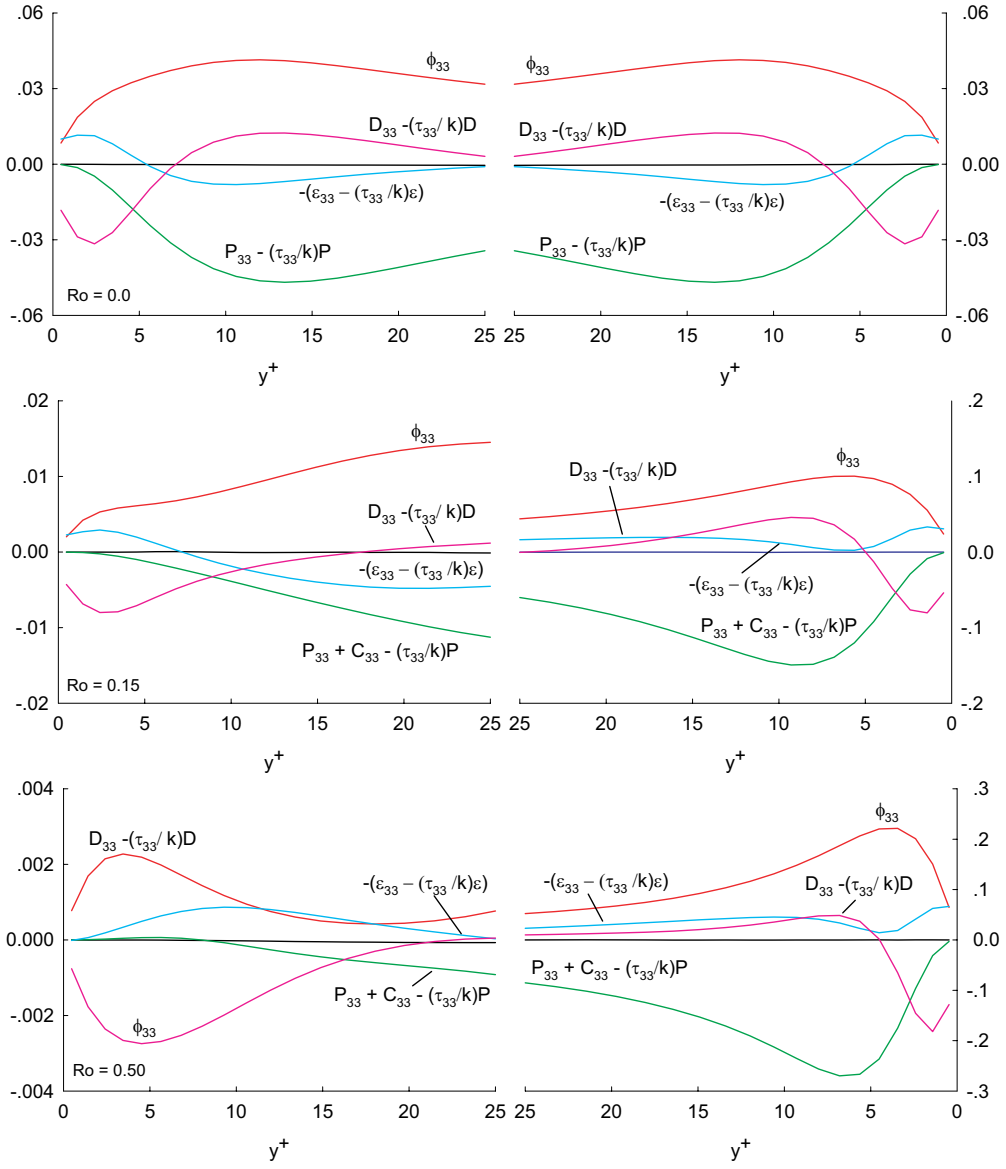

Figure 4.9: Scaled terms in the budget of b_{33} in wall coordinates (*lhs*: suction side, *rhs*: pressure side)

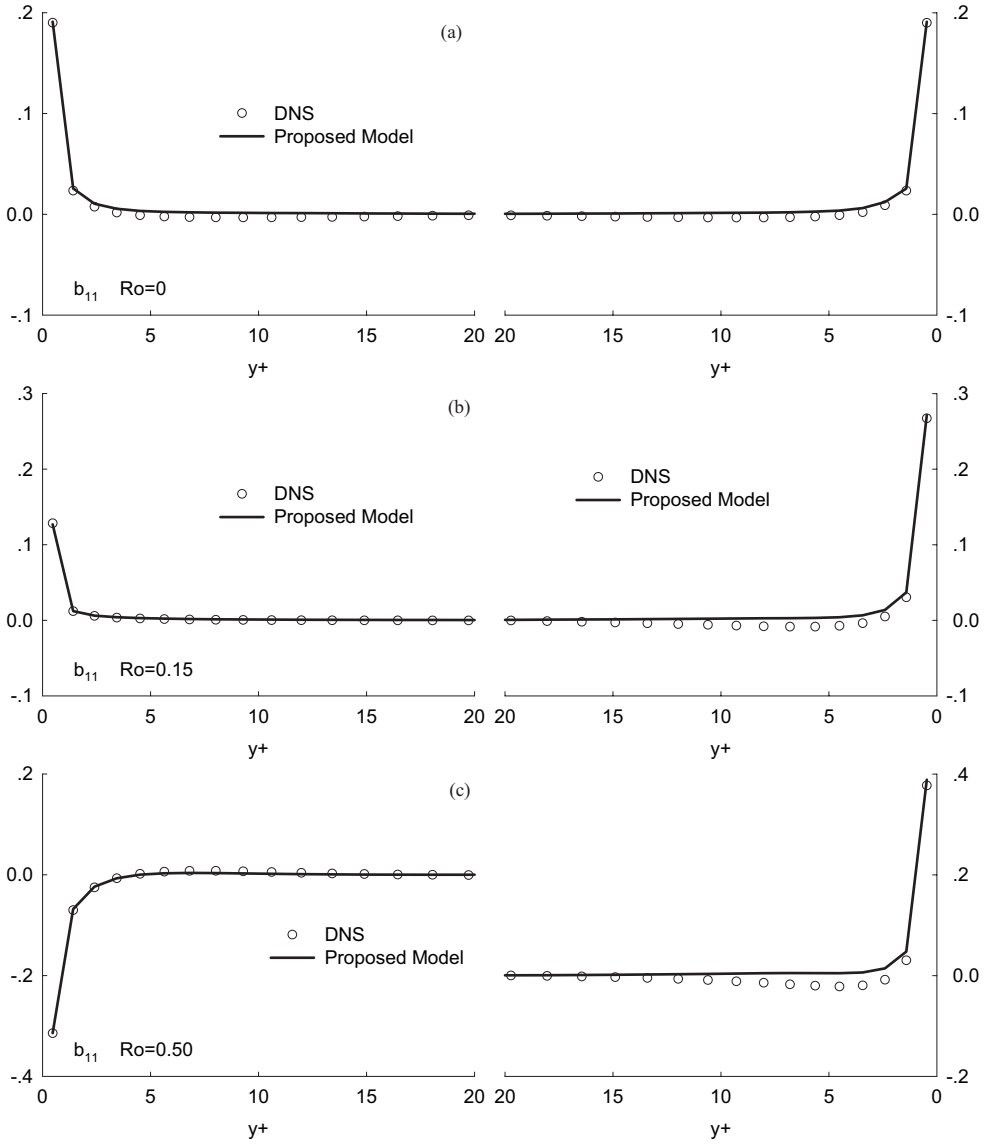

Figure 4.10: Validation of proposed diffusive transport constraint for b_{11}-component (*lhs*: suction side, *rhs*: pressure side)

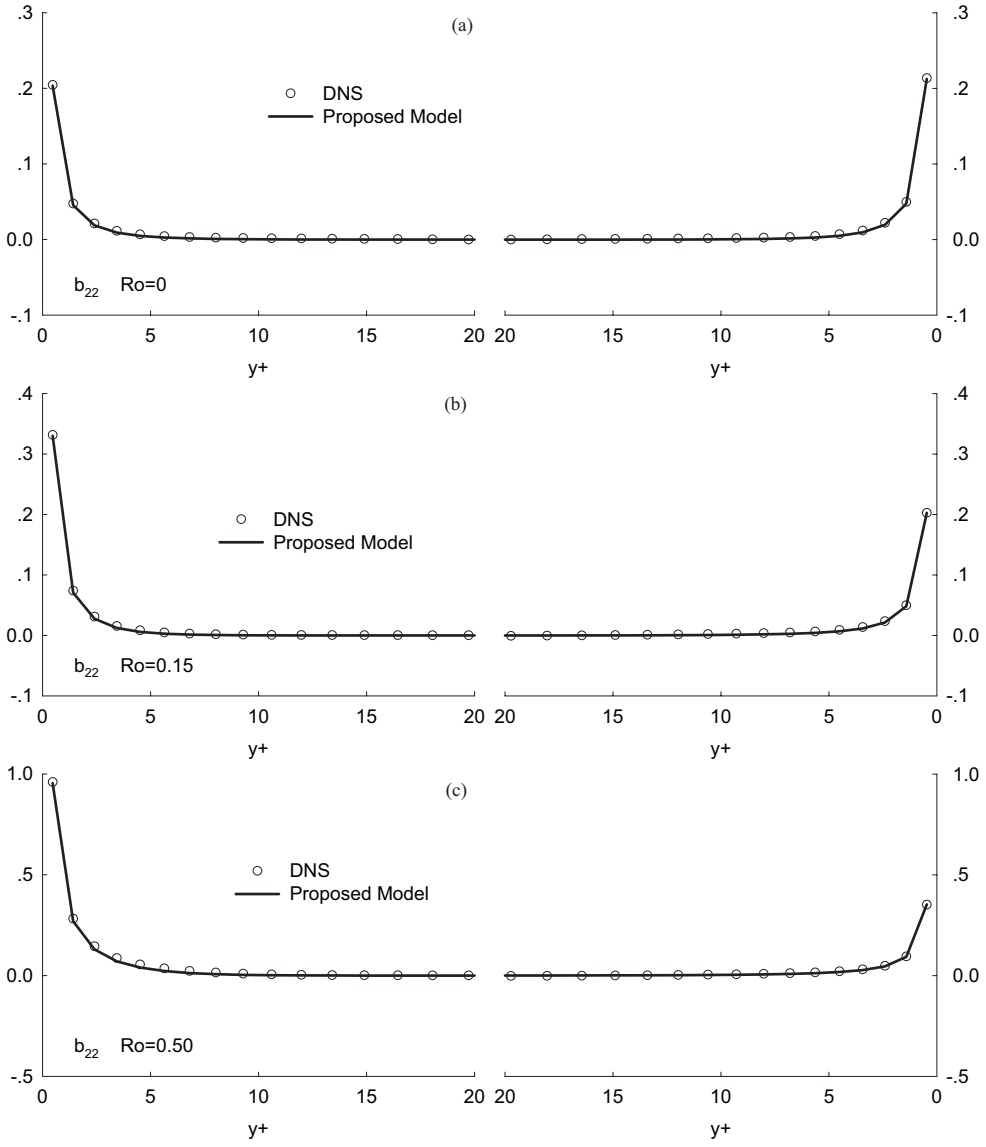

Figure 4.11: Validation of proposed diffusive transport constraint for b_{22}-component (*lhs*: suction side, *rhs*: pressure side)

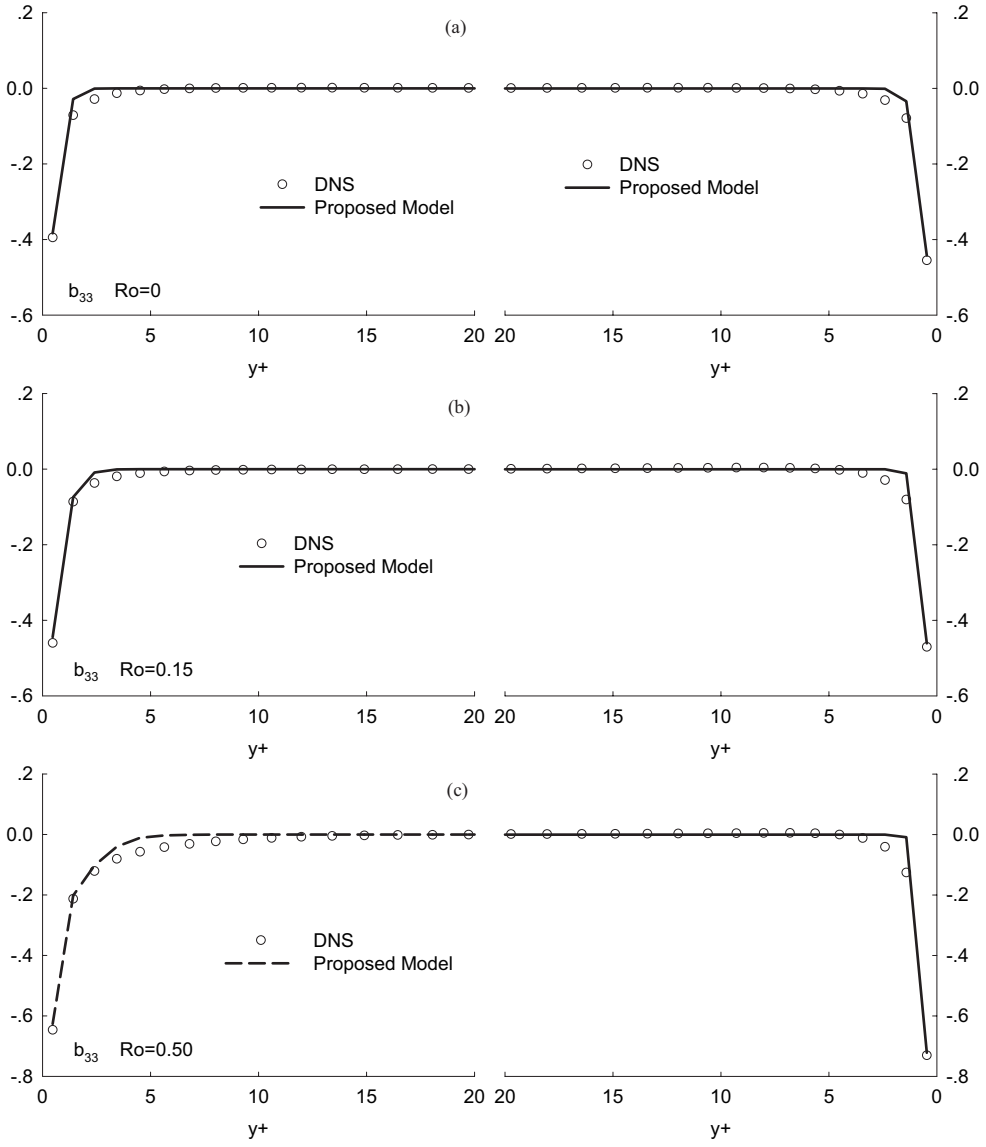

Figure 4.12: Validation of proposed diffusive transport constraint for b_{33}-component (*lhs*: suction side, *rhs*: pressure side)

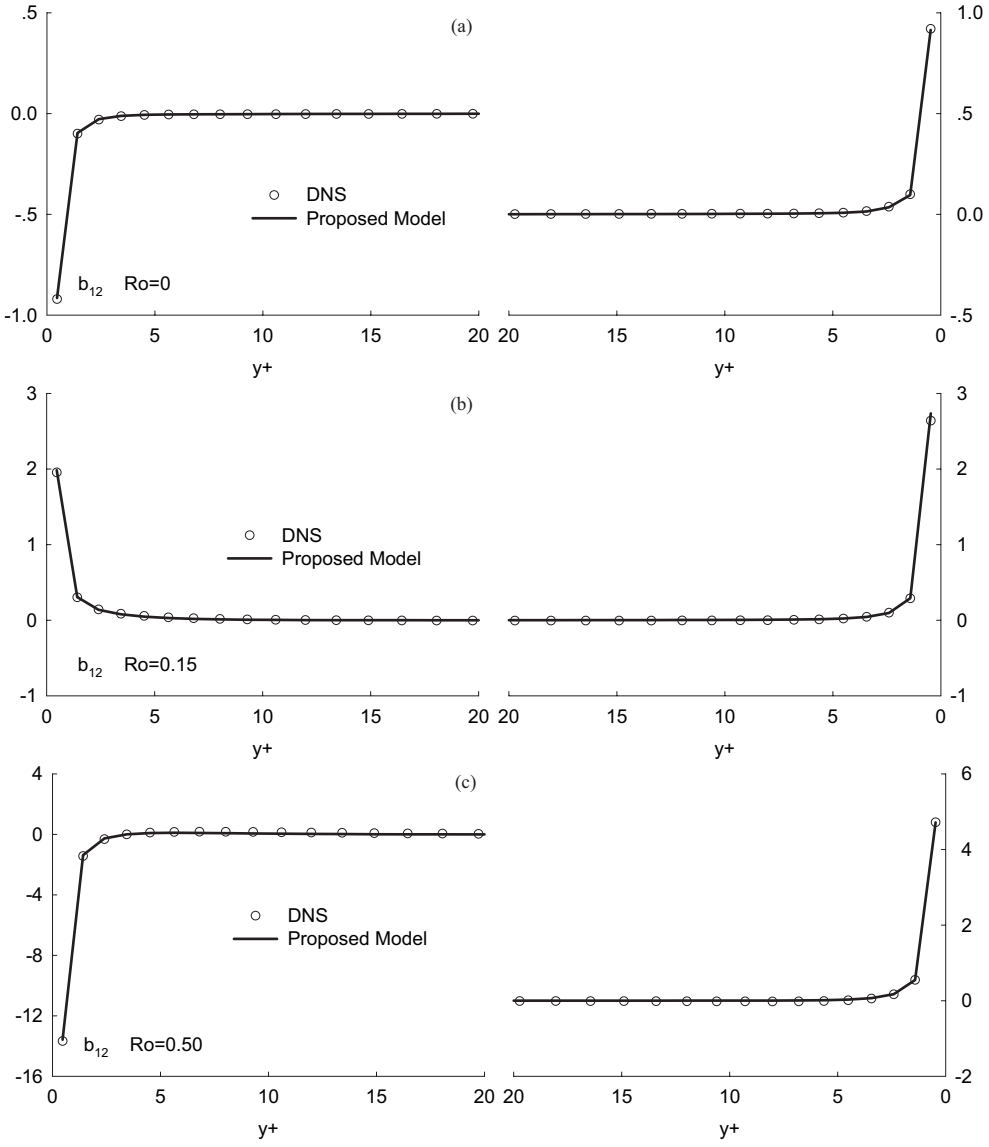

Figure 4.13: Validation of proposed diffusive transport constraint for b_{12}-component (*lhs*: suction side, *rhs*: pressure side)

$$\mathcal{D}_{ij} - \frac{\tau_{ij}}{k}\mathcal{D} = -\left[\phi_{ij} - \left(\varepsilon_{ij} - \frac{\tau_{ij}}{k}\varepsilon\right)\right] f_d, \tag{4.15}$$

with f_d being a function that restricts the effect of the redistribution term and dissipation term within the near-wall region. The form of f_d is specified so that it becomes unity at the wall and slowly decays away from the wall for, $y^+ \geq 10$. Such behavior is easily extracted from the functional form

$$f_d = 1 - \left[1 - \exp\left(-\frac{y^+}{6}\right)\right]^2 . \tag{4.16}$$

Substitution of Eq. (4.15) into Eq. (4.4) yields the modified ARSM equation

$$0 = \frac{1}{2k}\left(P_{ij} + C_{ij} - \frac{\tau_{ij}}{k}P\right) + \left[\frac{\phi_{ij}}{2k} - \frac{1}{2k}\left(\varepsilon_{ij} - \frac{\tau_{ij}}{k}\varepsilon\right)\right](1 - f_d) \ . \tag{4.17}$$

This equation shows that the diffusive transport constraint used in the formulation must balance both the redistribution and dissipation terms near the wall - effectively removing their near-wall effect. It should be noted that the validity of this form is unaffected by the system rotation since the balance between the redistribution and pressure transport and that between the viscous diffusion and dissipation persist regardless of the rotation number (see Figures 4.6 to 4.9). In another analysis of the non-rotating and rotating channel flow cases, Manceau (2005) also showed that the asymptotic behavior in the near-wall region was unaffected. In addition, while that study focused on the DRSM formulation, the alteration of the redistribution term was the focus of the near-wall elliptic blending formulation used.

Now an *a priori* test is performed on the proposed alternative form given in Eq. (4.15), of which both sides are scaled by $2k$ as for the case of extended one. Figure 4.10 shows the results for b_{11}-component where the newly proposed diffusive transport constraint (cf. Eq. (4.15)) gives very good agreement with DNS data in the wall vicinity for both non-rotating and rotating cases. The same level of agreements is achieved for both the b_{22}-component, Figure 4.11, and for the b_{12}-component, Figure 4.13. A slight discrepancy between the DNS and proposed model persists for the b_{33}-component, Figure 4.12, particularly near the pressure side. This is attributable to an increase in the production term there (cf. Figure 4.9). It adversely affects the balance between the diffusive transport term and its counterparts. A more advanced modeling strategy may be necessary to cope with this issue.

This evaluation showed that the newly proposed alternative diffusive transport constraint has the potential to yield an improved implicit form for the ARSM. This coupled with suitable models for the redistribution and dissipation rate terms.

4.5 Concluding Remarks

An assessment of the weak-equilibrium condition has been undertaken by means of an *a priori* evaluation of the fully developed channel flow with spanwise rotation using DNS data. The budget of the various terms in Eq. (4.4) confirms that the diffusive transport term is crucial in the near-wall region. Two diffusive transport constraints based on either zero anisotropy or an anisotropy proportional to the Reynolds stress anisotropy, are then evaluated using DNS data. The results show that neither of these conditions can hold for the near-wall region. An asymptotic analysis of the near-wall behavior for different terms in the budget equations shows that for b_{12}- and b_{22}-components, the diffusive transport term balances the redistribution term in the near-wall region; for b_{11}- and b_{33}-components, the diffusive transport and dissipation terms balance each other in the vicinity of the wall. Based on this asymptotic behavior, an alternative form of the diffusive transport constraint is proposed and evaluated. The results show that this new alternative diffusive transport constraint can be used to improve the predictive ability of the resultant ARSM.

Chapter 5

On the weak-equilibrium condition for algebraic heat flux model

5.1 Introduction

The objective of this chapter is the validity and modification of weak-equilibrium condition used to derive AFHM for flows in the non-inertial frames. The proper form of advection assumption will be derived by invoking the frame-invariant property to account for the rotation and curvature effects correctly. Moreover, it will also be shown that the transport equation for turbulent heat flux can be written in Euclidean-invariant form by introducing the Jaumann-Noll derivative. The diffusive transport constraint will also be addressed in detail to show its invalidity for flows in non-inertial frames. Based on the budget analyses, an attempt is made to achieve the near-wall correction of current diffusive transport constraint. The *a priori* test of the near-wall correction will be performed for the rotating channel flow with heat transfer by using DNS data.

5.2 Algebraic model for turbulent heat flux

Eq. (2.76) is the general model equation used for predicting the turbulent heat flux, however it is only valid for flows in inertial frames. As in non-inertial frames, certain modification must be made to Eq. (2.76) to account for system rotation and streamline curvature effects. Since the weak-equilibrium condition is the basis to derive the

algebraic approximation from transport model of normalized turbulent heat flux, it is straightforward to explore the extended weak-equilibrium condition that is valid both in inertial and non-inertial frames.

5.3 Frame invariant form of AHFM

5.3.1 Frame invariant form of transport equation for ξ_i

The transformation between inertial and non-inertial frames for the normalized heat flux transport equation is briefly described here. Following the works of Gatski & Wallin (2004) and Hamba (2006), the rectangular coordinates x_i^* in the non-inertial frame transforms to the coordinates in the inertial frame x_i as

$$x_i = Q_{ij} x_j^*, \tag{5.1}$$

where Q_{ij} is an orthogonal transformation tensor.

The system rotation tensor expressed in the x_i^* coordinates is given by

$$\Omega_{ij}^* = \frac{dQ_{ki}}{dt} Q_{kj} = \epsilon_{jik} \omega_k^*, \tag{5.2}$$

where ϵ_{ijk} is the permutation tensor, and ω_k^* is the angular rotation rate vector. The system rotation tensor expressed in the x_i coordinates Ω_{ij} is zero by definition.

Under above transformation rule, the variables appearing in the transport equation of normalized turbulent heat flux can be transformed as

$$b_{ij} = Q_{ik} b_{km}^* Q_{mj}^T, \tag{5.3a}$$

$$S_{ij} = Q_{ik} S_{km}^* Q_{mj}^T, \tag{5.3b}$$

$$W_{ij} = Q_{ik} \left(W_{km}^* + \Omega_{km}^* \right) Q_{mj}^T. \tag{5.3c}$$

$$\xi_i = Q_{ij} \xi_j^*, \tag{5.3d}$$

Relative to Euclidean transformation, it is readily seen that, b_{ij}, S_{ij} and ξ_i are all frame invariant while vorticity tensor W_{ij} is not. However, W_{ij} can be made frame invariant by adding a measure of the non-inertial frame rotation rate Ω_{ij}^*

$$\overline{W}_{ij}^* = W_{ij}^* + \Omega_{ij}^*. \tag{5.4}$$

Similarly, the material derivative of normalized turbulent heat flux $D\xi_j/Dt$ can be transformed as

$$\frac{D\xi_j}{Dt} = Q_{ji}\left(\frac{D\xi_i^*}{Dt} + \Omega_{ik}^*\xi_k^*\right). \tag{5.5}$$

The transport equation of normalized turbulent heat flux now can be transformed to the coordinates x_i^*, which can be written as

$$\frac{D\xi_i^*}{Dt} + \Omega_{ik}^*\xi_k^* = f_i^*\left(b_{km}^*, S_{km}^*, \overline{W}_{km}^*, \xi_m^*, \Theta_m^*\right). \tag{5.6}$$

The above result indicates that the normalized turbulent heat flux equation given by Eq. (5.6) is not frame invariant respect to a change of coordinate system under Euclidean transformation, since Eq. (5.5) is not frame invariant. This is not consistent with general understanding about mathematical expressions, which is nothing but a tool to describe physical laws, and should be independent from the choice of coordinate systems. This inconsistency can be overcome by introducing the Jaumann-Noll derivative (Trusov, 1987) also called corotational derivative (Thiffeault, 2001).

$$\frac{\bar{D}\mathbf{a}}{Dt} = \frac{D\mathbf{a}}{Dt} + \mathbf{\Omega a}, \tag{5.7a}$$

$$\frac{\bar{D}\mathbf{b}}{Dt} = \frac{D\mathbf{b}}{Dt} + \mathbf{b\Omega} - \mathbf{\Omega b}, \tag{5.7b}$$

with $\mathbf{a}$ and $\mathbf{b}$ being being a vector and a tensor respectively. Applying Eq. (5.7a) to Eq. (5.5), one can derive a frame-invariant form of the material derivative of normalized turbulent heat flux

$$\frac{\bar{D}\xi_j^*}{Dt} = \frac{D\xi_j^*}{Dt} + \Omega_{jk}^*\xi_k^*. \tag{5.8}$$

Eq. (5.6) then becomes

$$\frac{\bar{D}\xi_j^*}{Dt} = f_j^*\left(b_{km}^*, S_{km}^*, \overline{W}_{km}^*, \xi_m^*, \Theta_m^*\right). \tag{5.9}$$

It tells that the transport equation of normalized turbulent heat flux, Eq.(5.9), is now frame invariant, since the corotational derivative $\bar{D}\xi_j^*/Dt$ can be considered as a frame invariant variable as $\overline{W}_{ij}^*$ and the RHS of Eq. (5.9) is expressed in terms of frame invariant variables. Consequently, any model expression derived from Eq. (5.9) should also be frame invariant as argued by Weis & Hutter (2003).

5.3.2 Euclidean invariant form of AHFM

As stated by Hamba (2006), Eq. (5.9) is not suitable for curved flows, therefore it should be further generalized. To this end, the coordinate system $x_i^\dagger$ that is embedded in the flow and the coordinate system x_i^* in which the observer is fixed are considered here. The transformation rule between $x_i^\dagger$ system and inertial system is given by

$$x_i^\dagger = T_{ij} x_j, \tag{5.10}$$

where T_{ij} is a proper orthogonal transformation tensor.

By this transformation rule, the normalized turbulent heat flux equation can be described in the $x_i^\dagger$ system as

$$\frac{D\xi_i^\dagger}{Dt} + \Omega_{ik}^{(r)\dagger}\xi_k^\dagger = f_i^\dagger\left(b_{km}^\dagger, S_{km}^\dagger, W_{km}^\dagger + \Omega_{km}^{(r)\dagger}, \xi_m^\dagger, \Theta_m^\dagger\right), \tag{5.11}$$

where $\Omega_{ij}^{(r)\dagger} = T_{ik} dT_{kj}^T/dt$ is the rotation rate of the $x_i^\dagger$ system expressed in the $x_i^\dagger$ system.

Since the $x_i^\dagger$ system is independent of the inertial system x_i, Eq.(5.11) can be written in the inertial system as

$$T_{ij}^T \frac{D\xi_j^\dagger}{Dt} + \Omega_{ik}^{(r)}\xi_k = f_i\left(b_{km}, S_{km}, W_{km}, \xi_m, \Theta_m\right), \tag{5.12}$$

where $\Omega_{ij}^{(r)} = T_{ik}^T \Omega_{km}^{(r)\dagger} T_{mj}$ is the rotation rate of the $x_i^\dagger$ system expressed in the inertial system. By applying the weak-equilibrium condition $D\xi_i^\dagger/Dt$=0, the resultant implicit algebraic equation for a_j may have the form in the inertial system as

$$f_i\left(b_{km}, S_{km}, W_{km}, \xi_m, \Theta_m\right) - \Omega_{ik}^{(r)}\xi_k = 0. \tag{5.13}$$

Once again, considering the observer in the x_i^* coordinate system, it is straightforward to transform Eq. (5.12) to the non-inertial system x_i^*. It follows

$$Q_{ji} T_{ji}^T \frac{D\xi_j^\dagger}{Dt} + \Omega_{ik}^{(r)*}\xi_k^* = f_i^*\left(b_{km}^*, S_{km}^*, W_{km}^* + \Omega_{km}^\dagger, \xi_m^*, \Theta_m^*\right). \tag{5.14}$$

As stated by Gatski & Wallin (2004), irrespective of the coordinate system, the correct form of the weak-equilibrium condition should be

$$D\xi_j^\dagger/Dt = 0, \tag{5.15}$$

which is a extension of the original condition. Then the resultant implicit algebraic equation for ξ_j in the non-inertial system can be given by

$$\Omega_{ik}^{(r)*}\xi_k^* = f_i^*\left(b_{km}^*, S_{km}^*, W_{km}^* + \Omega_{km}^\dagger, \xi_m^*, \Theta_m^*\right). \tag{5.16}$$

It is clear that the AHFM written in Eq. (5.16) is frame invariant, since it is expressed in terms of frame invariant variables. It is important to note that Ω_{ij}^* is different from $\Omega_{ij}^{(r)*}$. The former represents a measure of the rotation rate of the flow, while the latter represents the rotation rate of the observer. If the x_i^* system coincides with the $x_i^\dagger$ system, $\Omega_{ij}^* = \Omega_{ij}^{(r)*}$ is obtained. Noted that $\Omega_{ij}^{(r)*}$ should be used for general cases. For instance of curved turbulent flows, which is usually analyzed relative to an observer fixed in an inertial frame. Consequently it arises a problem that how to measure $\Omega_{ij}^{(r)*}$ for such curved flows. There are some works related to this issue, such as Gatski & Jongen (2000); Girimaji (1997); Wallin & Johansson (2002), among others.

Now, Eq. (2.76), which is expressed in inertial frames can be rewritten in non-inertial frames as

$$\begin{aligned}\Omega_{ij}^{(r)*}\xi_j^* =& -C_b\left(2b_{ij}^* + \frac{2\delta_{ij}}{3}\right)\Theta_j^* - C_S S_{ij}^*\xi_j^* - C_W\left(W_{ij}^* + \Omega_{ij}^\dagger\right)\xi_j^* \\ & - \frac{\xi_i^*}{2}\left\{\tau\left(\frac{P_k}{\varepsilon_k} - 1 + 2C_{1\theta}\right) + \tau_\theta\left[\frac{P_\theta}{\varepsilon_\theta}\left(1 - 2C_{5\theta}\right) - 1\right]\right\}.\end{aligned} \tag{5.17}$$

Eq. (5.17), which is derived based on extended weak-equilibrium condition (Eq. (5.15)), has the ability to predict the normalized turbulent heat flux for flows in the non-inertial frames. By comparing with Eq. (2.76), one can tell that Eq. (5.17) has an extra term $\Omega_{ij}^{(r)*}\xi_j^*$, which describes the advection of ξ_i in the non-inertial frames, and the mean vorticity in Eq. (2.76) has been replaced with the absolute vorticity. By above measures, the system rotation and streamline curvature effects can be both included in the AHFM.

5.3.3 *A Priori* test of extended advection assumption

To demonstrate the validity of extended advection assumption, an *a priori* test will be performed using the DNS database (Elsamni & Kasagi, 2001; Kasagi & Iida, 1999; Nishimura & Kasagi, 1996). The test case adopted here is a fully developed turbulent flow in a plane channel, which is rotated at a specified angular velocity around its

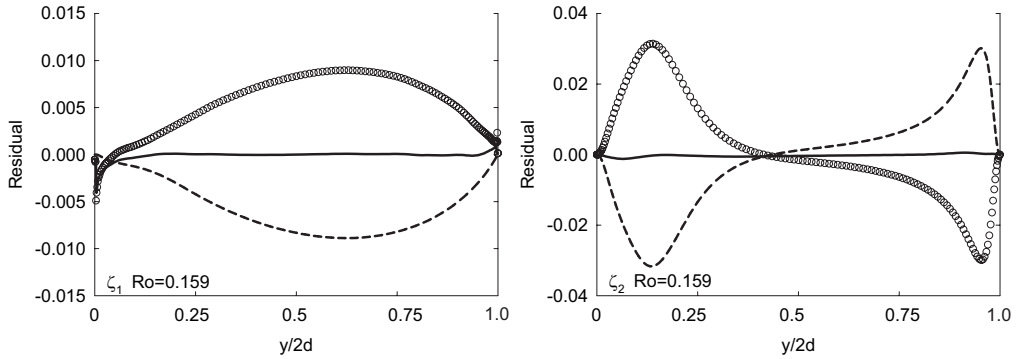

Figure 5.1: The test of extended advection assumption. Residual of Eq. (5.20)(circle) compared to that of Eq. (5.21)(solid line). The dash line is for the extra term $\Omega_{ij}\xi_j$

spanwise axis. The Coriolis force arising from the imposed system rotation enhances the turbulence along the pressure side, while reducing the turbulent activity along the suction side. The two walls are assumed to be kept at different, but constant temperatures, and any buoyancy effect is neglected. The DNS database used here is carried out for $Re_b = 4750$ and $Pr = 0.71$, where Re_b is the bulk Reynolds number based on the channel half width d and the bulk velocity U_b, and $Pr = \nu/\alpha$ is the Prandtl number. The rotation number is defined as

$$Ro = 2\omega_m d/U_b, \tag{5.18}$$

where ω_m is the system angular velocity.

By transforming Eq. (2.71) to the non-inertial frames and rewriting in a tensorial form, one can have

$$\begin{aligned}\frac{D\xi_i^*}{Dt} + \Omega_{ij}^*\xi_j^* = &-\left(2b_{ij}^* + \frac{2\delta_{ij}}{3}\right)\Theta_j^* - S_{ij}^*\xi_j^* - \left(W_{ij}^* + \Omega_{ij}^*\right)\xi_j^* + \mathcal{D}_i^a \\ &+ \frac{1}{k^{1/2}k_\theta^{1/2}}\left(\phi_{i\theta} - \varepsilon_{i\theta}\right) - \frac{\xi_i^*}{2}\left[\tau_k\left(\frac{P_k}{\varepsilon_k} - 1\right) + \tau_\theta\left(\frac{P_\theta}{\varepsilon_\theta} - 1\right)\right].\end{aligned} \tag{5.19}$$

By applying the original advection assumption, which applies to the left-hand side

of Eq. (5.19) to be zero, one has

$$0 = -\left(2b_{ij}^{*} + \frac{2\delta_{ij}}{3}\right)\Theta_{j}^{*} - S_{ij}^{*}\xi_{j}^{*} - \left(W_{ij}^{*} + \Omega_{ij}^{*}\right)\xi_{j}^{*} + \frac{1}{k^{1/2}k_{\theta}^{1/2}}\left(\phi_{i\theta} - \varepsilon_{i\theta}\right) - \frac{\xi_{i}^{*}}{2}\left[\tau_{k}\left(\frac{P_{k}}{\varepsilon_{k}} - 1\right) + \tau_{\theta}\left(\frac{P_{\theta}}{\varepsilon_{\theta}} - 1\right)\right] + \mathcal{D}_{i}^{a}. \quad (5.20)$$

By applying the extended assumption, Eq. (5.15), one has

$$\Omega_{ij}^{*}\xi_{j}^{*} = -\left(2b_{ij}^{*} + \frac{2\delta_{ij}}{3}\right)\Theta_{j}^{*} - S_{ij}^{*}\xi_{j}^{*} - \left(W_{ij}^{*} + \Omega_{ij}^{*}\right)\xi_{j}^{*} + \frac{1}{k^{1/2}k_{\theta}^{1/2}}\left(\phi_{i\theta} - \varepsilon_{i\theta}\right) - \frac{\xi_{i}^{*}}{2}\left[\tau_{k}\left(\frac{P_{k}}{\varepsilon_{k}} - 1\right) + \tau_{\theta}\left(\frac{P_{\theta}}{\varepsilon_{\theta}} - 1\right)\right] + \mathcal{D}_{i}^{a}. \quad (5.21)$$

With the specific models for the pressure temperature-gradient correlation $\phi_{i\theta}$, the dissipation term $\varepsilon_{i\theta}$ and diffusive transport term $\mathcal{D}_{i}^{a}$, Eqs. (5.20) and (5.21) are readily to arrive at the implicit form of AHFM respectively, such as Eq. (5.17). However, in order to validate the extended form of advection assumption, any other model influence should be isolated. Therefore, Eqs. (5.20) and (5.21) are used to perform the *a priori* test directly, without any model involved. The DNS database are employed for the supply of $\phi_{i\theta}$, $\varepsilon_{i\theta}$ and $\mathcal{D}_{i}^{a}$. The residuals of Eqs. (5.20) and (5.21) are computed, and smaller residuals suggest the better performance.

Since no models are introduced, the magnitude of any residual can be directly associated with the validity of the two assumptions. The results shown in Figure 5.1 are the distribution for $Ro = 0.159$. It is shown that the extended assumption gives practically zero residuals for all two components ξ_1 and ξ_2 across the channel which means that the extended assumption is able to fully account for the rotation effect for flows in non-inertial frames. This is in contrast to the original assumption where large residuals across the channel for all two components are shown.

5.4 The diffusive transport constraint

As known fact, the weak-equilibrium condition consists of advection assumption and diffusive transport constraint. The previous section has focused on the advection assumption, which is extended for the applicability to the non-inertial frames. In the following section, attention will be paid on the diffusive transport constraint. It is true

that the system rotation and streamline curvature can influence the transport process in turbulent flows significantly. This can be observed from numerous computations and experimental studies, such as Kasagi *et al.* (1992); Liu & Lu (2007); Matsubara & Alfredsson (1996); Wu & Kasagi (2004); Yamawaki *et al.* (2002). Consequently, the issue of whether the assumption for diffusive transport can hold in flows involving rotation and curvature effects arises. The same question for the diffusive transport assumption associated with Reynolds stress anisotropy tensor has been explored previously using budget analysis of Reynolds stress anisotropy equation together with the near-wall asymptotic behavior analysis. For the current study, the analogous strategy will be employed to address the issue of diffusive transport assumption associated with normalized turbulent heat flux.

5.4.1 Budget of normalized turbulent heat flux equation

In analogy with the derivation of transport equation for Reynolds stress anisotropy b_{ij} , one can obtain the transport equation of normalized turbulent heat flux ξ_i for fully developed rotating channel flow

$$0 = \left[P_{i\theta} - \frac{\xi_i}{2}\left(RP_k + \frac{P_\theta}{R}\right)\right] + \left[\mathcal{D}_{i\theta} - \frac{\xi_i}{2}\left(R\mathcal{D}_k + \frac{\mathcal{D}_\theta}{R}\right)\right] + \phi_{i\theta} - \left[\varepsilon_{i\theta} - \frac{\xi_i}{2}\left(R\varepsilon_k + \frac{\varepsilon_\theta}{R}\right)\right], \tag{5.22}$$

where $R = k_\theta^{1/2}/k^{1/2}$. One may interpret the terms on the RHS as production anisotropy, diffusive transport, pressure temperature-gradient correlation and dissipation anisotropy. It is noted that the $P_{i\theta}$ here includes the production due to mean temperature gradient $P_{j\theta}^T$, the production due to mean velocity gradient $P_{i\theta}^U$ and the Coriolis production $C_{i\theta}$. The weak-equilibrium assumption takes the diffusive transport as negligible, which leads to an algebraic approximation for the transport of normalized turbulent heat flux.

The budget of the various terms in Eq. (5.22) is evaluated by using DNS database (Elsamni & Kasagi, 2001; Kasagi & Iida, 1999; Nishimura & Kasagi, 1996). Figures 5.2(a) and (b) show the budget of ξ_1-component for non-rotating case, where the production anisotropy is the dominant source, while the pressure temperature-gradient correlation is the dominant sink. Moving towards the wall, the production anisotropy and pressure temperature-gradient correlation decay fast. The diffusive transport and

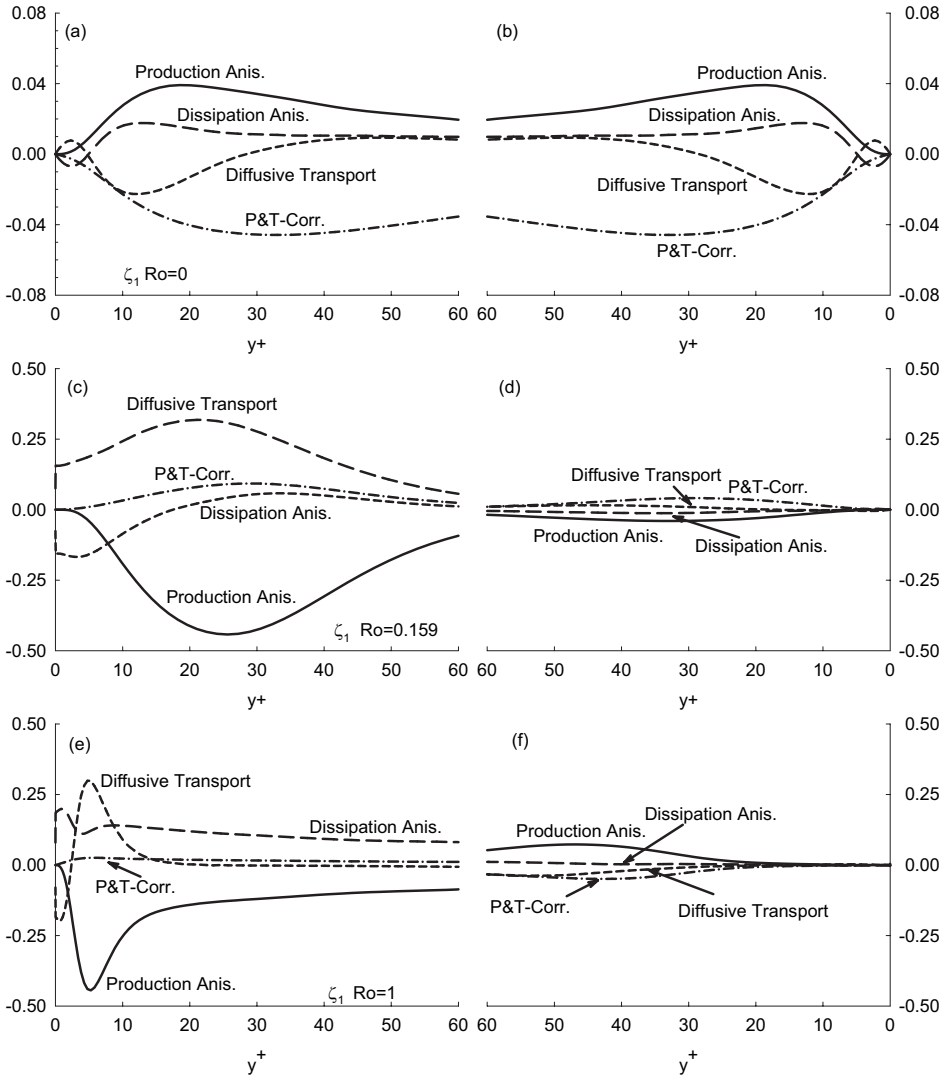

Figure 5.2: The budget of Eq. (5.22) for ξ_1 LHS: Pressure side, RHS: Suction side.

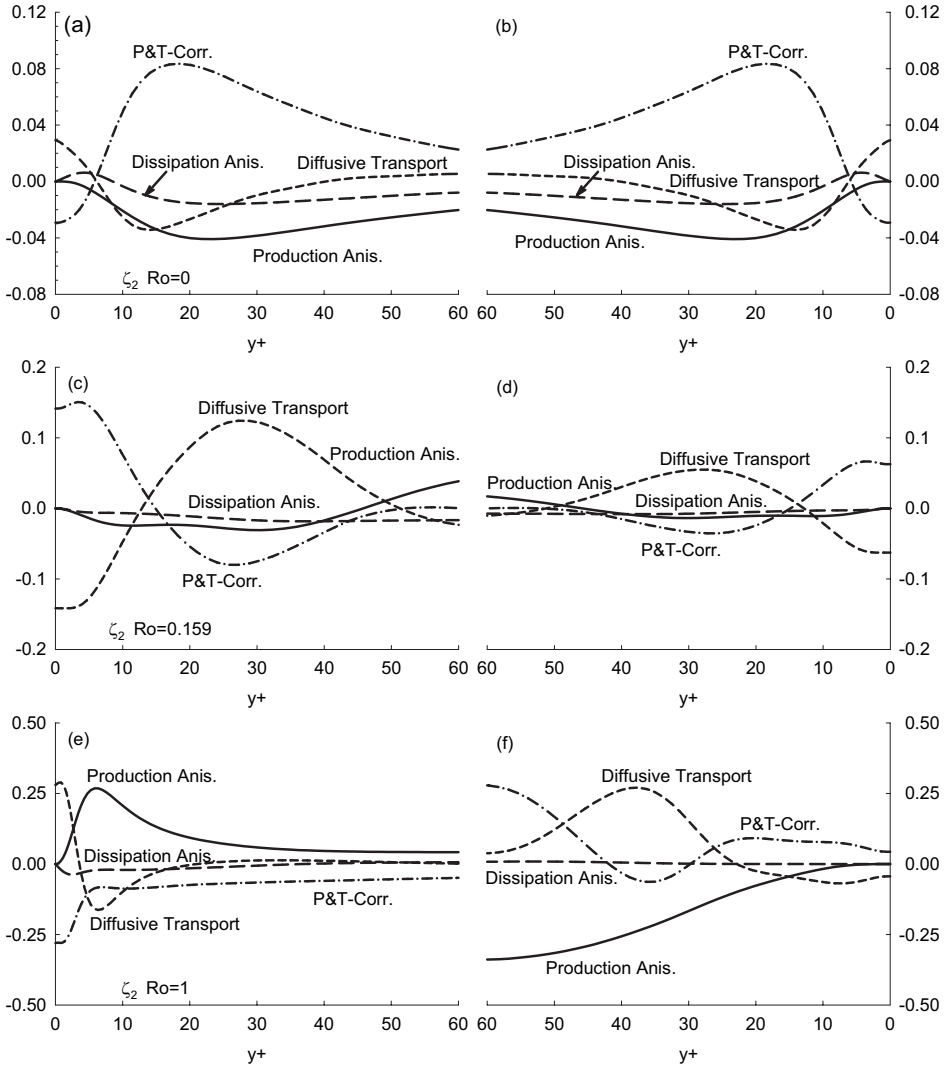

Figure 5.3: The budget of Eq. (5.22) for ξ_2 LHS: Pressure side, RHS: Suction side.

dissipation anisotropy appear as the dominant source and sink, of which are both related to the viscous effect caused by wall proximity for current studying case.

For the rotating cases, the significant influence of rotation effects can be observed by examining Figures 5.2(c) - 5.2(f), where the turbulent intensity is enhanced along pressure side, while reduced along suction side. The production anisotropy becomes dominant sink for the rotating case, which is contrary with the non-rotating case. The diffusive transport is obviously enhanced by the imposed rotation effect, since it becomes dominant source instead of being sink. The pressure temperature-gradient correlation is suppressed gradually with increasing rotation number, and becomes less important across the channel. The dissipation anisotropy is also remarkably influenced by the system rotation, since its sign is changed with different rotation numbers. Nevertheless, for the region near the wall, the diffusive transport and dissipation anisotropy, which are related to viscous effects, are crucial.

For ξ_2-component, the behavior of individual terms in the budget equation is different with that of ξ_1-component. Since it is wall-normal component, instead of viscous effect, the pressure fluctuation dominates the near-wall behavior of budget equation. For the non-rotating case, Figures 5.3(a) and 5.3(b) show that the dominant source is the pressure temperature-gradient correlation, while the production anisotropy is the sink. Moving to the wall, the production anisotropy and dissipation anisotropy become less important, while the pressure temperature-gradient correlation and diffusive transport, which are related to the pressure fluctuation, keep balance with each other, and obtain finite value on the wall. For the rotating cases, similar to ξ_1-component, the imposed rotation effects influence the budget remarkably. The diffusive transport becomes more important, while the dissipation anisotropy keeps being small across the channel. Similar to the non-rotating case, the diffusive transport and pressure temperature-gradient correlation, which are related to the pressure fluctuation, become more important near the wall.

For all events discussed above, the pressure temperature-gradient correlation balances the sum of the diffusive transport plus dissipation anisotropy, which indicates that the diffusive transport plays a crucial role in the budget of ξ_i transport equation for near-wall region. Consequently, the diffusive transport constraint, which neglects the diffusion/-transport term, is unlikely to hold there.

Table 5.1: Near-wall behavior of budget terms in Eq. (5.22)

i	1	2
Production	$\mathcal{O}(y^3)$	$\mathcal{O}(y^3)$
Diffusive transport	$\mathcal{O}(y)$	$-(1/\rho)\,\overline{b_\theta a_p}$
P&T-Corr.	$\mathcal{O}(y^2)$	$(1/\rho)\,\overline{b_\theta a_p}$
Dissipation	$\mathcal{O}(y)$	$\mathcal{O}(y)$

5.4.2 Modification of diffusive transport constraint

The analysis about the budget of ξ_i transport equation above has shown the invalidity of current diffusive transport constraint. In the previous chapter, a tempt has been made to resolve this problem by representing the diffusive transport by the sum of redistribution and dissipation anisotropy terms associated with Reynolds stress anisotropy. For current study, this proposal will be extended to the diffusive transport assumption associated with normalized turbulent heat flux. First, the near-wall behavior of individual term in the budget equation of ξ_i is analyzed. Based on that analysis, the near-wall correction of diffusive transport constraint is proposed. To analyze the near-wall behavior of individual terms in the budget equation, we expand the pressure, velocity and temperature fluctuations (So *et al.*, 2004; Wikström *et al.*, 2000) in the wall vicinity as follows

$$p = a_p + b_p y + c_p y^2 + \cdots , \tag{5.23a}$$

$$u = a_i + b_i y + c_i y^2 + \cdots , \tag{5.23b}$$

$$\theta = a_\theta + b_\theta y + c_\theta y^2 + \cdots , \tag{5.23c}$$

where $a_i = b_2 = a_\theta = 0$ (no-slip boundary condition, continuity and constant wall temperature). The expansions of $\overline{u\theta}$, $\overline{v\theta}$ and k_θ then become

$$\overline{u\theta} = \overline{b_\theta b_1} y^2 + \left(\overline{b_\theta c_1} + \overline{c_\theta b_1}\right) y^3 + \cdots , \tag{5.24a}$$

$$\overline{v\theta} = \overline{b_\theta c_2} y^3 + \left(\overline{b_\theta d_2} + \overline{c_\theta c_2}\right) + \cdots , \tag{5.24b}$$

$$k_\theta = \frac{1}{2}\overline{b_\theta^2} y^2 + \overline{b_\theta c_\theta} y^3 + \cdots . \tag{5.24c}$$

The budget terms in Eq. (5.22) are also expanded and listed in Table 5.1, where only the terms are of $\mathcal{O}(y^0)$ are listed. The budget terms that are at least of second order are omitted, since their wall limits are considered to be less important. For ξ_1-component, the diffusive transport and dissipation anisotropy are of lower orders compared to the production anisotropy and pressure temperature-gradient correlation, which indicates that they are more important in the near-wall region. The production anisotropy and pressure temperature-gradient correlation decay fast in the near wall region; while the diffusive transport balances the dissipation anisotropy up to the wall. For ξ_2-component, Table 5.1 shows that the diffusive transport and pressure temperature-gradient correlation are the major contributors near the wall, while the production anisotropy and dissipation anisotropy decay as of higher order and eventually vanish on the wall.

Above observation indicates that, for ξ_1- and ξ_2-component, the fact that diffusive transport balances the sum of pressure temperature-gradient correlation plus dissipation anisotropy suggests a possibility to arrive at the alternative form of diffusive transport constraint. One may use the sum of pressure temperature-gradient correlation plus dissipation anisotropy to represent the diffusive transport in the near-wall region. Based on above analyses, we propose an alternative form of diffusive transport constraint by the equation below:

$$\mathcal{D}_{i\theta} - \frac{\xi_i}{2}\left(R\mathcal{D}_k + \frac{\mathcal{D}_\theta}{R}\right) = -\left\{\phi_{i\theta} - \left[\varepsilon_{i\theta} - \frac{\xi_i}{2}\left(R\varepsilon_k + \frac{\varepsilon_\theta}{R}\right)\right]\right\} f_t, \tag{5.25}$$

where f_t is a model function. For present case, the following general form may be used

$$f_t = 1 - \left[1 - \exp\left(\frac{y^+}{\lambda}\right)\right]^2, \tag{5.26}$$

where $y^+ = yu_\tau/\nu$ and u_τ is the friction velocity. As well known fact, the Prandtl number Pr and the Reynolds number Re have the significant influence on the scalar field (Kawamura *et al.*, 1999, 1998; Kim & Moin, 1987). So & Speziale (1999) suggested any near-wall models should reflect a Pr dependence; otherwise, they would not be able to replicate the thermal asymptotes correctly as a wall is approached. The above arguments imply that the proposed diffusive transport constraint should be made parametric of Pr, which means that the λ should be incorporating with the Pr number. In current study, a constant value 6 for λ was chosen for time-being and its universal

validity should be task of future study. The proposed function is supposed to become unity for wall vicinity, and equal to 0 otherwise. Consequently, one can restricts the effects of pressure temperature-gradient correlation and dissipation anisotropy within the near-wall region.

From the above asymptotic behavior and budget analyses, one can tell that the near-wall diffusion and transport of ξ_i are mainly contributed by pressure transport and viscous diffusion, both of which must be properly approximated. For ξ_1-component, the pressure fluctuation parts of both sides in Eq. (5.25) are negligible, which leaves that the viscous diffusion part of LHS balances the viscous dissipation anisotropy part of RHS. For ξ_2-component, the viscous related parts of both sides in Eq. (5.25) are negligible, which leaves that the pressure transport part of LHS balances the pressure fluctuation part of RHS. These balances vary for different components, but this difference is automatically compensated. By adopting the present diffusive transport constraint, one can change Eq. (5.22) to

$$0 = \left[P_{i\theta} - \frac{\xi_i}{2}\left(RP_k + \frac{P_\theta}{R}\right)\right] + \left\{\phi_{i\theta} - \left[\varepsilon_{i\theta} - \frac{\xi_i}{2}\left(R\varepsilon_k + \frac{\varepsilon_\theta}{R}\right)\right]\right\}(1 - f_t)\,. \quad (5.27)$$

This equation indicates that the diffusive transport constraints need to be incorporated in the manner that both pressure temperature-gradient correlation and dissipation anisotropy disappear near the wall. It should be noted that the validity of this form is unaffected by the system rotation since the balance between the pressure temperature-gradient correlation and pressure transport and that between the viscous diffusion and dissipation anisotropy persist regardless of the rotation number as already seen in Figures 5.2 and 5.3.

An a priori test is performed to evaluate the present diffusive transport constraint given in Eq. (5.25), of which both sides are computed using the DNS data and compared with each other. Figure 5.4 shows the results for ξ_1-component, where the present diffusive transport constraint gives fairly good agreement with DNS data for $y^+ \leq 5$ both for non-rotating and rotating cases, which can be considered as an improvement compared with the original one. For ξ_2-component, Figures 5.5 shows that the present diffusive transport constraint can also give good agreement for $y^+ \leq 10$ compared to the DNS data.

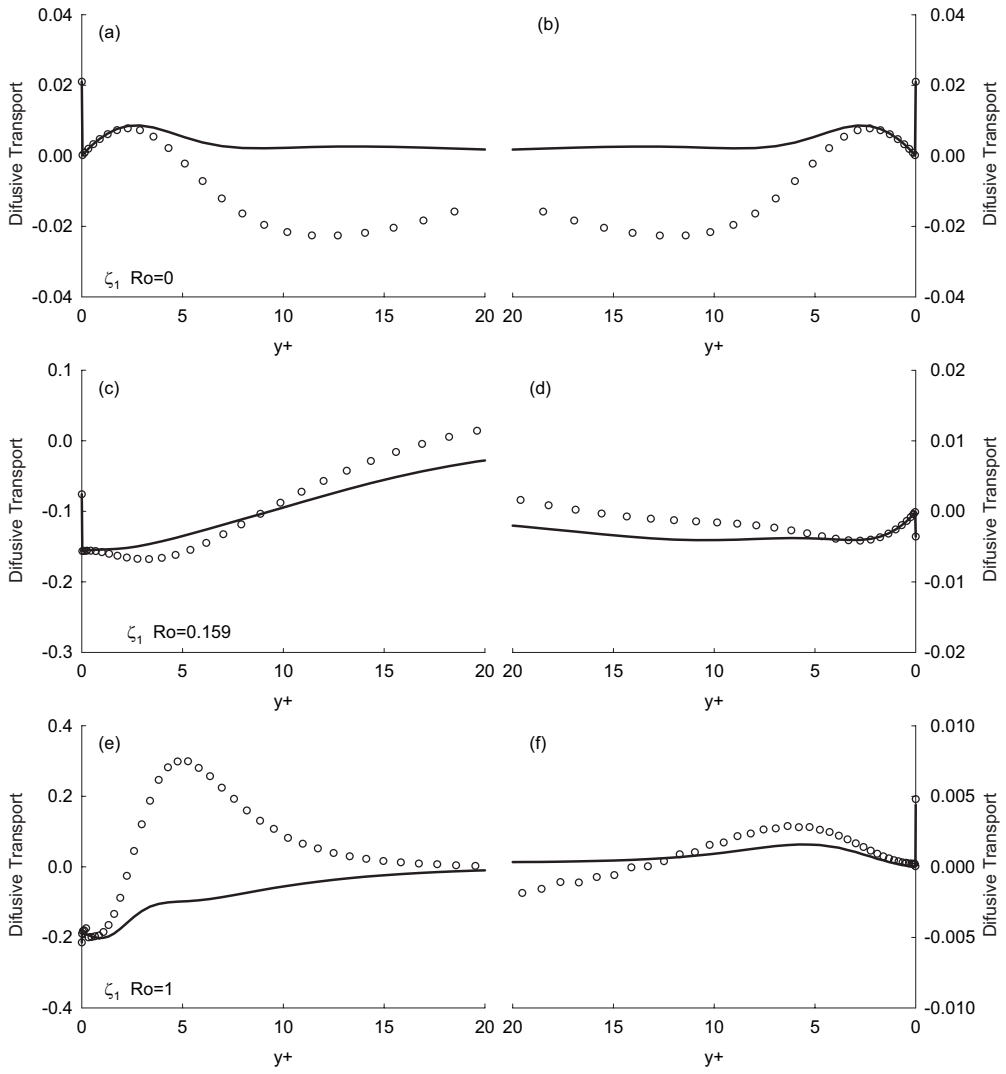

Figure 5.4: Validation of present near-wall correction of diffusive transport constraint for ξ_1 LHS: Pressure side, RHS: Suction side. The present constraint (solid line) compared to DNS (circle).

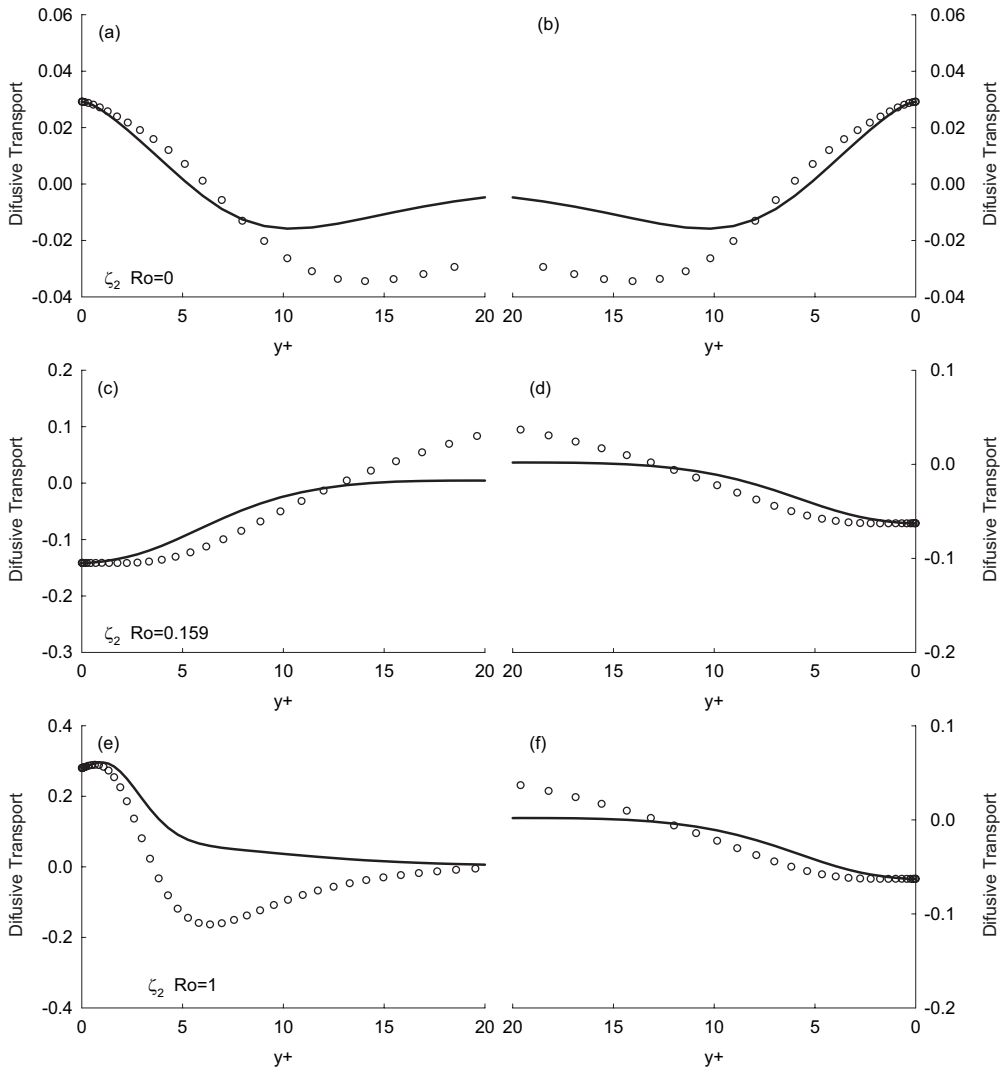

Figure 5.5: Validation of present near-wall correction of diffusive transport constraint for ξ_2 LHS: Pressure side, RHS: Suction side. The present constraint (solid line) compared to DNS (circle).

Whereas, compared with the Reynolds-stress case, where the extended constraint gives excellent agreement with DNS data for all Reynolds stress components, the extended constraint in present study remains noticeable discrepancy from DNS data in some cases. In both the Reynolds stresses and heat fluxes situations, the productions are assumed to be negligible. This assumption is well supported in the case of Reynolds stresses, of which, the production becomes negligible in the vicinity of the wall mostly. However, for the case of heat fluxes, the production remains small but noticeable values for $y^+ \leq 10$ sometimes, as shown in Figs. (5.2) and (5.3). Howsoever, the above evaluation indicates that present alternative diffusive transport constraint has the potential to advance the AHFM, once the accurate models for pressure temperature-gradient correlation and dissipation anisotropy in Eq. (5.22) are provided.

5.5 Concluding remarks

This chapter focuses on the validity and extensions of weak-equilibrium condition in the non-inertial frames. The weak-equilibrium condition, which consists of advection assumption and diffusive transport constraint, is the basis to derive the algebraic heat flux model from differential transport model. The frame invariant concept is invoked in this study to extend the original advection assumption for flows associated with rotation and curvature effects. Moreover, we derived the frame invariant form of AHFM by using the extended weak-equilibrium condition. It is also proven that the transport equation of normalized heat flux can be written in a Euclidean invariant way by introducing the Jaumann-Noll derivative.

The budget analyses of the various terms of exact transport equation for ξ_i show that the diffusive transport is crucial in the near-wall region. An asymptotic analysis of the near-wall behavior shows that, the diffusive transport keeps balance with the sum of pressure temperature-gradient correlation plus dissipation anisotropy in the wall vicinity, while production anisotropy is small. An alternative form of diffusive transport constraint is proposed and evaluated using DNS data. Evaluation shows that present alternative constraint has the potential to improve the predictive ability of resultant AHFM.

Chapter 6

Conclusion and Perspective

In the course of this study, the framework of RANS modeling is reviewed in detail. Some demonstrations using DRSM, NLEVM and EVM have been given for the case of fully developed rotating channel flow, and compared to the DNS computation. The results indicate that the DRSM, which is mathematically and physically better founded, is the most reliable one to represent the considered flow features.

The most important tasks accomplished in the present study are the development of algebraic models for Reynolds stress and turbulent heat flux, respectively. Instead of dealing with elaborate mathematical derivation, focus has been placed on the starting point of deriving such algebraic models, which is so-called weak-equilibrium condition. With the aid of DNS database, it has been discovered that the conventional weak-equilibrium condition tends to fail in the near-wall region. It is believed that, with the incorrect weak-equilibrium condition, the effort to derive the algebraic models with elaborate mathematical techniques will be certainly compromised. In the present study, by using the budget analysis and asymptotic analysis, the alternative form of diffusive transport constraint, both for Reynolds stress and turbulent heat flux, has been proposed, which offers a firmer foundation to derive algebraic models from DRSMs. The a priori tests suggest that the proposed forms have the potential to improve the predictive ability of resultant algebraic models.

In addition, the frame invariant concept is invoked in this study to extend the original advection assumption for flows associated with rotation and curvature effects. Moreover, we derived the frame invariant form of AHFM by using the extended weak-equilibrium condition. It is also proven that the transport equation of normalized heat

flux can be written in a Euclidean invariant way by introducing the Jaumann-Noll derivative.

It is noted that the comprehensive test of proposed models has not been conducted in the present study, although it is necessary in order to reveal the full potential of the proposed models. The successful implements of proposed constraints, both for ARSM and AHFM, requires reliable models for redistribution and dissipation terms, specially for the near-wall region. Accordingly, this requirement calls for more attention on the improvement of the redistribution and dissipation terms. Another interesting term, which draws attention in the course of present study, is the pressure transport term. Currently, this term has been handled together with the viscous diffusion. However, observation suggests the pressure transport plays a very important role in the near-wall region. Therefore, it should be modeled separately. Above objectives have also always been the demands by the further development of second-moment closure.

It has to be admitted that there has been some arguments about the role of algebraic models playing in the framework of RANS modeling. One may wonder if it is worth the effort to develop such algebraic models because of the troublesome numerical treatment. Additional modifications have to be made to include the noninertial effects. On the other hand, the DRSM accounts such effects naturally. While, in present stage, the most rational level of RANS modeling, the DRSM is not yet dominant in the practical applications because of the computation cost. In this situation, the algebraic models find their way and attract attentions, as what Pope (1999) refers to that the realistic goal is always the *optimal* turbulence model. Hopefully, it can be expected that rapid improvement of numerical method and computer resource would decrease the importance of the argument for algebraic model in the near future. Accordingly, the importance of DRSM models in practical applications would increase.

Appendix A

The transformation of W and S

The velocity U^* in the non-inertial frame $\mathbf{C}^*$ can be obtained by taking the time derivative, then the the spatial derivative of U^* is

$$\frac{\partial U^*}{\partial x^*} = \dot{Q}Q^T + Q\frac{\partial U}{\partial x}Q^T, \tag{A.1}$$

where $\dot{Q} = dQ/dt$ and $Q^T = \partial x/\partial x^*$.

Then following Eq.(A.1), the Euclidean transformation can be performed for strain-rate tensor S and the vorticity tensor W

$$\begin{aligned} S^* &= \frac{1}{2}\left(\frac{\partial U^*}{\partial x^*} + \left(\frac{\partial U^*}{\partial x^*}\right)^T\right) \\ &= \frac{1}{2}\dot{Q}Q^T + \frac{1}{2}Q\frac{\partial U}{\partial x}Q^T + \frac{1}{2}Q\dot{Q}^T + \frac{1}{2}Q^T\left(\frac{\partial U}{\partial x}\right)^T Q \\ &= \frac{1}{2}\dot{Q}Q^T + \frac{1}{2}Q\frac{\partial U}{\partial x}Q^T + \frac{1}{2}Q\dot{Q}^T + \frac{1}{2}(-Q)\left(\frac{\partial U}{\partial x}\right)^T(-Q^T) \\ &= \frac{d}{dt}\left(QQ^T\right) + QSQ^T, \end{aligned} \tag{A.2}$$

$$
\begin{aligned}
W^* &= \frac{1}{2}\left(\frac{\partial U^*}{\partial x^*} - \left(\frac{\partial U^*}{\partial x^*}\right)^T\right) && \text{(A.3)}\\
&= \frac{1}{2}\dot{Q}Q^T + \frac{1}{2}Q\frac{\partial U}{\partial x}Q^T - \frac{1}{2}Q\dot{Q}^T - \frac{1}{2}Q^T\left(\frac{\partial U}{\partial x}\right)^T Q \\
&= \frac{1}{2}\dot{Q}Q^T - \frac{1}{2}Q\dot{Q}^T + \frac{1}{2}Q\frac{\partial U}{\partial x}Q^T - \frac{1}{2}(-Q)\left(\frac{\partial U}{\partial x}\right)^T(-Q^T) \\
&= \frac{1}{2}\dot{Q}Q^T - \frac{1}{2}Q\dot{Q}^T + \underbrace{\frac{1}{2}\dot{Q}Q^T + \frac{1}{2}Q\dot{Q}^T}_{0} + \frac{1}{2}Q\frac{\partial U}{\partial x}Q^T - \frac{1}{2}(-Q)\left(\frac{\partial U}{\partial x}\right)^T(-Q^T), \\
&= \dot{Q}Q^T + QWQ^T. && \text{(A.4)}
\end{aligned}
$$

For the strain-rate tensor S^*, since $QQ^T = I$

$$S^* = QSQ^T. \qquad \text{(A.5)}$$

For the vorticity tensor, one may deduce to

$$W^* = Q\left(W + \Omega\right)Q^T. \qquad \text{(A.6)}$$

Appendix B

The transformation of $\overline{u_j\theta}^*$

$$\begin{aligned}
\overline{u_j\theta}^* &= \lim_{\alpha\to\infty}\frac{1}{N}\sum_{\alpha=1}^{N}\left(u_j^{*(\alpha)}\theta^{*(\alpha)}\right)\\
&= \lim_{\alpha\to\infty}\frac{1}{N}\sum_{\alpha=1}^{N}\left(Q_{ji}u_i^{(\alpha)}\theta^{(\alpha)}\right)\\
&= Q_{ji}\lim_{\alpha\to\infty}\frac{1}{N}\sum_{\alpha=1}^{N}\left(u_i^{(\alpha)}\theta^{(\alpha)}\right)\\
&= Q_{ji}\overline{u_i\theta}. \qquad \text{(B.1)}
\end{aligned}$$

Appendix C

The transformation of $\frac{D\overline{u_j\theta}}{Dt}$

$$
\begin{aligned}
\frac{D\overline{u_j\theta}^*}{Dt} &= \frac{\partial\overline{u_j\theta}^*}{\partial t} + u_k^*\frac{\partial\overline{u_j\theta}^*}{\partial x_k} \\
&= \frac{\partial Q_{ji}\overline{u_i\theta}}{\partial t} + Q_{km}u_m\frac{\partial Q_{ji}\overline{u_i\theta}}{Q_{km}\partial u_m} \\
&= \dot{Q}_{ji}\overline{u_i\theta} + Q_{ji}\frac{\partial\overline{u_i\theta}}{\partial t} + Q_{ji}u_m\frac{\partial\overline{u_i\theta}}{\partial x_m} \\
&= Q_{jl}\Omega_{li}\overline{u_i\theta} + Q_{ji}\left(\frac{\partial\overline{u_i\theta}}{\partial t} + u_m\frac{\partial\overline{u_i\theta}}{\partial x_m}\right) \\
&= Q_{ji}\Omega_{ik}\overline{u_k\theta} + Q_{ji}\frac{D\overline{u_i\theta}}{Dt} \\
&= Q_{ji}\left(\Omega_{ik}\overline{u_k\theta} + \frac{D\overline{u_i\theta}}{Dt}\right) \\
&= Q_{ji}\frac{\bar{D}\overline{u_i\theta}}{Dt}.
\end{aligned}
\tag{C.1}
$$

Appendix D

The incorporation of proposed diffusive transport constraint with ARSM

D.1 The basic equation set

The explicit algebraic stress model of Gatski & Speziale (1993), applicable to inertial and noninertial frames, is given by

$$\begin{aligned} b_{ij} = & -a_1 C_\mu^* \tau S_{ij} - a_1 a_2 C_\mu^* \tau^2 \left(S_{ik}\tilde{W}_{kj} - \tilde{W}_{ik}S_{kj} \right) \\ & + 2a_1 a_3 C_\mu^* \tau^2 \left(S_{ik}S_{kj} - \frac{1}{3} S_{mn}S_{mn}\delta_{ij} \right), \end{aligned} \tag{D.1}$$

where

$$C_\mu^* = \left[1 - \frac{4}{3}a_3^2 g^2 \left(\frac{k}{\varepsilon}\right)^2 S_{mn}S_{mn} + 4a_2^2 g^2 \left(\frac{k}{\varepsilon}\right)^2 \tilde{W}_{mn}\tilde{W}_{mn}\right]^{-1}, \tag{D.2a}$$

$$g = \left[\left(C_1^1/2 + 1\right)\frac{P}{\varepsilon} + C_1^0/2 - 1\right]^{-1}, \tag{D.2b}$$

$$\tilde{W}_{ij} = -\, c_\omega e_{mij}\Omega_m, \tag{D.2c}$$

$$c_\omega = \frac{C_4 - 4}{C_4 - 2}. \tag{D.2d}$$

The coefficients are defined as $a_1 = 0.487$, $a_2 = 0.8$, $a_3 = 0.375$, $C_1^0 = 3.4$, $C_4 = 0.4$ and $C_1^1 = 1.8$.

Above Gatski-Spezial algebraic Reynolds stress relations can be further simplified for the case of fully developed rotating channel flow

$$\tau_{12} = -\, g a_1 C_\mu^* \frac{k^2}{\varepsilon}\frac{dU}{dy}, \tag{D.3a}$$

$$\tau_{11} = \frac{2}{3}k + \frac{4}{3}g^2 C_\mu^* a_3 a_1 \frac{k^3}{\varepsilon^2}S_{12}^2 + 4a_2 a_1 \frac{k^3}{\varepsilon^2}S_{12}\tilde{W}_{12}, \tag{D.3b}$$

$$\tau_{22} = \frac{2}{3}k + \frac{4}{3}g^2 C_\mu^* a_3 a_1 \frac{k^3}{\varepsilon^2}S_{12}^2 - 4a_2 a_1 \frac{k^3}{\varepsilon^2}S_{12}\tilde{W}_{12}, \tag{D.3c}$$

$$\tau_{33} = \frac{8}{3}k - \frac{8}{3}g^2 C_\mu^* a_3 a_1 \frac{k^3}{\varepsilon^2}S_{12}^2. \tag{D.3d}$$

Above stress relations need to be coupled with Equations for turbulent kinetic energy and the turbulent dissipation rate, which are

$$0 = -\frac{1}{\rho}\frac{\partial P_{eff}}{\partial x} - \frac{d}{dy}\overline{uv} + \nu\frac{d^2U}{dy^2}, \tag{D.4a}$$

$$0 = P - \varepsilon + \frac{d}{dy}\left[\left(\nu + \frac{\nu_t}{\sigma_\varepsilon}\right)\frac{dk}{dy}\right], \tag{D.4b}$$

$$0 = C_{\varepsilon 1}^* P\frac{\varepsilon}{k} - f_2 C_{\varepsilon 2}^* + \frac{d}{dy}\left[\left(\nu + \frac{\nu_t}{\sigma_\varepsilon}\right)\frac{d\varepsilon}{dy}\right], \tag{D.4c}$$

where

$$\nu_t = f_\mu C_\mu k\tau, \qquad \tau = k/\varepsilon. \tag{D.5}$$

Note that the P_{eff} is affected by the Ro, which is $2\Omega d/U_m$.

To sum up, the coefficients in the GS ARSM are listed in Table (D.1)

Table D.1: Coefficients in the GS ARSM

Item	Value
f_μ	1.0
C_μ	0.094
f_2	$\left[1-\exp\left(-\frac{y^+}{6.5}\right)\right]^2$
$C^*_{\varepsilon 1}$	1.44
$C^*_{\varepsilon 2}$	1.83
σ_k	1
σ_ε	1.3
a_1	0.487
a_2	0.8
a_3	0.375
C_4	0.4
C_1^0	3.4
C_1^1	1.8

D.2 The incorporation

In the present study, only straightforward incorporation is considered. Recall that the proposed diffusive transport constraint for ARSM is given by

$$\mathcal{D}_{ij}-\frac{\tau_{ij}}{k}\mathcal{D}=-[\phi_{ij}-(\varepsilon_{ij}-\frac{\tau_{ij}}{k}\varepsilon)]f_d. \tag{D.6}$$

Direct incorporation of Eq. (D.6) into the exact transport equation for Reynolds

stress anisotropy tensor b_{ij} leads to

$$0 = \frac{1}{2k}\left(P_{ij} + C_{ij} - \frac{\tau_{ij}}{k}P\right) + \left[\frac{\phi_{ij}}{2k} - \frac{1}{2k}\left(\varepsilon_{ij} - \frac{\tau_{ij}}{k}\varepsilon\right)\right](1 - f_d). \tag{D.7}$$

Following the explicit method presented by Gatski & Speziale (1993), Eq. (D.7) can be made explicit for b_{ij}. Actually, in the Gatski & Speziale (1993) model, the dissipation anisotropy term is set to zero. This fact suggests that the effect of proposed constraint will only be reflected by the changing of redistribution term. Consequently, it is readily to recognized that the resultant ARSM, which is revised by incorporating the proposed constraint, will remain the same form as Eq. (D.1). However, the corresponding model coefficients should be modified as following

$$\begin{aligned}
&\hat{a}_1 = \frac{2}{3} - \frac{\beta C_2}{2}, \quad \hat{a}_2 = 1 - \frac{\beta C_4}{2}, \quad \hat{a}_3 = 1 - \frac{\beta C_3}{2}, \\
&\hat{a}_4 = \tau\left[\left(\frac{\beta {C_1}^1}{2} + 1\right)\frac{P}{\varepsilon} + \frac{\beta {C_1}^0}{2} - 1\right]^{-1}, \\
&\beta = 1 - f_d.
\end{aligned}$$

D.3 Results and comments

The ARSM equation set introduced in the previous section is solved by the finite difference method with 201 non-uniformly distributed nodes in the y direction, and the first node was situated at $y^+ \leq 0.5$. The distance between each node is increased with an expansion rate of 1.05. The boundary condition for k is 0 and for the dissipation rate ε

$$\varepsilon = 2\nu\left(\frac{\partial\sqrt{k}}{\partial y}\right). \tag{D.8}$$

To stabilize the computation, the discretization of momentum equation (Eq.(D.4a)) is re-managed as following.

$$\overline{uv} = -\nu_{t1}\frac{dU}{dy}, \tag{D.9}$$

$$\nu_{t1} = g a_1 C_\mu^* \frac{k^2}{\varepsilon}. \tag{D.10}$$

The momentum equation can be arranged as

$$0 = -\frac{1}{\rho}\frac{\partial P_{eff}}{\partial x} + \frac{d}{dy}\left(\nu_{t1}\frac{dU}{dy}\right) + \nu\frac{d^2U}{dy^2}, \tag{D.11}$$

$$= -\frac{1}{\rho}\frac{\partial P_{eff}}{\partial x} + \frac{d}{dy}\left(\Gamma\frac{dU}{dy}\right), \tag{D.12}$$

with $\Gamma = \nu_{t1} + \nu$.

The diffusion terms are discretized using CDS

$$\left[\frac{d}{dy}\left(\Gamma\frac{dU}{dy}\right)\right] \approx \frac{\left(\Gamma\frac{dU}{dy}\right)_{i+\frac{1}{2}} - \left(\Gamma\frac{dU}{dy}\right)_{i-\frac{1}{2}}}{\frac{1}{2}\left(x_{i+1} - x_{i-1}\right)}. \tag{D.13}$$

Furthermore, the CDS approximations for the first order derivative are

$$\left(\Gamma\frac{dU}{dy}\right)_{i+\frac{1}{2}} \approx \Gamma_{i+\frac{1}{2}}\frac{U_{i+1} - U_i}{x_{i+1} - x_i}, \tag{D.14}$$

$$\left(\Gamma\frac{dU}{dy}\right)_{i-\frac{1}{2}} \approx \Gamma_{i-\frac{1}{2}}\frac{U_i - U_{i-1}}{x_i - x_{i-1}}, \tag{D.15}$$

where

$$\Gamma_{i+\frac{1}{2}} = \frac{1}{2}\left(\Gamma_{i+1} + \Gamma_i\right), \tag{D.16a}$$

$$\Gamma_{i-\frac{1}{2}} = \frac{1}{2}\left(\Gamma_i + \Gamma_{i-1}\right). \tag{D.16b}$$

$$\tag{D.16c}$$

The resulting algebraic equation for momentum at node i reads

$$A_p^i U_i + A_E^i U_{i+1} + A_W^i U_{i-1} = Q_i. \tag{D.17}$$

Consequently, the coefficients of the algebraic equation (Eq. (D.17)) are

$$A_E^i = \frac{2\nu + \nu_{t1,i+1} + \nu_{t1,i}}{h_{i+1}\left(h_{i+1} + h_i\right)}, \tag{D.18a}$$

$$A_W^i = \frac{2\nu + \nu_{t1,i} + \nu_{t1,i-1}}{h_i\left(h_{i+1} + h_i\right)}, \tag{D.18b}$$

$$A_P^i = -\left(A_E^i + A_W^i\right), \tag{D.18c}$$

$$Q_i = \frac{1}{\rho}\frac{\partial P_{eff}}{\partial x}, \tag{D.18d}$$

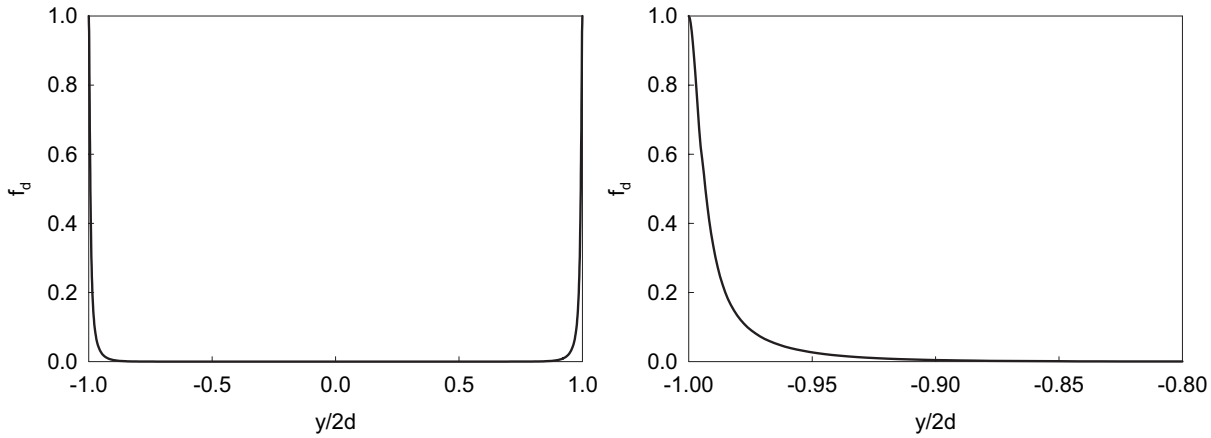

Figure D.1: Model coefficient f_d

with $h_i = x_i - x_{i-1}$.

The discretization of k and ε equations follows the similar manner. The computation is conducted for $Ro = 0$ and 0.2. The results for original Gatski-Speziale ARSM (referred as ARSM), and the revised ARSM after incorporation of proposed diffusive transport constraint (referred as ARSMC), are presented in the following plots.

D.3.1 Stationary case

First of all, the distribution of model coefficient f_d is shown in Fig. D.1. This coefficient is supposed to become unity at the wall and slowly decays away from the wall for $y^+ \leq 10$, which is well represented in Fig. D.1.

In Fig. D.2, the mean velocity profile are shown both for original ARSM and revised ARSM. By examining Fig. D.2, one can tell that by original GS model, fairly well agreement with DNS data is achieved. And by the revised ARSM, improvement is not obtained. In Fig. D.3, the plots for Reynolds stress components are presented. Similar with the mean velocity, the revised version of ARSM did not bring improvements comparing to the original one.

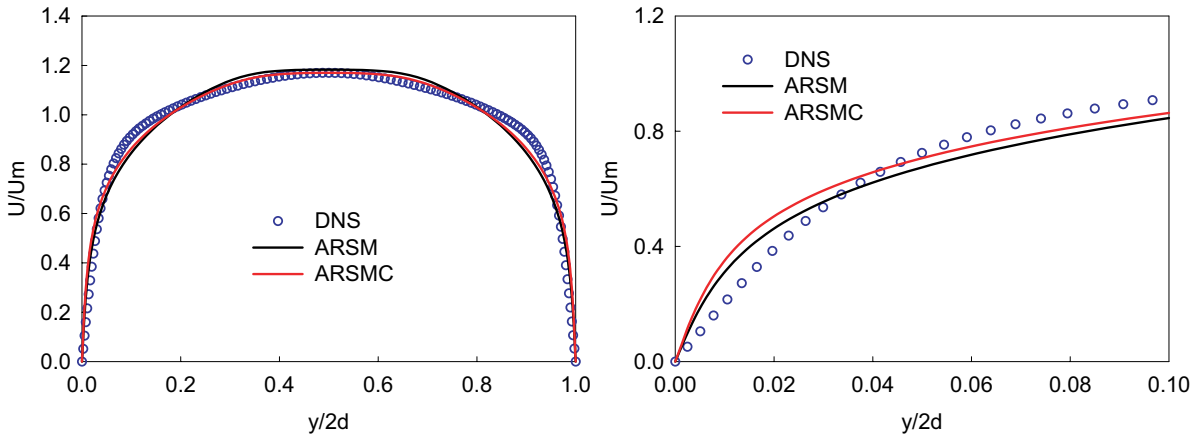

Figure D.2: Mean velocity profile for $Ro = 0$

D.3.2 Rotating case of $Ro = 0.2$

For the rotating case of $Ro = 0.2$, Both the original ARSM and revised ARSM possess certain ability to represent the rotation effect as shown in Fig. D.4. Nevertheless, there still exists noticeable discrepancy between the DNS and the original ARSM. Once again, the revised version of ARSM yet brings any improvement comparing with original ARSM. This observation also stands for the plots of other Reynolds stress components (Fig. D.5).

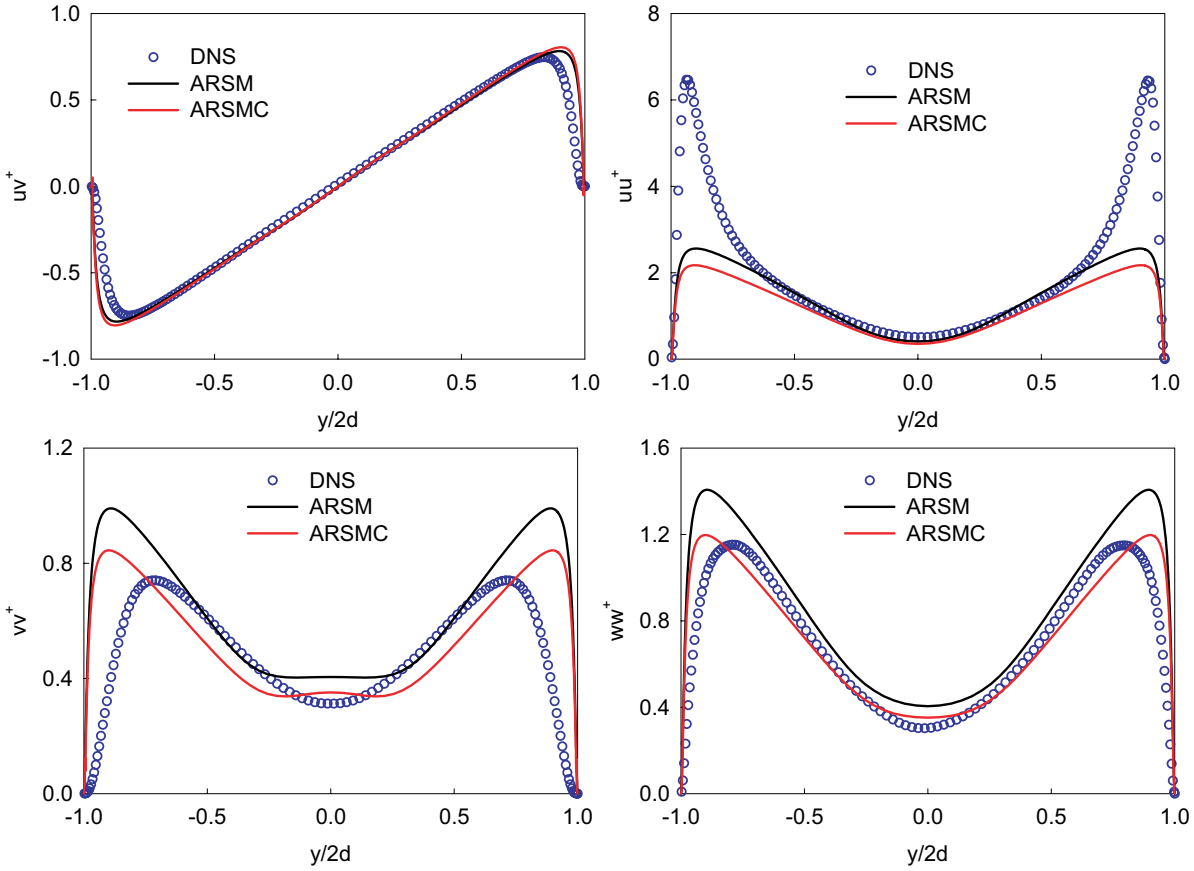

Figure D.3: Reynolds stress components for $Ro = 0$

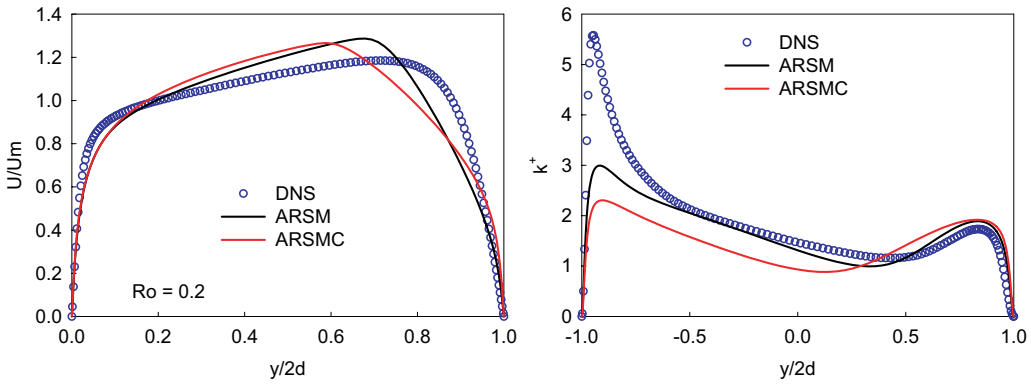

Figure D.4: Mean velocity and kinetic energy for $Ro = 0.2$

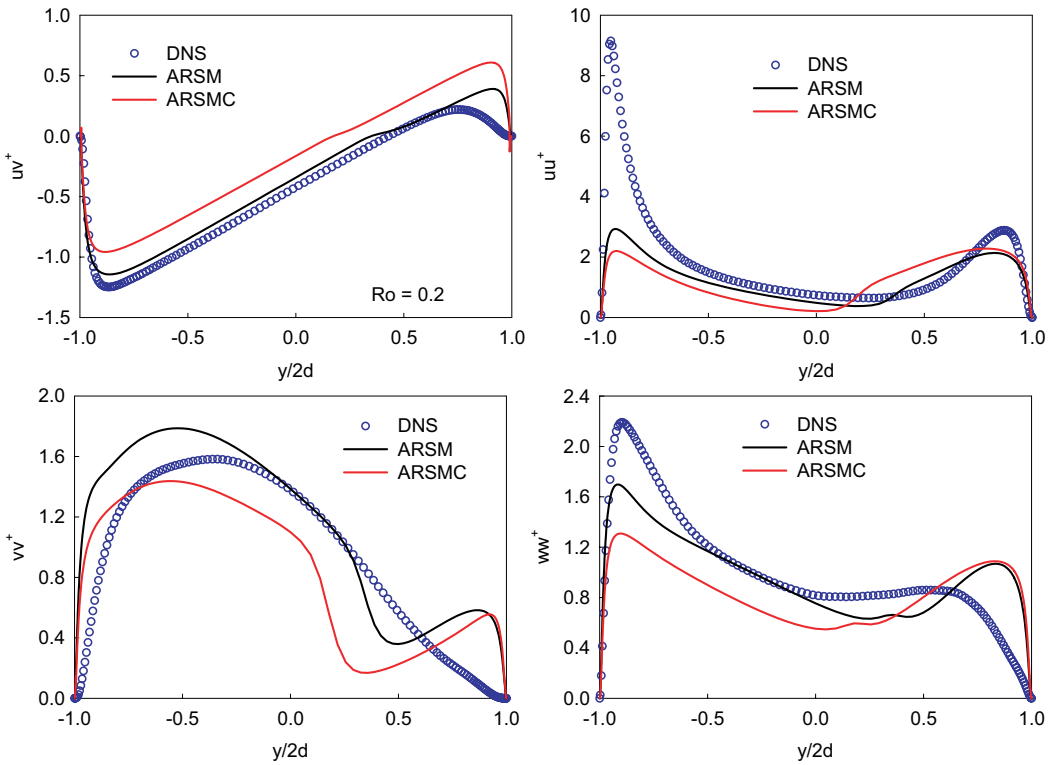

Figure D.5: Reynolds stress components for $Ro = 0.2$

References

ABE, K. & SUGA, K. 2001 Towards the development of a Reynolds-averaged algebraic turbulent scalar-flux model. *Int. J. Heat and Fluid Flow* **22** (1), 19–29. 5

ALVELIUS, K. 1999 Studies of turbulence and its modelling through large eddy- and direct numerical simulation. PhD thesis, Royal Institute of Technology, Stockholm, Sweden. 37

ANDERSSON, H. I. & KRISTOFFERSEN, R. 1993 Reynolds-stress budgets in rotating channel flow. In *Proceedings of Ninth Symposium on Turbulent Shear Flows, pp. 16C18. Kyoto, Japan*. 5

ANTONELLO, M. & MASI, M. 2007 A simplified explicit algebraic model for the Reynolds stresses. *Int. J. Heat and Fluid Flow* **28** (5), 1092–1097. 17

BREDBERG, J. 2001 On two-equation eddy-viscosity models. *Tech. Rep.*. Internal Report 01/8, Chalmers University of Technology. 29

CAMBON, C., JACQUIN, L. & LUBRANO, J. L. 1992 Toward a new Reynolds stress model for rotating turbulent flows. *Phys. Fluids* **4**, 812. 37

CEBECI, T. & BRADSHAW, P. 1984 *Physical and computational aspects of convective heat transfer*. Springer. 32

CELIK, I. 2005 RANS/LES/DES/DNS: the future prospects of turbulence modeling. *J. Fluid Engrg.* **127**, 829–830. 2

CHOU, P. Y. 1945 On the velocity correlations and the solution of the equations of turbulent fluctuation. *Quart. Appl. Math* **3** (3), 38–45. 14

CRAFT, T. J., GANT, S. E., IACOVIDES, H. & LAUNDER, B. E. 2004 A new wall function strategy for complex turbulent flows. *Numerical Heat Transfer, Part B: Fundamentals* **45** (4), 301–318. 3

CRAFT, T. J., LAUNDER, B. E. & SUGA, K. 1996 Development and application of a cubic eddy-viscosity model of turbulence. *Int. J. Heat and Fluid Flow* **17** (2), 108–115. 31

CRAFT, T. J., LAUNDER, B. E. & SUGA, K. 1997 Prediction of turbulent transitional phenomena with a nonlinear eddy-viscosity model. *Int. J. Heat and Fluid Flow* **18** (1), 15–28. 29

DOL, H. S., HANJALIĆ, K. & KENJEREŠ, S. 1997 A comparative assessment of the second-moment differential and algebraic models in turbulent natural convection. *Int. J. Heat and Fluid Flow* **18** (1), 4–14. 6, 32

DURBIN, P. A. & PETTERSSON, B. A. 2001 *Statistical theory and modeling for turbulent flows*. Wiley New York. 10

DUTZLER, G. K., PETTERSSON-REIF, B. A. & ANDERSSON, H. I. 2000 Relaminarization of turbulent flow in the entrance region of a rapidly rotating channel. *Int. J. Heat and Fluid Flow* **21** (1), 49–57. 38, 46

ELSAMNI, O. & KASAGI, N. 2001 The effects of system rotation with three orthogonal rotating axes on turbulent channel flow. In *The 7th International Congress on Fluid Dynamics and Propulsion, Cairo, Egypt, December 18-20*. 89, 92

GATSKI, T. B. 2004 Constitutive equations for turbulent flows. *Theor. Comp. Fluid Dyn.* **18** (5), 345–369. 6, 13

GATSKI, T. B. & JONGEN, T. 2000 Nonlinear eddy viscosity and algebraic stress models for solving complex turbulent flows. *Prog. Aerospace Sci.* **36** (8), 655–682. 5, 89

GATSKI, T. B. & RUMSEY, C. L. 2001 Linear and non-linear eddy viscosity models. In *Closure Strategies for Turbulent and Transitional Flows*. Cambridge University Press. 5, 20, 21, 66, 69

GATSKI, T. B. & SPEZIALE, C. G. 1993 On explicit algebraic stress models for complex turbulent flows. *J. Fluid Mech.* **254**, 59–78. 16, 17, 21, 22, 23, 109, 112

GATSKI, T. B. & WALLIN, S. 2004 Extending the weak-equilibrium condition for algebraic Reynolds stress models to rotating and curved flows. *J. Fluid Mech.* **518**, 147–155. 3, 5, 6, 27, 33, 86, 88

GIRIMAJI, S. S. 1996 Fully explicit and self-consistent algebraic Reynolds stress model. *Theor. Comp. Fluid Dyn.* **8** (6), 387–402. 17, 23

GIRIMAJI, S. S. 1997 A Galilean invariant explicit algebraic Reynolds stress model for curved flows. *Phys. Fluids* **9**, 1067–1077. 5, 6, 89

GRUNDESTAM, O. 2006 Modelling and simulation of turbulence subject to system rotation. PhD thesis, Royal Institute of Technology, Stockholm, Sweden. 28

GRUNDESTAM, O., WALLIN, S. & JOHANSSON, A. V. 2005*a* An explicit algebraic Reynolds stress model based on a nonlinear pressure strain rate model. *Int. J. Heat and Fluid Flow* **26** (5), 732–745. 17

GRUNDESTAM, O., WALLIN, S. & JOHANSSON, A. V. 2005*b* Techniques for deriving explicit algebraic Reynolds stress models based on incomplete sets of basis tensors and predictions of fully developed rotating pipe flow. *Phys. Fluids* **17**, 115103. 17

GRUNDESTAM, O., WALLIN, S. & JOHANSSON, A. V. 2008 Direct numerical simulations of rotating turbulent channel flow. *J. Fluid Mech.* **598**, 177–199. 5, 37

HAASE, W., AUPOIX, B., BUNGE, U. & SCHWAMBORN, D. 2006 *FLOMANIA - a European initiative on flow physics modelling: results of the European-Union funded project, 2002-2004*. Springer. 3, 15

HADŽIĆ, I. 1999 Second-moment closure modelling of transitional and unsteady turbulent flows. PhD thesis, Delft University of Technology. 2

HAMBA, F. 2006 Euclidean invariance and weak-equilibrium condition for the algebraic Reynolds stress model. *J. Fluid Mech.* **569**, 399–408. 3, 5, 6, 27, 86, 88

HANJALIĆ, K. 2005*a* Turbulence and transport phenomena - modelling and simulation. Lecture Note. 12, 14

HANJALIĆ, K. 2005*b* Will RANS survive LES? a view of perspectives. *J. Fluid Engrg.* **127**, 831–839. 2

HANJALIĆ, K. & JAKIRLIĆ, S. 1993 A model of stress dissipation in second-moment closures. *Appl. Sci. Res.* **51** (1-2), 513–518. 40

HANJALIĆ, K. & LAUNDER, B. E. 1972 A Reynolds stress model of turbulence and its application to thin shear flows. *J. Fluid Mech.* **52** (04), 609–638. 14

HATTORI, H., MORITA, A. & NAGANO, Y. 2006 Nonlinear eddy diffusivity models reflecting buoyancy effect for wall-shear flows and heat transfer. *Int. J. Heat and Fluid Flow* **27** (4), 671–683. 6, 33, 34

HELLSTEN, A. 2004 New two-equation turbulence model for aerodynamics applications. PhD thesis, Helsinki University of Technology. 2, 14

HOWARD, J.H.G., PATANKAR, S.V. & BORDYNUIK, R.M. 1980 Flow prediction in rotating ducts using Coriolis-modified turbulence models. *J. Fluid Engrg.* **102**, 46–461. 29, 56, 57

JAKIRLIĆ, S., HANJALIĆ, K. & TROPEA, C. 2002 Modeling rotating and swirling turbulent flows: a perpetual challenge. *AIAA J.* **40** (10), 1984–1996. 63

JOHANSSON, A. V. 2002 Engineering turbulence models and their development, with emphasis on explicit algebraic Reynolds stress models. *CISM Courses Lect.* **442**, 253C300. 2, 3

JOHANSSON, A. V. & WALLIN, S. 1996 A new explicit algebraic Reynolds stress model. In *The 6th European Turbulence Conference, Lausanne, Switzerland*, pp. 31–34. 17

JOHNSTON, J. P., HALLEENT, R. M. & LEZIUS, D. K. 1972 Effects of spanwise rotation on the structure of two-dimensional fully developed turbulent channel flow. *J. Fluid Mech.* **56** (03), 533–557. 37, 56, 64

JONGEN, T. 1998 Simulation and modeling of turbulent incompressible fluid flows. PhD thesis, Swiss Federal Institute of Technology. 21, 23

JONGEN, T. & GATSKI, T. B. 1998*a* A new approach to characterizing the equilibrium states of the Reynolds stress anisotropy in homogeneous turbulence. *Theor. Comp. Fluid Dyn.* **11** (1), 31–47. 17

JONGEN, T. & GATSKI, T. B. 1998*b* General explicit algebraic stress relations and best approximation for three-dimensional flows. *Int. J. Eng. Sci.* **36** (7), 739–763. 21, 23

JONGEN, T., MACHIELS, L. & GATSKI, T. B. 1998*a* Predicting noninertial effects with linear and nonlinear eddy-viscosity, and algebraic stress models. *Flow, Turbulence and Combustion* **60** (2), 215–234. 6, 17

JONGEN, T., MOMPEAN, G. & GATSKI, T. B. 1998*b* Predicting S-duct flow using a composite algebraic stress model. *AIAA J.* **36** (3), 327–335. 6

KASAGI, N. & IIDA, O. 1999 Progress in direct numerical simulation of turbulent heat transfer. In *The 5th ASME/JSME Joint Thermal Engineering Conference, March 15-19, San Diego, California*. 89, 92

KASAGI, N., TOMITA, Y. & KURODA, A. 1992 Direct numerical simulation of passive scalar field in a turbulentchannel flow. *J. Heat Transfer* **114**, 598–606. 92

KAWAMURA, H., ABE, H. & MATSUO, Y. 1999 DNS of turbulent heat transfer in channel flow with respect to Reynolds and Prandtl number effects. *Int. J. Heat and Fluid Flow* **20** (3), 196–207. 97

KAWAMURA, H., OHSAKA, K., ABE, H. & YAMAMOTO, K. 1998 DNS of turbulent heat transfer in channel flow with low to medium-high Prandtl number fluid. *Int. J. Heat and Fluid Flow* **19** (5), 482–491. 97

KIM, J. & MOIN, P. 1987 Transport of passive scalars in a turbulent channel flow. In *6th Symposium on Turbulent Shear Flows, Toulouse, France, Sept. 7-9.*. 97

KIM, J., MOIN, P. & MOSER, R. 1987 Turbulence statistics in fully developed channel flow at low Reynolds number. *J. Fluid Mech.* **177**, 133–166. 5, 38, 42, 64

KRISTOFFERSEN, R. & ANDERSSON, H. I. 1993 Direct simulations of low-Reynolds-number turbulent flow in a rotating channel. *J. Fluid Mech.* **256**, 163–197. viii, 5, 8, 37, 38, 53, 54, 57, 63, 64, 65

LAI, YG & SO, RMC 1990 Near-wall modeling of turbulent heat fluxes. *Int. J. Heat Mass Transfer* **33**, 1429–1440. 6

LAMBALLAIS, E., LESIEUR, M. & MÉTAIS, O. 1996 Effects of spanwise rotation on the vorticity stretching in transitional and turbulent channel flow. *Int. J. Heat and Fluid Flow* **17** (3), 324–332. 37, 38

LAMBALLAIS, E., MÉTAIS, O. & LESIEUR, M. 1998 Spectral-dynamic model for large-eddy simulations of turbulent rotating channel flow. *Theor. Comp. Fluid Dyn.* **12** (3), 149–177. viii, 5, 37, 38, 46, 53, 54, 64

LAUNDER, BE, PRIDDIN, CH & SHARMA, BI 1977 The calculation of turbulent boundary layers on spinning and curved surfaces. *J. Fluid Engrg.* **99**, 231–239. 29, 56

LAUNDER, B. E., MORSE, A., RODI, W. & SPALDING, D. B. 1972 Prediction of free shear flows: a comparison of the performance of six turbulence models. In *Conference on Free Turbulent Shear Flows, NASA Rept. SP-321, pp. 361-426.*, , vol. 1, pp. 20–21. 41

LAUNDER, B. E., REECE, G. J. & RODI, W. 1975 Progress in the development of a Reynolds-stress turbulence closure. *J. Fluid Mech.* **68** (03), 537–566. 14, 19, 24

LAUNDER, B. E. & SHIMA, N. 1989 Second-moment closure for the near-wall sublayer- Development and application. *AIAA J.* **27** (10), 1319–1325. 39, 40, 57

LIU, N.-S. & LU, X.-Y. 2007 Direct numerical simulation of spanwise rotating turbulent channel flow with heat transfer. *Int. J. Numer. Meth. Fluids* **53** (11), 1689–1706. 37, 46, 92

LUMLEY, J. L. 1978 Computational modeling of turbulent flows. *Adv. Appl. Mech.* **18**, 123–176. 24

MANCEAU, R. 2005 An improved version of the elliptic blending model. Application to non-rotating and rotating channel flows. In *Proc. 4th Int. Symp. Turb. Shear Flow Phenomena, Williamsburg, VA, USA*. 3, 83

MANSOUR, N. N., KIM, J. & MOIN, P. 1988 Reynolds-stress and dissipation-rate budgets in a turbulent channel flow. *J. Fluid Mech.* **194**, 15–44. 12, 43, 73

MATSUBARA, M. & ALFREDSSON, P. H. 1996 Experimental study of heat and momentum transfer in rotating channel flow. *Phys. Fluids* **8**, 2964. 37, 92

MATSUBARA, M. & ALFREDSSON, P. H. 1998 Secondary instability in rotating channel flow. *J. Fluid Mech.* **368**, 27–50. 37

MOMPEAN, G., GAVRILAKIS, S., MACHIELS, L. & DEVILLE, M. O. 1996 On predicting the turbulence-induced secondary flows using nonlinear $k-\varepsilon$ models. *Phys. Fluids* **8**, 1856. 29

MOORE, J. 1967 Effect of coriolis forces on turbulent flow in rectangular channels. *Tech. Rep.*. MIT Gas Turbine Lab. Rep. 74. 64

NAGANO, Y. & HATTORI, H. 2003 Direct numerical simulation and modelling of spanwise rotating channel flow with heat transfer. *J. Turbul.* **4** (1), 1–15. 6

NAJI, H., MOMPEAN, G. & YAHYAOUI, O. E. 2004 Evaluation of explicit algebraic stress models using direct numerical simulations. *J. Turbul.* **5** (38), 1–25. 26

NISHIMURA, M. & KASAGI, N. 1996 Direct numerical simulation of combined forced and natural turbulent convection in a rotating plane channel. In *The 3rd KSME/JSME Thermal and Fluid Engineering Conference, Kyongju, Korea*. 89, 92

PALLARES, J. & DAVIDSON, L. 2000 Large-eddy simulations of turbulent flows in stationary and rotating channels and in a stationary square duct. *Tech. Rep.*. Report 00/03, Dept. of Thermo and Fluid Dynamics, Chalmers University Of Technology. 38, 46

PATEL, V. C., RODI, W. & SCHEUERER, G. 1985 Turbulence models for near-wall and low Reynolds number flows- A review. *AIAA J.* **23** (9), 1308–1319. 43

PIOMELLI, U. & LIU, J. 1995 Large-eddy simulation of rotating channel flows using a localized dynamic model. *Phys. Fluids* **7**, 839. 37

POPE, SB 1983 Consistent modeling of scalars in turbulent flows. *Phys. Fluids* **26**, 404. 34

POPE, S. B. 1975 A more general effective-viscosity hypothesis. *J. Fluid Mech.* **72** (02), 331–340. 16, 21, 25

POPE, S. B. 1999 Modeling complex turbulent flows. In *Modeling complex turbulent flows* (ed. M. D. Salas, N. Hefner & L. Sakell), pp. 53–67. Kluwer Academic Publishers. 104

POPE, S. B. 2000 *Turbulent flows*. Cambridge University Press. 1

REYNOLDS, W. C. 1976 Computation of turbulent flows. *Annu. Rev. Fluid Mech.* **8** (1), 183–208. 13

RODI, W. 1972 The prediction of free turbulent boundary layers by use of a two-equation model of turbulence. PhD thesis, University of London. 4, 17

RODI, W. 1976 A new algebraic relation for calculating the Reynolds stresses. *Zeitschrift fuer angewandte Mathematik und Mechanik* **56**, 219–221. 4, 16, 17, 18

RODI, W. 2006 DNS and LES of some engineering flows. *Fluid Dynamics Research* **38** (2-3), 145–173. 2

RODI, W. & SCHEUERER, G. 1983 Calculation of curved shear layers with two-equation turbulence models. *Phys. Fluids* **26**, 1422. 4, 18

ROGERS, M. M., MANSOUR, N. N. & REYNOLDS, W. C. 1989 An algebraic model for the turbulent flux of a passive scalar. *J. Fluid Mech.* **203**, 77–101. 6

ROKNI, M. 2000 A new low-Reynolds version of an explicit algebraic stress model for turbulent convective heat transfer in ducts. *Numer. Heat Transfer, Part B* **37** (3), 331–363. 6

ROSENAU, P. 1989 Extending hydrodynamics via the regularization of the Chapman-Enskog expansion. *Phys. Rev. A* **40** (12), 7193–7196. 19

ROTTA, J. 1951 Statistische Theorie nichthomogener Turbulenz. *Zeitschrift für Physik A Hadrons and Nuclei* **131** (1), 51–77. 14, 24

RUMSEY, C. L., GATSKI, T. B., ANDERSON, K. W. & NIELSEN, E. J. 2001 Isolating curvature effects in computing wall-bounded turbulent flows. *Int. J. Heat and Fluid Flow* **22** (6), 573–582. 4, 18

RUMSEY, C. L., GATSKI, T. B. & MORRISON, J. H. 1999 Turbulence Model Predictions of Extra-Strain Rate Effects in Strongly-Curved Flows. *AIAA Paper* pp. 99–0157. 17

RUMSEY, C. L., GATSKI, T. B. & MORRISON, J. H. 2000 Turbulence model predictions of strongly curved flow in a U-duct. *AIAA J.* **38** (8), 1394–1402. 4, 18

SHABANY, Y. & DURBIN, P. 1997 Explicit algebraic scalar flux approximation. *AIAA Journal* **35** (6), 985–989. 6

SHABBIR, A. & SHIH, T. H. 1992 Critical assessment of Reynolds stress turbulence models using homogeneous flows. *Tech. Rep.*. NASA TM 105954. 24

SHIH, T-H., ZHU, J. & LUMLEY, J. L. 1995 A new Reynolds stress algebraic equation model. *Comput. Methods Appl. Mech. Engrg.* **125** (1-4), 287–302. 30, 57, 58

SO, R. M. C., JIN, L. H. & GATSKI, T. B. 2004 An explicit algebraic Reynolds stress and heat flux model for incompressible turbulence: Part I Non-isothermal flow. *Theor. Comp. Fluid Dyn.* **17** (5), 351–376. 6, 33, 34, 96

SO, R. M. C., LAI, Y. G., ZHANG, H. S. & HWANG, B. C. 1991 Second-order near-wall turbulence closures-A review. *AIAA J.* **29**, 1819–1835. 41

SO, R. M. C., SARKAR, A., GERODIMOS, G. & ZHANG, J. 1997 A dissipation rate equation for low-Reynolds-number and near-wall turbulence. *Theor. Comp. Fluid Dyn.* **9** (1), 47–63. 43

SO, R. M. C. & SOMMER, T. P. 1996 An explicit algebraic heat-flux model for the temperature field. *Int. J. Heat Mass Transfer* **39** (3), 455–465. 6

SO, R. M. C. & SPEZIALE, C. G. 1999 A review of turbulent heat transfer modeling. *Annual Review of Heat Transfer* **10**, 177–219. 32, 97

SPEZIALE, CG 1998 A review of material frame-indifference in mechanics. *Appl. Mech. Rev.* **51** (8), 489–504. 6, 27

SPEZIALE, C. G. 1979 Invariance of turbulent closure models. *Phys. Fluids* **22**, 1033–1037. 6, 27

SPEZIALE, C. G. 1987 Second-order closure models for rotating turbulent flows. *Quart. Appl. Math.* **45**, 721–733. 29

SPEZIALE, C. G. 1991 Analytical methods for the development of Reynolds-stress closures in turbulence. *Annu. Rev. Fluid Mech.* **23** (1), 107–157. 13

SPEZIALE, C. G., SARKAR, S. & GATSKI, T. B. 1991 Modelling the pressure–strain correlation of turbulence: an invariant dynamical systems approach. *J. Fluid Mech.* **227**, 245–272. 20

SPEZIALE, C. G. & XU, X. H. 1996 Towards the development of second-order closure models for nonequilibrium turbulent flows. *Int. J. Heat and Fluid Flow* **17** (3), 238–244. 17

TAFTI, D. K. & VANKA, S. P. 1991 A numerical study of the effects of spanwise rotation on turbulent channel flow. *Phys. Fluids* **3**, 642. 37

TAULBEE, D. B. 1992 An improved algebraic Reynolds stress model and corresponding nonlinear stress model. *Phys. Fluids* **4**, 2555–2561. 16, 19, 24, 29

TAULBEE, D. B., SONNENMEIER, J. R. & WALL, K. M. 1994 Stress relation for three-dimensional turbulent flows. *Phys. Fluids* **6**, 1399–1401. 16

THIFFEAULT, J. L. 2001 Covariant time derivatives for dynamical systems. *J. Phys. A: Math. Gen.* **34**, 5875–5885. 87

TRUSOV, P. V. 1987 Corotation derivatives and defining relations in the theory of large plastic strains. *J. Appl. Mech. Tech. Phys.* **28** (2), 311–316. 87

WALLIN, S. 2000 Engineering turbulence modeling for CFD with a focus on explicit algebraic Reynolds stress models. PhD thesis, Royal Institute of Technology, Stockholm, Sweden. 28

WALLIN, S. & JOHANSSON, A. V. 2000 An explicit algebraic Reynolds stress model for incompressible and compressible turbulent flows. *J. Fluid Mech.* **403**, 89–132. 17, 23, 25, 26

WALLIN, S. & JOHANSSON, A. V. 2002 Modelling streamline curvature effects in explicit algebraic Reynolds stress turbulence models. *Int. J. Heat and Fluid Flow* **23** (5), 721–730. 5, 17, 28, 89

WEIS, J. & HUTTER, K. 2003 On Euclidean invariance of algebraic Reynolds stress models in turbulence. *J. Fluid Mech.* **476**, 63–68. 6, 27, 87

WIKSTRÖM, P. M., WALLIN, S. & JOHANSSON, A. V. 2000 Derivation and investigation of a new explicit algebraic model for the passive scalar flux. *Phys. Fluids* **12**, 688. 6, 7, 33, 34, 96

WILCOX, D. C. 1993 *Turbulence modeling for CFD*. DCW Industries. 29

WU, H. & KASAGI, N. 2004 Turbulent heat transfer in a channel flow with arbitrary directional system rotation. *Int. J. Heat Mass Transfer* **47** (21), 4579–4591. 92

XU, X. H & SPEZIALE, C. G. 1996 Explicit algebraic stress model of turbulence with anisotropic dissipation. *AIAA J.* **34**, 2186–2189. 17

YAMAWAKI, D., OBI, S. & MASUDA, S. 2002 Heat transfer in transitional and turbulent boundary layers with system rotation. *Int. J. Heat and Fluid Flow* **23** (2), 186–193. 92

YING, R. & CANUTO, V. M. 1996 Turbulence modelling over two-dimensional hills using an algebraic Reynolds stress expression. *Boundary Layer Meteorol.* **77** (1), 69–99. 23